Retrovirus induced expression of inhibitory ligands on myeloid cells and the regulation of cytotoxic CD8+ T cells

Inaugural Dissertation

for

the Doctoral Degree of

Dr. rer. nat.

from the Faculty of Biology

University of Duisburg-Essen

Germany

Submitted by

Paul David

from Sikaria, India

April 2019

Die der vorliegenden Arbeit zugrunde liegenden Experimente wurden am Institut für Virologie in der Abteilung für experimentelle Virologie der Universität Duisburg-Essen durchgeführt.

1. Gutachter: Prof. Dr. Ulf Dittmer
2. Gutachter: Prof. Dr. Monika Lindemann

Vorsitzender des Prüfungsausschusses: Prof. Dr. Wiebke Hansen

Tag der mündlichen Prüfung: 05.06.2019

Table of Contents

Dedicated to my Mother and Father in law

1. Introduction

1.1 Retroviruses

Retroviruses are a large group of enveloped, single-stranded RNA viruses that replicate in a host through the process of reverse transcription. These viruses belong to the family *Retroviridae* and can be found in all vertebrates. The family *Retroviridae* consists of seven genera (*Alpha*, *Beta*, *Gamma*, *Delta*, *Epsilon*, *Lentivirus* and *Spumavirus*). Some retroviruses are associated with immune related pathology in humans. Infection with human immunodeficiency virus type 1 (HIV-1, *Lentivirus*) or HIV-2 leads to the progression of acquired immune deficiency syndrome (AIDS). The infection with human T-cell leukemia virus type 1 (HTLV-1, *Deltaretrovirus*) induces T cell leukemia.

1.1.1 Morphology of Retroviruses

Retroviruses are generally spherical, enveloped particles with an average diameter ranging from between 100 to 200 nm.

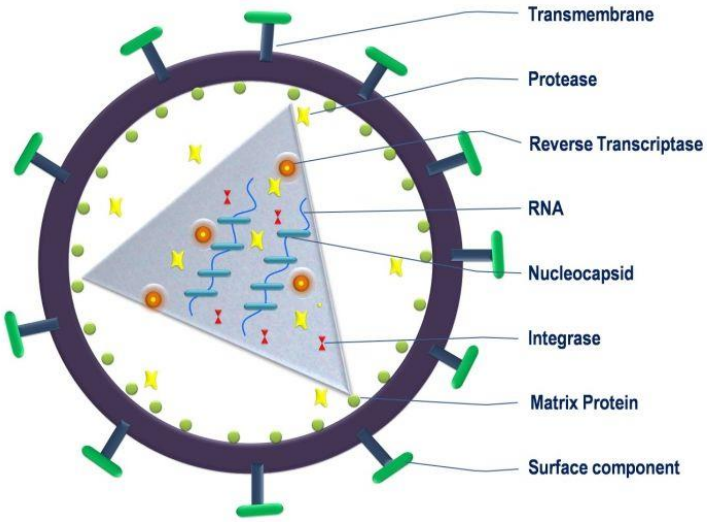

Figure 1.1 Schematic cross section of the retrovirus. The lipid bilayer is shown as two concentric outer circles on which the envelope protein complex are embedded (adapted from Stanford University Press 2008).

Different retroviruses (Fig. 1.1) have the same virion part, which includes the outer envelope coat and the inner capsid, which contains two copies of the genetic material in form of single-stranded positive sense RNA (ssRNA), and viral enzymes. The envelope consists of lipids that are obtained

from the host plasma membrane during the budding process and from glycoproteins such as gp120 and gp41 in case of HIV. The inner surface of the envelope membrane is covered with matrix proteins, which surrounds the nucleocapsid. This nucleocapsid contains the diploid single-stranded RNA molecules, the reverse transcriptase, as well as the integrase and other proteins.

The genomes of all infectious retroviruses contain the three major genes *gag* (group specific antigens), *env* (envelope, glycoproteins) and *pol* (polymerase, reverse transcriptase, integrase, protease). Complex retroviruses, such as HIV, also have genes that code for regulatory and accessory proteins.

1.1.2 The retroviral life cycle (Replication of retroviruses)

There are seven steps in the replication cycle of a retrovirus (Fig. 1.2). The first step is attachment, in which the retrovirus uses one of its glycoproteins to attach to one or more particular cell-surface receptors on the host cell. Some retroviruses likewise use an optional receptor, referred to as the co-receptor. The second and third steps are penetration and uncoating individually. Retroviruses infiltrate the host cell by direct fusion of the virion envelope with the plasma membrane of the host. The fourth step is replication, which happens after the retrovirus undergoes partial uncoating thereby releasing its genome and essential enzymes (reverse transcriptase (RT), integrase, polymerase, and protease). At this stage, the RNA genome is converted by RT into double-stranded DNA, followed by integration into the host genome, transcription and translation of viral proteins. The fifth step is assembly, where retrovirus capsids are assembled in an immature form. The sixth step is budding, where the immature viral particle acquires the host plasma membrane, and the last step is maturation and release, in which the gag and pol proteins of the retrovirus are cleaved by the retroviral protease, thus forming the mature and infectious form of the virus (1).

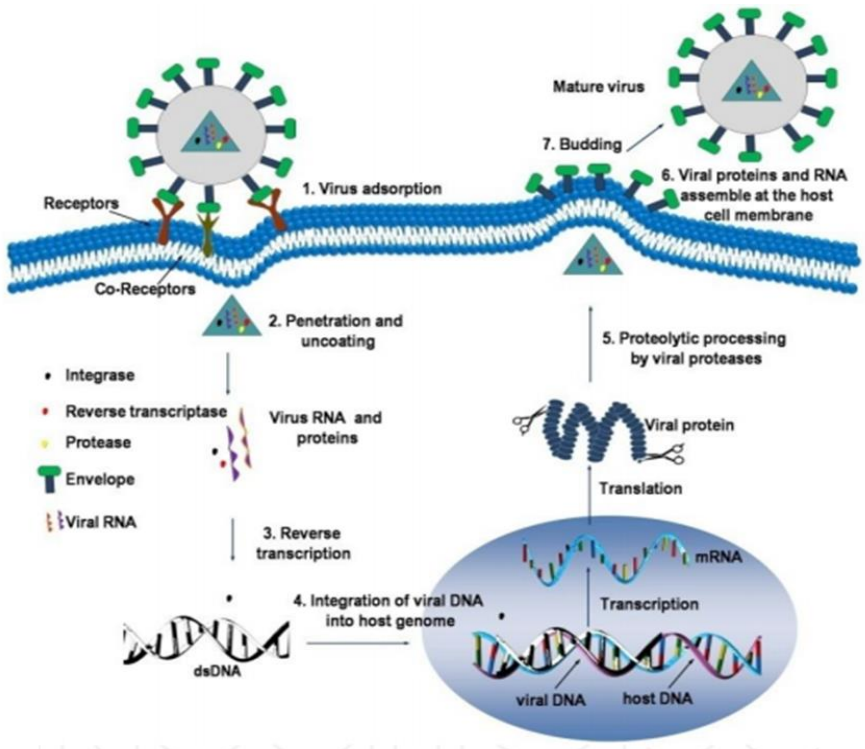

Figure 1.2 Replication of retroviruses. (Adapted from Stanford University Press 2008).

1.1.3 Friend Virus (FV)

FV was discovered by Charlotte Friend in 1957 (2). FV is an ecotropic gammaretrovirus complex composed of the Friend murine leukemia virus (F-MuLV) and the spleen focus-forming virus (SFFV). F-MuLV is a replication competent helper virus that is non-pathogenic in adult mice. SFFV is a replication-defective virus which induces pathology (3). SFFV cannot produce its own particles so it spreads by being packaged into F-MuLV-encoded particles produced in cells co-infected by both viruses. Pathology in susceptible adult mice is characterized by a polyclonal proliferation of erythroid precursor cells resulting in massive splenomegaly. Interestingly, erythroblasts ($Ter119^{+}$) cells are the main target cells for viral replication during the acute phase of FV infection, whereas B cells and, to a lesser extent monocytes, are the main virus reservoir during chronic infection (4). As FV infected cells express viral gp55 and glycoGag on their cell surface (5), the FV model provides the unique possibility to directly detect and analyze virus-infected cells with antibodies (Ab) against the viral proteins.

1.1.4 F-MuLV

Genome organization of F-MuLV

Genomic RNA of F-MuLV consists of two identical molecules of RNA, each approx. 38s in size (6). The genome of F-MuLV is similar to other mammalian and avian type-C viruses. The genome of F-MuLV can be divided into four genetic regions, which are (in a 5' to 3' order):

(i) *gag* gene - encodes for structural proteins,

(ii) *pol* gene – encodes for RNA-dependent DNA polymerase and other viral enzymes,

(iii) *env* gene – encodes for 70000 D glycoprotein coat of the virus,

(iv) *c* gene ('common') for which a gene product has not been indicated (7).

1.1.5 Pathogenesis of Friend virus in mice

F-MuLV is apathogenic in adult mice but can cause splenomegaly, anemia and erythroleukemia in new-born mice that have not yet developed an effective adaptive immune system (2). The FV complex is able to induce severe splenomegaly and lethal erythroleukemia associated with generalized immunosuppression in immunocompetent susceptible adult mice (8). The initial step of FV-induced disease is caused by a false proliferation signal induced by the binding of SFFV gp55 envelope glycoproteins to erythropoietin receptors on nucleated erythroid cells (5). This results in a vast expansion in the population of actively dividing cells susceptible to FV infection and provides a perfect target population for further infection.

The second step is the transformation phase where SFFV genomes integrate into the Spi1 site common to FV-induced erythroleukemias (3). Resistant strains of mice can mount immune responses with sufficient speed and potency to prevent the accumulation of transformation-associated events and thus averting the development of erythroleukemia (9). This results in enhanced transcription factor PU.1 levels in erythroid cells and inhibits their commitment to differentiation (10). At a later time point, the loss of p53 (tumor suppressor gene) function often occurs resulting in full cell transformation (8). However, even these resistant strains of mice are never able to completely clear virus-infected cells and they develop a life-long chronic infection (10).

1.1.6 Resistance to FV infection

The progression of FV-induced disease is reliant on an initial dose of virus and the mouse strain's genetic background. Mice have several host genes that are important for susceptibility to FV infection. These host genes constitute the Friend virus susceptibility factors Fv (1-6) (non-immunological) and at least four genes in the major histocompatibility complex (MHC) (immunological), which impact cellular and antibody mediated immune responses to FV infection (11). There are several genes that intervene with the infection (Fv1 and Fv4) and others that intervene with the immune response (Rfv1-3) or coordinate erythroid cell proliferation and differentiation (Fv2, Fv5) (12). Fv2r inhibits the polyclonal cell activation of erythroid progenitor cells thereby confining splenomegaly, whereas Fv2s makes mice susceptible to FV-induced splenomegaly. The Fv2 gene encodes for the tyrosine kinase Stk/RON, which in its short form (sf-Stk) accounts for the susceptible phenotype, whereas in resistant mice a longer form of Stk is present that cannot mediate the signaling from gp55 (10). The H-2D genes are important for the effective presentation of viral T cell epitopes. For example, mice bearing H-2Db/b have a high incidence of recovery from FV leukemia due to efficient presentation of FV-epitopes (11, 13).

1.1.7 Human Immunodeficiency Virus (HIV)

HIV is a retrovirus that invades cells in the immune system and leads to the progression of advanced acquired immune deficiency syndrome (AIDS). According to the WHO there are approximately 37 million HIV patients living worldwide (14). The virus demolishes a type of white blood cell in the immune system called T-helper cells or CD4+ T cells (CD: cluster of differentiation), and replicates inside these cells. This increases the risk and impact of opportunistic infections and cancers. However, a person can carry HIV without experiencing symptoms for a long time. Unfortunately, HIV is a lifelong infection. Modern treatment and managing the disease can effectively prevent the replication of HIV and prevent the development of AIDS.

1.1.8 Problems of HIV animal studies.

Humans and chimpanzees are hosts for HIV-1, and for this reason either *in vitro* studies with human blood or *in vivo* studies with chimpanzees can be done. Although chimpanzees are susceptible to HIV-1 infection, the replication is greatly inhibited and usually there is no progression to AIDS (15, 16). Simian immunodeficiency virus (SIV) is very similar to HIV-1 and has been used in its natural host (sooty mangabeys), although the infection does not induce immune

activation, and progression to an AIDS-like syndrome is rare. However, the infection of rhesus macaques with SIV results in a decline of CD4+ T cells and a progression to AIDS (17).The downside of these *in vivo* models for HIV-1 infection is that they are very expensive to conduct, and very low numbers of animals are available due to ethical issues. Furthermore, these animals are not inbred and thus there is a great level of genetic heterogeneity often making the results of such studies difficult to interpret.

The humanized mice model has proven to be highly informative and has a huge potential for advancing the future of HIV research (18). There are limitations to the humanized mice model, which include the relatively small volume of peripheral blood and PBMCs for viral analysis and *ex vivo* functional analysis and as well as the mice's relatively short life span (19). Apart from this, the structure of secondary lymphoid tissue does not fully match with humans and IgG immune response is not optimal (20).

1.2 Innate immune response

Immune response against viral pathogens is a complex of pathways which starts after recognition or the sensing of the virus's foreign biological structures. The subsequent immune reaction leads to abrogation of viral replication and the elimination of the infected cells. The immune response against viruses is divided into the innate and adaptive immune responses.

1.2.1 Sensing of retroviruses

Infected cells determine foreign structures of pathogens via different germline encoded pattern recognition receptors (PRRs). PRRs recognizes viral molecules by engaging with pathogen associated molecular patterns (PAMPs), which are present and produced during infection of host`s cells, viral replication and the spread of virus (21). Innate sensing of HIV is performed by membrane-bound sensors, cytosolic sensors, restriction factors, cloaking and cellular nucleases.

Membrane-bound sensors: PRRs are roughly branched into two groups: membrane-bound receptors like Toll-like receptors and cytoplasmic receptors such as cyclic GMP-AMP synthase (cGAS) or IFN-γ-inducible protein 16 (IFI16). TLR3 recognizes the double-stranded RNA produced during retroviral replication, TLR4 recognizes the envelope protein, TLR7 and TLR8 recognize the viral ssRNA, while TLR9 recognizes viral RNA–DNA hybrids. Both groups trigger

the expression of IFNs and produce vast amount of IFN-stimulated genes with pro-inflammatory functions (22-25).

Cytosolic Sensors: HIV utilizes CD4 and CCR5 or CXCR4 to infect CD4+ T cells, macrophages, and monocyte-derived dendritic cells (MDDCs). After membrane fusion, the viral capsid enters the cytosol (26). The viral DNA sensors are activated when the ssRNA is reverse transcribed into dsDNA. This involves the formation of reverse transcription intermediates (IRIs), and various RNA, RNA/DNA hybrid, and DNA species which may act as PAMPs for the stimulation of cytosolic sensors. The formation of cyclic GMP-AMP dinucleotide (cGAMP) and the activation of adapter protein STING leads to the ultimate induction of IRF3 dependent expression of type I IFNs and other cytokines (27). Another cytosolic sensor which induces IFN in macrophages through the STING dependent pathway is IFI16. Apart from DNA sensors, there are several RNA sensors such as RIG-1 and MDA5 (28).

Restriction factors: Compiled evidence indicates that restriction factors may not only act as effectors of the innate immune response but also directly recognize viral infections. TRIM5α acts as a PRR which triggers the activation of TGF-β activated kinase 1 (TAK1) and NF-κB upon the detection of the HIV-1 capsid (29). Recent studies indicate the role of tetherin/BST2 as PRR that activates NF-κB and initiates production of pro-inflammatory cytokines (30).

Cloaking of reverse transcription process: Although HIV target cells have the potential to identify viral nucleic acid, the virus nevertheless is able to escape immune sensing. One possible mechanism for this is the safeguard of RTIs from immune recognition. Recent studies demonstrated that the viral capsid remains largely unharmed (31). The stability of the viral capsid seems to be a crucial determinant of immune sensing. The interaction of the viral capsid with cellular cofactors may help HIV-1 to avoid immune sensing. Mutation in the viral capsid of the HIV-1 particle rattles the interaction with cellular cofactors and activates the immune sensors to induce an antiviral state in macrophages (32).

Cellular nucleases and HIV-1 sensing: HIV-1 misuses the cellular nucleases to avoid immune sensing. The three main cellular enzymes which assist HIV-1 in escaping immune sensing are three prime repair exonucleases 1 (TREX-1), SAMHD1 and the cellular RNase H2 endonuclease complex (33-35).

Modulation of innate sensing by HIV-1: Signaling through PRRs converge into the induction of a few transcription factors, like NK-κB, IRF3, IRF7 and the nuclear factor of activated T cells (NF-AT) (36). The gene products of HIV-1 such as Nef and Tat promote NF-κB activation. HIV-1 accessory proteins play a crucial role in modulating NF-κB activities. Vpu reduces NF-κB activation by reducing tetherin cell surface levels and further suppresses the downstream canonical signaling of NF-κB (37). Vpu also squelches IRF3 via lysosome-mediated degradation or caspase-mediated cleavage. Vpu inhibits TLR7-mediated IFN-1 production by exploiting the tetherin and ILT7 interaction. Apart from Vpu, Vpr has a role in the activation of structure-specific endonuclease regulator SLX4, which has a crucial role in cleaving RTIs, hence avoiding innate sensing (38).

1.2.1.2 Restriction factors

Eventually the oldest antiviral protection pathways are the restriction mechanisms. This protective mechanism is activated in infected cells soon after viral PAMPs recognition which further leads to the modulation or the inhibition of cellular processes which are necessary for viral replication and spread (39). These host cellular proteins are called restriction factors and are induced by interferons and are considered to be the first line of defense against viruses (Fig. 1.3). The main restriction factors which are explored in detail are APOBEC3G, tetherin, sterile alpha motif and histidine-aspartate domain 1 (SAMHD1), and TRIM5α (Fig. 1.2). The 6 other novel restriction factors which were recently discovered are endoplasmic reticulum a1,2-mannosidase I (ERManI), translocator protein (TSPO), guanylate-binding protein 5 (GBP5), serine incorporator (SERINC3/5) and zinc-finger antiviral protein (ZAP) (Fig. 1.3).

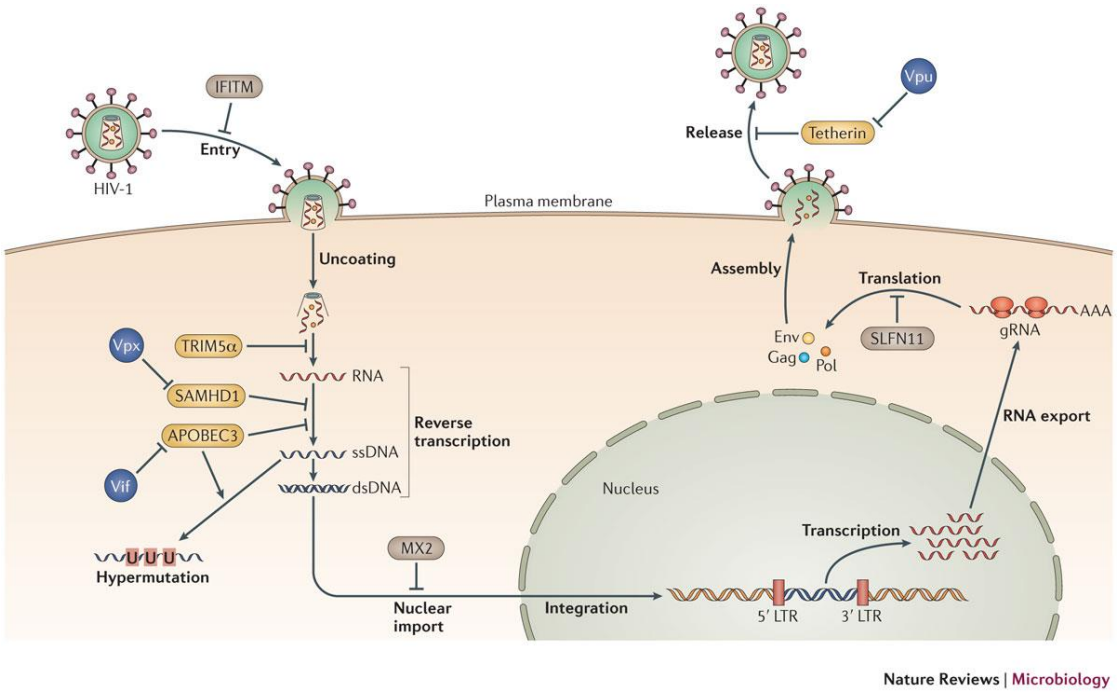

Figure 1.3 HIV-1 restriction and resistance factors. In the absence of virally encoded antagonists (or viral escape), host cell proteins called HIV-1 restriction factors (yellow) inhibit various stages of the replication cycle. The tripartite motif-containing protein 5α (TRIM5α) promotes the accelerated fragmentation of viral cores, preventing cDNA synthesis. SAM and HD domain-containing protein 1 (SAMHD1) depletes the cellular levels of 2′-deoxynucleoside 5′-triphosphates (dNTPs), which are required for efficient cDNA synthesis. APOBEC3 (apolipoprotein B mRNA-editing enzyme, catalytic polypeptide-like 3) proteins interfere with the processivity of HIV-1 reverse transcriptase and induce hypermutation of viral cDNA by cytidine deamination. Tetherin prevents the release of budded virions from the infected cell. Several viral proteins (blue) antagonize these cellular restriction factors. Viral infectivity factor (Vif) antagonizes APOBEC3 proteins, viral protein unique (Vpu) antagonizes tetherin, and the HIV-2 viral protein X (Vpx) antagonizes SAMHD1. HIV-1 resistance factors (brown) inhibit other stages of viral replication and are not counteracted by the virus. Myxovirus resistance 2 (MX2) prevents the nuclear import and integration of viral cDNA. Schlafen 11 (SLFN11) suppresses the translation of viral proteins. Interferon-induced transmembrane proteins (IFITMs) inhibit viral entry by interfering with membrane fusion. dsDNA, double-stranded DNA; gRNA, viral genomic RNA; LTR, long terminal repeat; ssDNA, single-stranded DNA (40).

1.2.1.3 Interferons

Interferons (IFNs) are a group of signaling proteins (41) secreted by host cells to counter the occupancy of viruses. There are three different classes of IFNs in humans, type I (IFN-α, IFN-β, IFN-ε, IFN-κ and IFN-ω), type II (IFN-γ), and type III (IFN-λ) (42). HIV-1 is identified by innate immune sensors that provoke the production of type I IFNs which concurrently controls HIV replication and promotes intrinsic immune activation. It remains controversial as to whether the effect of type I IFNs are constructive or destructive (43). Type I IFN plays a crucial role in stimulating restriction factors which limits HIV replication. These restriction factors are essential at every stage of the HIV replicative cycle, from reverse transcription (SAMHD1 and APOBEC3) to nuclear entry (MX2) to transcription (Schlafen 11) and budding (tetherin) (44-49). Type I IFN signaling is beneficial during acute retrovirus infection. The *in vivo* blockade of IFNAR signaling results in increased SIV infection during acute infection (50). Treatment with IFNα2 during chronic HIV infection resulted in decreased HIV RNA and p24 antigen levels (44). *In vitro* and humanized mice studies showed the importance of IFNα8 and IFNα14 in controlling HIV replication to a greater extent than IFNα2 (51, 52).

Other than its beneficial effect in controlling HIV replication, type I IFN also has a role in pro-inflammatory response. Increased type I IFNs in circulation is the outcome of poor CD4+ T cell recovery (53, 54). Type I IFNalso upregulates CCR5 (HIV co-receptor) and leads to the induction of pDC that produces CCR5 ligands, which further results in the creation and recruitment of more target cells which in turn promotes CD4+ T cell depletion (55, 56). During chronic LCMV infection, the blockade of type I IFN signaling enhanced antigen specific CD4+ T cell responses. Type I IFNs are associated with the stimulation of activation and proliferation of CD8+ T cell (57, 58). Finally, there is a lot to be explored in order to determine the functionality of type I IFNs, which can be used to inhibit or cure HIV infection. During FV infection, B6 mice showed increased levels of type I IFN responses, and a lack of type I IFNs led to significantly higher viral loads in the spleen and plasma. Type I IFNs play a crucial role during innate immunity and suggest a new approach for antiretroviral therapy based on type I IFN application (59).

1.2.1.4 Complement system

The complement system is the key part of the innate immune system and acts as a bridge between the innate and adaptive immune systems. It consists of 30 soluble proteins and three different

pathways (classical, alternative and mannose-binding lectin (MBL)) for its activation (60-62). The end product of all these three pathways is the formation of the membrane attack complex (MAB), by which complement forms lytic pores and destroys the virus and infected cells (63).

1.2.2 Cellular innate immune responses against retroviruses

1.2.2.1 Natural Killer cells (NK cells)

NK cells are part of the innate immune system and play a crucial role in combatting cancers as well as various viruses including retroviruses. These cells express activating and inhibitory receptors on their cell surface which recognize MHC molecules. The interplay between MHC molecules and regulatory receptors on NK cells regulate the NK cell response. Activated NK cells eliminate target cells by releasing cytotoxic granules and secreting proinflammatory cytokines and chemokines. (64).

1.2.2.2 Innate lymphoid cells

The discovery of a new innate lymphocyte population was made several years ago in mice and primates, and this population is essential for mucosal homeostasis, microbial regulation and immune defense. Innate lymphoid cells (ILCs) are a growing family of immune cells that have phenotypic and functional similarity with T cells. These cells are divided into three subpopulations based on phenotype and functionality: ILC1 has similarities with NK cells and produces type I cytokines (IFN-γ and TNF-α) but differs in the complex cytotoxic function which is inherited by NK cells. ILC2 has coinciding functions with Th2 and is identified by its reliance on GATA3, and the production of IL-5 and IL-13 (65, 66). ILC3 has resemblance to Th17 and is classified by its reliance on transcription factors RORγt and AHR, and the secretion of IL-17 and IL-22 (67).

1.2.2.3 Myeloid cells

Myeloid cells originate from hematopoietic stem cells in the bone marrow and contribute majorly to the leukocytes population (68). Myeloid cells comprise of monocytes, macrophages, neutrophils, basophils, eosinophils, dendritic cells (DC) and megakaryocytes. Myeloid cells play a significant role in the maintenance of tissue homeostasis and the development of immune responses against pathogens (69).

1.2.2.4 Monocytes

Monocytes are the largest cells in the normal peripheral blood (14-20µm diameter); they have a peculiar morphologic appearance which includes an uneven cell shape, a nucleus with oval or kidney like shape, cytoplasmic vesicles and a huge nucleus to cytoplasm ratio (3:1) (70). Human monocytes are categorized into three different subtypes centered on the differential expression of CD14 and CD16: classical monocytes (CD14++CD16-), intermediate monocytes (CD14++CD16+), and non-classical monocytes (CD14+CD16++) (71). The key marker of human monocytes is CD14 which is a glycoprotein and myelomonocytic differentiation antigen which functions as an accessory protein to the toll-like receptor (TLR)-4.

During HIV infection, monocytes are the target for the virus as they express CD4 receptors and chemokine co-receptors for the entry of this pathogen. *In vivo* and *in vitro* data demonstrated that HIV-infected circulating monocytes are rare in comparison to CD4 T cells. 1% of monocytes are a reservoir for HIV throughout the course of infection and are known to prevent the elimination of virus in HIV-infected individuals (72).

1.2.2.5 Macrophages

Macrophages originate from blood monocytes. Macrophages are specialized cells which are involved in the detection, phagocytosis and destruction of bacteria and other harmful organisms. Macrophages migrate and circulate to almost all the tissue parts inspecting for pathogens and eradicating dead cells. Additionally these cells are able to produce reactive oxygen species like nitric oxide which kill phagocytosed bacteria. Macrophages present antigens to T cells and initiate inflammation by releasing cytokines like IL-1, IL-6 and TNF-α. Macrophage polarization illustrates the functionality of macrophages. M1 type symbolizes pro-inflammatory and M2 symbolizes anti-inflammatory macrophages (73). M1 macrophages produce ROS and high levels of pro-inflammatory cytokines (74). *In vitro* studies have reflected that M1 cells inhibit HIV infection, whereas M2 cells inhibit the viral replication at the post integration stage (75). However, macrophages express elevated levels of C type lectins which promote the macrophage-mediated transfer of HIV to CD4 T cells (76). Infected macrophages are important for the production and harboring of HIV for long periods. They can cross the blood-tissue barrier and transmit HIV to all the tissues and organs. Thus, infected macrophages are important for the pathogenesis, dissemination, and persistence of HIV throughout the body during infection.

Tissue macrophages are important contributors to HIV pathogenesis, whereas their defined importance has not been addressed during long-term suppressive ART. Humanized myeloid only mice (MoM) data demonstrated that using ART, the HIV infection of tissue macrophages was suppressed. The study also showed a rapid decline in the plasma viral load and dramatic enhancement in the cell associated viral RNA and DNA (77).

1.2.2.6 Granulocytes

Granulocytes are the poly-morphonuclear cells and are composeed of neutrophils, basophils and eosinophils. Neutrophils are bone marrow-derived leucocytes with a short life span. During an emergency they migrate to the tissues and exert numerous antimicrobial and pro-inflammatory functions (78). HIV doesn't infect neutrophils, however HIV infection leads to neutropenia which is a common state during advanced HIV infection (79). Saitoh *et al*. reported that neutrophils use neutrophil extracellular traps (NETs) to capture and ameliorate HIV (80). TLR7 and TLR8 receptors of neutrophils after binding to viral nucleic acid induce the production of ROS, which then stimulates NET formation and finally results in the removal of HIV (80, 81).

1.2.2.7 Dendritic cells and antigen presentation

Dendritic cells (DCs) are named after their tree-like or dendrite shapes and are crucial for the commencement of adaptive immunity. DCs are derived from the bone marrow and, like macrophages, belong to the group of professional antigen presenting cells.

The recognition of invading pathogens by DCs leads to their activation, causing the upregulation of MHC class I and class II, as well as co-stimulatory molecules which further initiates an effective T cell response. After migration to lymphoid organs, DCs present non-self-peptides bound to MHC molecules on their surface to naïve CD4+ and CD8+ T cells. CD4+ T cells only interact with peptide bound to MHC class II, while CD8+T cells only recognize peptides bound to MHC class I. Whereas all nucleated body cells express MHC class I, MHC class II is only present on professional antigen presenting cells (APCs), like DCs. There are two different pathways leading to the presentation of a peptide on an MHC molecule. Peptides presented on MHC class I molecules are of cytosolic or endoplasmic reticulum (ER) origin, whereas peptides presented on MHC class II molecules are derived from endosomes. All peptides are usually of pathogenic origin and they result from different routes of infection or pathogen encounter. For

MHC class I loading endogenous antigens are generated. These are derived from misfolded proteins of cellular or pathogenic origin, or proteins produced within an infected cell. These proteins are then cleaved into smaller peptides by the proteasome. The unloaded MHC class I molecule is initially located at the luminal side of the ER membrane. Therefore, peptides must be transported into the ER lumen via the transporter associated with antigen processing (TAP). TAP has the highest affinity for peptides with a length of 8 to 10 amino acids and with hydrophobic and basic carboxy-terminal amino acids, which present the optimal size and anchor charge for MHC class I binding. The process of MHC class I peptide-complex assembly is highly chaperone guided. The fully assembled complex is then transported to the surface of the cell via the Golgi apparatus, where it can be recognized by specific CD8+ T cells (82). MHC class II loading occurs in a different process with peptides derived from exogenous antigens captured through phagocytosis or endocytosis. The internalized antigens become degraded in increasingly acidified compartments (early endosome – endolysosome – lysosome) containing hydrolytic enzymes. In this process oligopeptides with a length of 13 to 18 amino acids are produced, which are able to bind to the peptide binding groove of the MHC class II complex (83). The assembly of the two chains of the MHC class II complex takes place in the ER, where an invariant chain blocks the peptide binding groove from binding endogenous peptides and stabilizes the complex. After passing through the Golgi apparatus, the MHC class II invariant chain-complex is included in the endosomal-lysosomal pathway (84). The invariant chain is degraded, leaving only a small fragment blocking the peptide binding groove (CLIP, class II-associated invariant chain peptide). In a chaperon-mediated pathway, the CLIP is released and replaced by a peptide produced by the endosomal-lysosomal pathway. The MHC class II peptide-complex is then presented on the surface of APCs, where it can be recognized by specific CD4+ T cells (85). Thus, DCs link the innate and adaptive immune systems. DCs also upregulate the expression of stimulatory CD80, CD86 molecules (86). DCs of hematopoietic origin are divided into myeloid DCs (mDCs) and plasmacytoid DCs (pDCs). mDCs secrete high levels of IL-12, whereas pDCs can prime antiviral immune responses by producing type I IFNs.

1.2.2.8 Myeloid cells as a reservoir of HIV.

Although most research focusses on CD4+ T cells for the cure of HIV, myeloid cells in general, and macrophages in particular, have been given less attention (87). Monocytes and macrophages

belong to the myeloid lineage and have special features which makes them a likely HIV reservoir (88). Even though monocytes differentiate into macrophages, several reports have shown the detection of HIV in peripheral monocytes (89). Studies have shown the migration of HIV infected intermediate monocytes (CD14+CD16+) to the CNS and the establishment of a viral reservoir (90). HIV infection cannot not enter abundantly present classical monocytes (91), so it rather targets intermediate monocytes which are less in number, and some studies could not even detect the HIV-DNA in monocytes (92)(93). Hence, theses infected cells could migrate to different tissues and differentiate into macropahges. Macrophages from different organs like CNS (94), lungs (95), liver (96) and intestine (97) have shown the presence of HIV DNA.

DCs being the professional APCs are one of the main targets for pathogens like HIV. The most influential response of DCs to the HIV reservoir seems to be its ability to deport HIV to antigen specific CD4+ T cells (98).

1.2.2.9 Myeloid derived suppressor cells (MDSCs)

Myeloid derived suppressor cells (MDSC) are a heterogeneous cell population which arises from common myeloid progenitors in the bone marrow. Few reports suggest that MDSCs are arrested in the immature phase of differentiation (99). They have strong immunosuppressive effects on cytotoxic T cells. The increased levels of proinflammatory cytokines and other inflammatory mediators direct the expansion and recruitment of MDSC during chronic virus infection (100). The loss of T cell function during HIV-1 disease progression has been associated with higher frequencies of MDSC and has also been positively correlated with viral loads (101) and with the loss of T cell function (102).

Mouse MDSCs can be further divided into two subtypes, monocytic (CD11b+Ly6C+) and granulocytic (CD11b+Ly6G+). In humans, the MDSCs are generally defined as high density myeloid cells expressing CD33, CD14 and low levels of HLA DR (103). MDSCs use different suppressive effector pathways simultaneously. The production of arginase (ARG1), iNOS, TGFβ, IL-10, COX2, indoleamine 2,3-dioxygenase (IDO), are the most prominent ways to control the functionality of lymphocytes (104). MDSC suppresses both antigen-specific and non-specific T cell activation in the mouse model (105). Granulocytic and monocytic MDSC suppresses T cells by the reduction of L-arginine within the tumor microenvironment which leads to the arrest of T cells in Go-G1 (106). In addition, MDSCs suppresse T cell activation by segregating cysteine,

enabling T cells to receive cysteine, which is necessary for antigen activation, proliferation and differentiation (106). MDSCs affect the reduction of CD4+ and CD8+ T cells in homing lymph node, which results in the down-regulation of L-selectin which helps in leucocyte extravasation to inflated areas (107). Interestingly, the inhibition of MDSC *in vivo* and *in vitro* results in decreased Tregs proliferation and tumor-induced tolerance in antigen specific T cells (108). In FV infection, MDSCs are activated and expand during acute infection. gMDSCs express arginase 1, higher counts of PD-L1 and CD39 on the cell surface, and these molecules are involved in the suppression of CD8+ T cells (109).

1.3 Adaptive Immune responses

The adaptive immune system, also known as acquired immunity, uses specific antigens to strategically mount an immune response. Unlike the innate immune system, which attacks only based on the identification of general threats, the adaptive immunity is activated by exposure to defined antigens, and forms an immunological memory to learn about the threat and immediately respond after second infection. The adaptive immune response is much slower to respond to pathogens than the innate immune response, which is primed and ready to fight. The adaptive immunity is further divided into the humoral and cellular which are mediated by B and T lymphocytes.

B cells. The differentiation of B cells from hematopoietic stem cells takes place in the bone marrow. The key effector functions of B cells are the production of antigen-specific antibody and antigen presentation. The production of antibodies by B cells are either T cells dependent or independent (110). However, the activation of B cells are controlled by T cells, which is why they are called T helper cells.

T cells originate from stem cells in the bone marrow and develop in the thymus, a small lymphoid organ located between the lungs. In the thymus, the developing T cells start expressing T cell receptors (TCR) and other molecules like CD4 and CD8. Furthermore, only the cells with functional TCRs are subjected to positive and negative selection in order to distinguish their own components of the immune system from foreign ones. In positive selection, immature T cells bind with the MHC molecules. If the T cells TCRs are incapable of binding to MHC complexes, the T cells undergo apoptosis. If the T cells TCR successfully bind to MHC complexes, they receive survival signals and thus are positively selected. The subsequent recognition of complexes of

endogenous MHC molecules, in combination with pathogenic antigens, triggers the activation of these T cells, thereby initiating an immune response. This process creates a repertoire of T cells that can recognize a wide variety of antigens. While the ability of T cells to recognize antigen-MHC complex is important for their ability to fight pathogens and other foreign cells, it is equally important that these T cells do not recognize and attack their own cells. This is where negative selection comes into play.

T cells can be divided into different subtypes based on their function and can be distinguished by the expression of different surface molecules, which are called clusters of differentiation (CD). CD4 and CD8 are glycoproteins and belong to the Ig superfamily. CD4 are expressed on populations of lymphocytes with helper functions. CD8 are expressed on T lymphocytes with cytotoxic features. CD4 and CD8 act as a co-receptors and, together with the T cell receptors (TCR), play an important role in the recognition of antigens. Recognition of foreign antigens expressed by MHC molecules expressed on APCs lead to activation of the T cells and initiates further immune responses.

T helper cells functionally can be divided into different subpopulations. The pro- CD4+ T helper cells of type 1 (T_H1) produce inflammatory cytokines like TNFα, IFNγ and IL-2. CD4+ type 2 T cells (T_H2) are responsible for the activation and regulation of B cells. Two other subpopulations of CD4+ T cells produce regulatory cytokines IL-9 and IL-17 and in this way can be divided into CD4+ T cells of type 9 (T_H9) and type 17 (T_H17). IL-17 induce inflammation associated with pathogens, autoimmune and allergic reactions. IL-9 preferentially regulate the proliferation and apoptosis of hematopoietic cells. Follicular helper T cells (T_{FH}) play an essential role in the formation of germinal centers (GCs) of lymph nodes. B cells within GCs are known as GC B cells and undergo rapid proliferation and antibody diversification, allowing the production of many types of antibodies, with a greater affinity for their targets. Defects in T_{FH} help to B cells have been observed in HIV-infected patients and contribute to the inability of patients to produce effective HIV specific antibodies. Given the contribution of T_{FH} to a number of human diseases, a better understanding of these cells could one day be therapeutically beneficial. Additionally to the helper function, some CD4+ T cells progress into cytotoxic effector CD4+ T cell populations. This population of CD4+ T cells develops before the polarization of different subsets of T_H cells. The transcription factors which regulate the cytotoxicity of CD4+ cytotoxic cells are T-bet and Eomes

(111). The one important subpopulation of CD4+ T cells is a regulatory T cells (Tregs). The main role of regulatory CD4+ T cells is to abrogate the activation of the immune system and thus they are essential for the prevention of autoimmune diseases. On the other hand, the suppression of immune responses by Tregs may also lead to the early suppression of effector functions of immune cells during viral infection, thus preventing the elimination of the virus (112, 113).

CD8+ T cells belong to the main effector cells of an adaptive immune response against viral infections. Upon activation, they recognize virus-infected cells via MHC I-presented antigens and can kill them directly through various mechanisms.

1.3.1 Activation of CD8+ T cells

T cells become activated or stimulated mainly by three different signals or steps. Once the T cells leave the thymus, they circulate around the body until the point they recognize their antigens on the surface of antigen presenting cells (APCs). The T cell receptor (TCR) on T cells then binds to the MHC complex on the surface of APC, which triggers the initial activation, proliferation and differentiation of the T cells. In addition to TCR binding to antigen loaded MHC, T cells require a number of secondary signals to become activated and respond against pathogens. The binding of ligands CD80 or CD86 expressed on APC with CD28 receptor provides the additional costimulatory signal for the activation and proliferation of naïve CD8+ T cells. Inflammatory cytokines provides another costimulatory signal which is necessary for the differentiation of cytotoxic T cells. The activation of antigen-specific T cells leads to the production of huge amounts of T cells with similar specificity (114, 115).

1.3.2 CD8+ T cells and their effector molecules

The important effector molecules secreted by CD8+ T cells are the pro-inflammatory cytokines interferon gamma (IFN-γ), interleukin 2 (IL-2) and tumor necrosis factor alpha (TNF-α) (118-120). However, these cytokines may also be secreted by other immune cells, such as e.g. CD4 + T cells, NK cells or APCs. IFN-γ is the only member of the type II IFN family and has a prominent role in the activation of macrophages, the immigration of lymphocytes to the site of infection, the maturation and differentiation of various immune cells, increases the activity of NK cells, and regulates B cell function (121). IFN-γ may also inhibit viral replication or induce viral elimination by up-regulating MHC I molecules and the immunoproteasome, thereby enabling an efficient recognition of virus-infected cells by CD8+ T cells. In addition, IFN-γ has a direct antiviral effect

through the induction of antiviral proteins and may also have an anti-proliferative and pro-apoptotic effect (121).TNF-α is also a pleiotropic cytokine and has various effects on different immune cells. It exists in a soluble form, but can also be membrane-bound to develop its effect. TNF-α binds to its receptor, the TNFα receptor (TNFR). It consists of two subunits, TNFRI and TNFRII. TNFRI is expressed on all cells and its binding is associated with most TNF-α-induced effects. Activation of the TNFR signaling cascade induces various signaling pathways which are associated with cell activation, cell differentiation, and cytokine production (122). Furthermore, the binding of TNFR, by both soluble and membrane-bound TNF-α, triggers the programmed cell death, i.e. apoptosis, in target cells. TNF-α induces the transcriptional activation and the expression of reactive oxygen or nitrogen species as well as the activation of various caspases. IL-2 is the major growth factor of T cells and has vital role in their activation and expansion. The major producers of IL-2 are CD4+ T cells, but CD8+ T cells can also secrete large amounts of IL-2 (123). Autocrine IL-2 supports the continuous expansion of CD8+ T cells and induces the production of other cytokines (such as IFN-γ, perforin or GzmB) (124), thereby CD8+ T cells can achieve more effector functions. In addition, IL-2 is needed to develop an immunological CD8+ T cell memory (125).

1.3.3 Mechanisms of CD8+ T cell-mediated elimination of infected cells

Cytotoxic T cells play a crucial role in the immune defense against viruses, bacteria and other intracellular pathogens. Upon activation, there are two major mechanisms by which CD8+ T cells kill infected or tumor cells. The first mechanism is by releasing cytotoxic granules which contain cytotoxic molecules like perforin and Gzms (126, 127). The interaction between TCR of CD8+ T cells and the antigen-MHC I complex induces the targeted displacement of intracellular granules to the contact point between CD8+ T cells and infected cells, the so-called immunological synapse. There, both cell membranes fuse and the contents of the granules are deflated in the resulting intracellular space, thereby inducing the cell death of the target cell. In this exocytosis-induced apoptosis, perforin is responsible for forming pores in the membrane of the target cell so that GzmA and GzmB can invade. The endocytosis of the Gzms is mediated by the cation-independent mannose-6-phosphate receptor and then induces proteolytic cleavage of caspases, which can lead to DNA fragmentation (deoxyribonucleic acid) and apoptosis (128). In addition, Gzms can induce caspase-independent mitochondrial decay leading to the release of cytochrome c, another pro-

apoptotic protein (129). To protect themselves from the action of their own secreted granules, CD8+ T cells express Gzm-specific inhibitors (130).

The second way to induce CD8+ T cell-mediated killing of target cells is activated after the interaction of death ligands like FasL with the death receptors Fas on the surface of target cells. Activated CD8+ T cells express FasL on their cell surface, which binds to its receptor, Fas, on the surface of the infected or malignant cells (131). This binding causes the Fas molecules on the surface of the target cell to trimerise, which pulls together signaling molecules. This leads to the activation of the caspase cascade, which also results in the apoptosis of the infected or malignant target cells. Additionally to FasL, TRAIL expressed on CD8+ T cells can trigger the caspase activation and apoptosis of target cells by either DR4 (Death Cell Receptor 4) or DR5 (132).

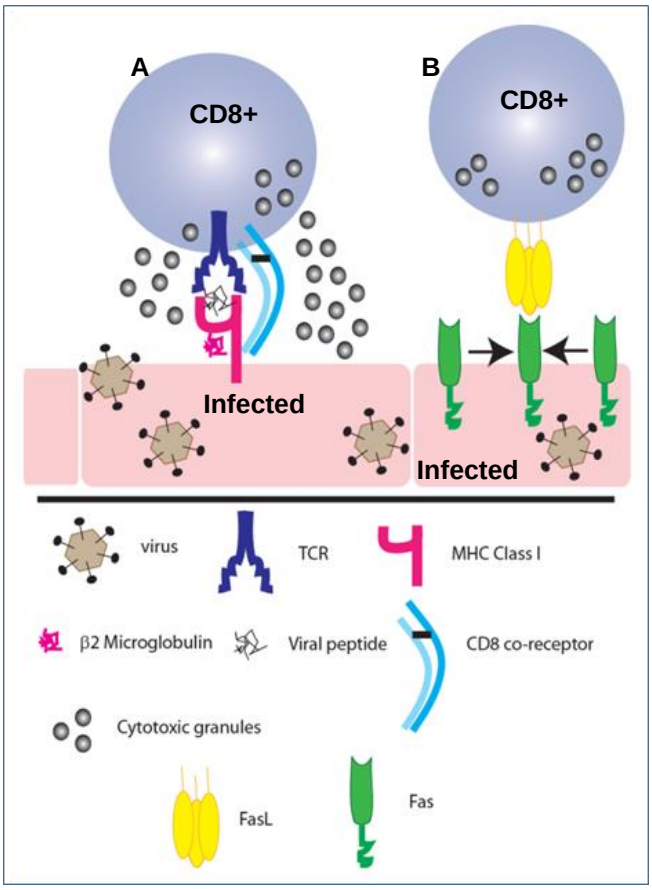

Fig 1.4 T cell and antigen presenting cell interactions

1.3.4 Memory formation of CD8+ T cells

The CD8+ T cell response is generally characterized into three different phases. In the initial phase, CD8+ T cells become activated, expand, and gain effector functions, which contributes significantly to the elimination of virus-infected cells (120). This is followed by the contraction phase, which leads to a reduction in the number of CD8+ T cells. The remaining CD8+ T cells become memory CD8+ T cells and thus reach the third phase, in which an immunological memory is established (Figure 1.5A). Two to three weeks after the CD8+ T cell expansion has reached its maximum, the majority (90 to 95%) of the activated effector CD8+ T cells die due to apoptosis (133). The remaining antigen-specific CD8+ T cells remain as a reservoir of long-lived memory CD8 + T cells (Figure 1.5 B). However, memory CD8+ T cells differ from effector CD8 + T cells, both in their phenotype and function and gene expression (120). Thus, 5 to 10% of effector CD8+ T cells express high levels of CD127, the α-chain of the IL-7 receptor. Precisely these CD8+ T cells preferentially survive the infection and later transform to memory CD8+ T cells (134). In contrast, in this phase of memory formation effector CD8+ T cells, which express only low levels of CD127, disappear. In addition, CD8+ T cells down-regulate CD62 ligand (CD62L) during the effector phase. CD62L is a member of the selectin family and is normally expressed by many lymphocytes. Its function is important for cell adhesion. When immune cells are activated, selectin is downregulated, thus enabling its mobility. Once memory CD8+ T cells have developed, CD62L is upregulated again and allows localization in central lymphoid organs (120).

The establishment of an immunological memory allows a rapid reactivation of virus-specific T cells with effective immune defense in a second infection with the same virus.

1.3.5 Dysfunctional CD8+ T cells in chronic viral infections

During chronic viral infections, the functions of CD8+ T cells may be severely impaired. They first lose their effector functions, e.g. the ability to secrete cytokines (initially IL-2 followed by TNF-α) (135). Dysfunctional CD8+ T cells are also characterized by the increased expression of inhibitory receptors whose normal function is to control auto reactivity or excess immune responses and associated pathological damage. Although inhibitory receptors are also expressed by CD8 + T cells during the effector phase, the increased and long-lasting expression of these receptors is a hallmark of dysfunctional CD8+ T cells during chronic infection (136). The inhibitory signaling pathway regulated by the PD-1 (Programmed cell death-1) receptor and

binding of its ligands PD-1 ligand (PD-L1) and PD-L2 may inhibit the cytotoxic functions of CD8+ T cells (137). In addition, there are other inhibitory molecules, e.g. CTLA-4 (cytotoxic T lymphocyte antigen 4), which can be expressed by T cells. CTLA-4 is a homologue to CD28 and, because it has a higher affinity, binds preferentially to CD80 or CD86, thus preventing the ongoing co-stimulation and activation of CD8+ T cells (138).

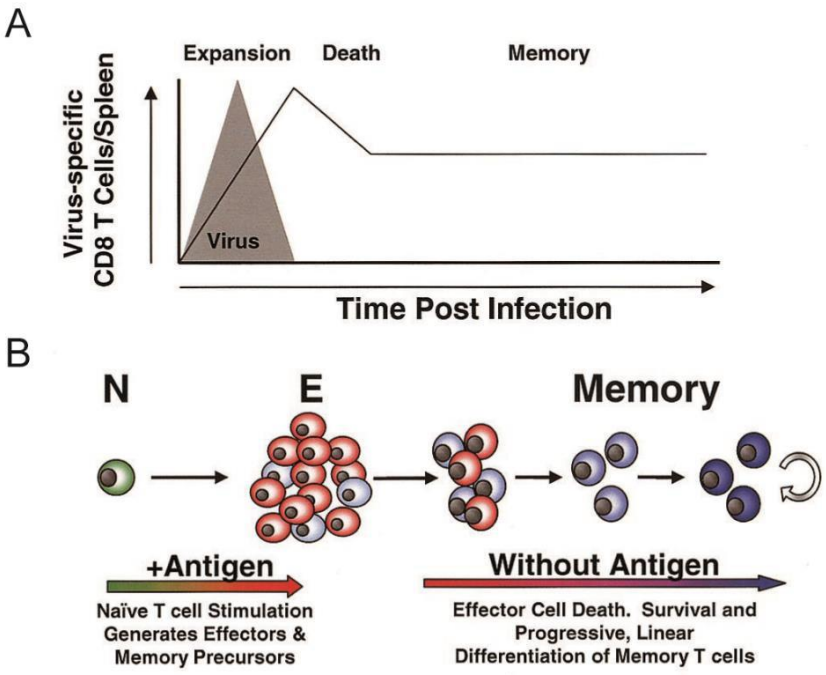

Fig. 1.5 The dynamics of a CD8+ T cell response during acute virus infection.

(A) CD8+ T cells response to an acute viral infection undergoes an expansion phase, culminating in the generation of effector CD8 T cells and viral clearance. The expansion phase is followed by a death phase, when 90 to 95% of the effector T cells die. The surviving 5 to 10% of the effector CD8 T-cell pool further differentiates and generates a memory T-cell population that is maintained long term in the absence of the antigens. **(B)** Memory CD8 T-cell generation is linear and progressive. The effector T cells that survive the death phase further differentiate, giving rise to memory T cells that continue to differentiate in the absence of the antigens and acquire the ability to persist in the absence of the antigens via homeostatic turnover (Fig. adapted from (120)).

Tim-3 (T cell immunoglobulin mucin 3) is commonly expressed on TH1 cells and some CD8+ T cells and acts as a negative regulator capable of inducing its own apoptosis. Tim-3 is also up-regulated by CD8+ T cells during the chronic phase and is a hallmark of dysfunction (139, 140).

1.3.6 Checkpoint inhibitors

PD-1 belongs to the immunoglobulin superfamily (IgSF) of surface proteins and is composed of ~20 amino acids stalk region, a transmembrane domain and intracellular domain containing both ITIM and ITSM, and exerts its inhibitory effect by recruitment of SHP-1 and SHP-2 molecules (137). The expression of PD-1 is distributed on activated T cells, B cells, DCs, NKT, and monocytes. The ligands of PD-1 are PD-L1 and PD-L2. **PD-L1** is widely expressed on hematopoietic and non-hematopoietic cells, whereas **PD-L2** is widely expressed on APCs. PD-1 ligation hinders by the activation of cell survival factors and the expression of transcription factors like T-bet, GATA-3 and Eomes. It also inhibits the cell cycle progression and proliferation of T cells. Blockage of PD-1/PD-L1 pathway during acute LCMV infection restores the functionality, proliferation of T cells (141, 142).

BTLA (CD272) belongs to IgSF and possesses an intracellular motif similar to PD-1 which exerts its inhibitory effect by the recruitment of SHP-1 and SHP-2 molecules. BTLA is expressed on T cells, B cells, DCs and myeloid cells (137). **CD160** does not belong to the IgSF and is a glycoylphosphatidylinosital (GPI)-anchored receptor, inhibiting T cell activation by reducing phosphorylation of CD3ξ. However, its inhibitory mechanisms remain elusive. CD160 is expressed on T cells and NK cells. Both BTLA and CD160 bind to **HVEM (CD270)**, which belongs to TNFR super family 14. HVEM is expressed on naïve T cells, B cells, DCs, NK cells, and myeloid cells. BTLA and CD160 ligation to HVEM results in an inhibitory effect. Therapies targeting HVEM to block BTLA and CD160 binding are being developed to enhance immune responses and vaccination (reviewed in (143)).

CTLA-4 contains YxxM motif and exerts its inhibitory effect by the recruitment of SHP-2 and PI3K. CTLA-4 is expressed by activated T cells. CD80 and CD86 are the ligands which bind to CTLA-4. **CD80/CD86** are expressed on B cells, monocytes, DCs, and T cells. Multiple models have shown the influence of CTLA-4 during TCR signaling. These include the competitive antagonism of CD28 and inhibition of lipid raft and microcluster formation. Blockade of CTLA-4 is associated with autoimmune and immunopathology (144).

Lag3 also belongs to IgSF and possess the KIEELE motif by which it inhibits the expansion of T cells. Lag3 is expressed on T cells, B cells and NK cells. Lag3 binds to **MHC II**, which is expressed on DCs, macrophages, B cells, monocytes, and thymic epithelial cells. Lag3 plays a crucial role in modulating DCs function and promoting the suppressive effect of Tregs. Blockage of Lag3 results in an enhanced number of memory CD4 and CD8 T cells in mice infected with the Sendai virus, and T cell expansion in the gamma herpes virus model (145).

Tim-3 is a type I glycoprotein receptor and possess Y235 and Y242 motif. Although Tim3 does not contain ITIM and ITSM, it possesses intracellular tyrosine kinase phosphorylation motifs. It exerts its inhibitory effect by recruiting Lck, Fyn, p85 PI3K, and Bat3 molecules (146). Tim3 is expressed on T cells, B cells, NK cells, NKT cells, DCs and macrophages. Tim3 binds to 4 different ligands. These are the carcinoembryonic antigen cell adhesion molecule 1 (**Caecam-1**), **Galectin-9**, **Phosphatidylserine** (PtdSr), and the high mobility group protein B1 (**HMGB1**) (147). The ligands are mainly expressed on T cells, DCs, macrophages, eosinophils, and endothelial cells. Blockage of Tim3/Galectin-9 during autoimmune and chronic inflammatory disease restored the effector function of T cells (148).

2B4 has originally been identified on mouse NK cells and subsets of cytotoxic T cells (149-151). CD48 (17D6, 5-8A10, 6.28, BCM1, BLAST, B-LAST-1, HM48-1, Ly-m3, MEM-102) is the ligand which interacts with 2B4 and regulates T cell activation (152, 153). **CD48** is expressed on the surface of B and T lymphocytes, NK cells, DCs, monocytes, neutrophils, mast cells, eosinophils, and endothelial cells. Taken together, T cells start to upregulate inhibitory receptors after they become activated. The ligands for these inhibitory receptors are broadly expressed in different tissues and on several cell types. Inflammatory cytokines like IFN-γ, IL-2 and TNF-α enhance the expression of inhibitory ligands on cells in inflamed tissues (154-157). Thus, inhibitory ligands can control the proliferation and cytotoxicity of activated lymphocytes and prevent the collateral damage of inflamed tissues and organs caused by overshooting immune responses.

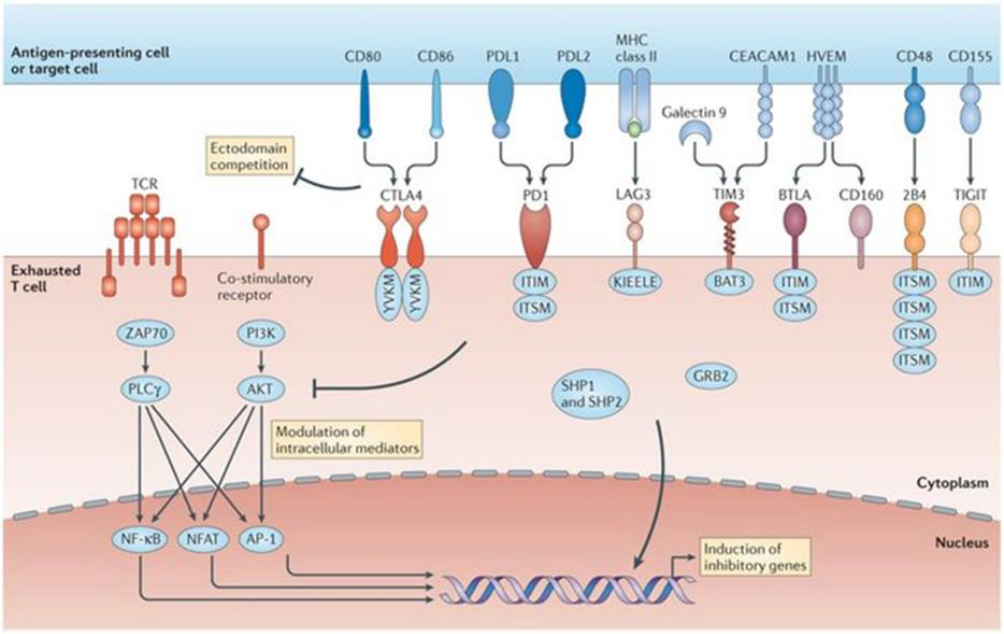

Fig 1.6 Molecular pathways of inhibitory receptors associated with T cell exhaustion. Ligand and receptor pairs for inhibitory pathways are depicted, showing the intracellular domains of receptors that contribute to T cell exhaustion. (158).

1.3.7 Regulatory T cells

Regulatory T cells belong to the subset of CD4+ T cells and play an important role in suppressing the proliferation and function of effector T cells (159). Like other T cells, Tregs mature in the thymus. Tregs generally express CD25, which is the receptor of IL-2 and transcriptional repressor of forkhead box protein 3 (Foxp3), the transcription factor of these CD4+ T cells (160, 161).

There are two subsets of CD4+ Tregs, They differ in their developmental origin, specificity, mechanisms and dependence on TCR and co-stimulatory signaling. They are classified as natural Tregs (nTreg) or induced Tregs (iTreg). nTregs are characterized by their selective surface expression of Neuropilin-1 (Nrp-1) (162, 163). Tregs that arise in the periphery are called induced Tregs (iTregs). This cell population is generated from naïve CD25+ or CD25- T cells in the periphery upon antigen presentation by semi-mature DCs and under the influence of IL-10, transforming growth factor β (TGF-β) and possibly IFN-α (164, 165).

There are different suppressive mechanisms which are utilized by Tregs. Tregs can secrete inhibitory cytokines, such as IL-10, TGF-β, and IL-35, and apply these soluble factors as a main

mechanism of suppression. Metabolic disruption by Tregs includes by high- affinity CD25 dependent IL-2 cytokine-deprivation-mediated apoptosis, cyclic adenosine monophosphate (cAMP)-mediated inhibition, and CD39 and/or CD73 generated, adenosine receptor 2A (A2AR) mediated immunosuppression (167, 168). Another mechanism is to target DCs and include the modulation of maturation and function of DCs through the lymphocyte-activation gene 3 (Lag3)–MHC-class-II-mediated suppression of DC maturation, and CTLA4–CD80/CD86-mediated induction of indoleamine 2,3- dioxygenase (IDO) (169-173).

Aims and scope of the work

Subpopulations of myeloid cells are key players in the regulation of cellular immune responses. During retroviral infection, cytotoxic virus-specific CD8+ T Lymphocytes (CTLs) efficiently control acute virus infections but become exhausted or dysfunctional during chronic phase of infection. The signaling from checkpoint receptors expressed on the surface of CTLs provide the inhibition and induce the dysfunctionality and apoptosis of these effector cells. The subpopulations of myeloid cells are the targets for retroviruses and able to express different ligand for checkpoint receptors. The first aim of these study was to define which subpopulations of myeloid cells are the targets for replication of acute Friend virus (FV) and perform the detailed characterization of inhibitory ligands expressed on infected and non-infected myeloid subpopulations. Simultaneously the expression of receptors for these ligands on virus-specific CD8+ T cells will be necessary to characterize.

Additionally to checkpoint receptors/ligands the regulatory T cells (Tregs) and myeloid-derived suppressor cells (MDSCs) play an important role in the regulation of CTL responses during acute and chronic retroviral infections. The second aim of this study was to define the contribution of all these mechanisms for the regulation of CTLs. In order to address this question, the selective elimination of MDSCs or Tregs individually or in combination with the blocking of checkpoint receptors will be necessarily performed during acute FV infection. Expansion and the functionality of CTLs and the interplay between MDSC, Tregs and inhibitory receptors and their ligands are the necessary estimate in these experiments. Simultaneous depletion of different inhibitory mechanisms will allow us to gain deep insight into mechanisms of immunoregulation and find the new approaches for restoration of dysfunctional T cells.

2 Materials

2.1 Laboratory animals

2.1.1 Wild-type mice

C57BL/6 (B6)	Resistance genotype H-2b/b, Fv1b/b, Fv2r/r, Rfv3r/r Harlan Winkelmann GmbH, Borchen, Germany

2.1.2 Congenic and Transgenic mice

TCRtg CD8 TCR transgenic mice	The D^bGagL TCR Tg (T cell receptor transgenic) mice were specific for the D^bGagL FV epitope. Mice were maintained at the animal facilities in the University Hospital Essen, Germany
DEREG mice	Generated by Dr. Tim Sparwasser's group (Institut für Infektionsimmunologie, Twincore, Zentrum für Experimentelle und Klinische Infektionsforschung, Hannover, Germany) and maintained at the animal facilities of University Hospital Essen. DEREG (depletion of regulatory T cell) mice were generated from bacterial artificial chromosome (BAC) technology. These mice carry a DTR-eGFP transgene under the control of an additional FoxP3 promoter. Usage of DEREG mice allows both detection and inducible depletion of $FoxP3^+$ Treg cells
PD-L1 KO	Generated by Lieping Chen (Department of Immunology, Mayo Clinic College of Medicine, Rochester, USA) and maintained at the animal facilities in the university hospital Essen, Germany. In this mice exon 1 and large

part of exon 2 of the endogenous B7-H1 allele is replaced with a Neo-resistance cassete by a gene targeting vector, which leads to deletion of the sequence encoding the signal peptide and also the majority of the extracellular IgV domain of PD-L1.

2.2 Cell lines and viruses

2.2.1 Cell lines

Mus dunni cell line which is permissive for all four classes of murine leukemia virus (MuLV) was used to determine the productivity of virus infected cells *in vitro*. *Mus dunni* were maintained in complete RPMI medium supplemented along with 10% FCS and 0.5% penicillin/streptomycin.

2.2.2 Friend virus

The FV stock used for the experiments was a FV complex containing two retroviral complexes, β-tropic Friend murine leukemia virus (F-MuLV) and the polycythemia-inducing spleen focus forming virus (SFFV). Here the F-MuLV was tagged with green fluorescent dye called m-Wasabi. The tagging of m-Wasabi enabled us to distinguish the infected and non- infected cells.

2.3 Equipment and materials

The equipment and materials used in this study are listed in Tables 2.1 and 2.2 below

Table 2.1 Equipment

Item	Manufacturer
Biofuge fresco	Heraeus, München
Centrifuge 5415 C	Eppendorf, Hamburg
CO_2 incubator	Thermo, Dreieich
Freezer	LIEBHERR, Ochsenhausen

Heating block	Granz, QBC
Infrared lamps	Philips, Amsterdam
Laminar flow	KOJAIR, Meckenheim
LSRII flow cytometer	Becton Dickinson, Heidelberg
Neubauer cell counting chamber	Becton Dickinson, Heidelberg
Reflected –light microscope CK 2	Hund, Wetzlar
Refrigerator	LIEBHERR, Ochsenhausen
Single channel pipettes (10, 20, 100, 200, 1000µl)	Eppendorf, Hamburg
Sorvall centrifuge fresco	Thermo, Dreieich

Table 2.2: Materials

Material	Manufacturer
Beakers	Schott, Mainz
Cannulae (G23; G25; G27)	Becton Dickinson, Heidelberg
Cell culture flasks (T25; T75)	Greiner bio-one, Frickenhausen
Cell culture plates, sterile (6; 24 and 96 well)	Greiner bio-one, Frickenhausen
Cell microstrainer (70µm)	Falcon BD, Heidelberg
Disposables syringes (5ml; 10ml; 25ml)	Braun, Melsungen
Erlenmeyer flask	Schott, Mainz
FACS tubes	Becton Dickinson, Heidelberg
Filters	Becton Dickinson, Heidelberg

Forceps, pointed and curved	Oehmen, Essen
Parafilm	American National Can, Chicago
Pipette boy	Hirschmann, Eberstadt
PP screw-cap tubes (15ml; 50ml)	Greiner bio-one, Frickenhausen
Reaction tubes (1.5ml; 2ml)	Eppendorf, Hamburg
Scissors, large and small	Oehmen, Essen
U-shaped microplates	Greiner bio-one, Frickenhausen

2.4 Chemicals and Medium

Unless not mentioned, the chemicals below were purchased from Applichem, Merck, Roth and Sigma.

3-amino-9-ethylcarbazole (AEC), acetic acid, ammonium chloride (NH_4Cl), autoMACS run and wash buffer (Miltenyii Biotec), β-mercaptoethanol (β-ME), bovine serum albumin (BSA), brefeldin A (BFA), dimethyl sulfoxide (DMSO), ethanol, ethylendiaminetetraacetic acid (EDTA), FACS Clean (BD Biosciences), FACS Flow (BD Biosciences), FACS Rinse (BD Biosciences), fetal calf serum (Biochrom), Ficoll (GE Healthcare), 37% formaldehyde, formalin, glucose, hydrogen peroxide (H_2O_2), incidine 8%, isopropanol, L-Glutamine, magnesium chloride ($MgCl_2$), penicillin-streptomycin (Pen-Strep), phosphate buffer saline (PBS) (Gibco), polybrene A, RPMI-1640 media (Gibco), sodium carbonate (Na_2CO_3), sodium acetate (CH_3COONa), sodium azide (NaN_3), sodium pyruvate, trypan blue, trypsin-EDTA.

2.5 Antibiotics

Penicillin / Streptomycin (Gibco)

2.6 Buffers and Medium

All buffers and solutions were prepared using double distilled water.

Table 2.3 Buffers and medium

Medium	Composition
Culture medium	500 ml RPMI 1640 (Gibco) 10% FCS (Gibco) 0.5% Penicillin/Streptomycin mixture
DC medium	500 ml RPMI 1640 (Gibco) 10% FCS (Gibco) 0.5% Penicillin/Streptomycin mixture 0.5% Sodium pyruvate 0.5% L- Glutamine 0.05% β-mercaptoethanol GM-CSF and IL-4
FACS Buffer	1000 ml PBS 0.02% Sodium azide 0.5% BSA
Freezing medium	40% FCS 10% DMSO 50% RPMI medium
MACS Buffer	1000 ml PBS 0.5% BSA 2mM EDTA

2.7 Antibodies

Anti-mouse and anti-human antibodies were purchased from eBIosciences (Invitrogen), Biolegend, BD Bioscience, Thermo fischer and RD.

2.7.1 Mouse reactive antibodies

Table 2.4 List of antibodies used for staining of mouse cells

Antibody	Fluorochrome	Clone	Company
AB720 (a-MuLV Env, Isotype IgG2b)	AF647	N/A	Invitrogen (Thermo fischer)
PD-L1 anti-mouse	BV605	10F.9G2	Biolegend
PD-L2 anti -mouse	PerCP-eFluor	122	eBiosciences
CD11b anti-mouse/human	BV605	M1/70	Biolegend
CD11c anti-mouse	BV510	N418	Biolegend
NK1.1 anti-mouse	APC/Cy7	PK136	Biolegend
CD19 anti-mouse	APC/Cy8	6D5	Biolegend
CD3 anti-mouse	APC/Cy9	17A2	Biolegend
Ter-119 anti-mouse	APC/Cy10	TER-119	Biolegend
Ly6C anti-mouse	BV421	HK1.4	Biolegend
Ly6G anti-mouse	AF700	1A8	Biolegend

CD80 anti-mouse	FITC	16-10A1	BD
Ki67 anti-mouse	PE-Cy7	SoLA15	eBiosciences
CD43 anti-mouse	FITC	1B11	Biolegend
CD8 anti-mouse	AF700	53-6.7	Biolegend
CD4 anti-mouse	BV605	RM4-5	Biolegend
F4/80 anti-mouse	PE	BM8	Biolegend
HVEM (CD270) anti-mouse	PE	LH1	Thermo Fischer Scientific
BTLA (CD272) anti-mouse	PE	6F7	eBiosciences
CD160 anti-mouse	APC	7H1	Biolegend
PD-1 anti-mouse	BV421	29F.1A12	Biolegend
Tim3 anti-mouse	APC		RD
CD80 anti-mouse	PE/Cy7	16-10A1	Biolegend
CD86 anti-mouse	BV605	GL-1	Biolegend
Lag3 (CD223) anti-mouse	PerCP/Cy5.5	C9B7W	Biolegend
GzmB anti-mouse/human	APC	GB11	invitrogen
IFN-g anti-mouse	PE/Dazzle	XMG1.2	Biolegend

IL-2 anti-mouse	PE	JES6-5H4	eBiosciences
TNF-a anti-mouse	BV510	MP6-XT22	Biolegend
CD62L anti-mouse	PE/Cy7	MEL-14	eBiosciences
CD43 anti-mouse	PerCP	1B11	Biolegend
KLRG1 anti-mouse	BV421	2F1/KLRG1	Biolegend
2B4 (CD244) anti-mouse	PE/Cy7	M2B4	Biolegend
F4/80 anti-mouse	PE/Cy7	BM8	Biolegend
MHC II anti-mouse	BV605	M5/113.15.2	Biolegend
TNF-a anti-mouse	PE/Cy7	MP6-XT22	Biolegend
PD-L1 anti-mouse	PE/Cy7	10F.9G2	Biolegend
CD69 anti-mouse	BV510	H1.2F3	Biolegend
BTLA (CD272) anti-mouse	APC	6A6	Biolegend
CD107a anti-mouse	PerCP-eFluor710	eBio1D4B	eBiosciences
MHC II anti-mouse	FITC	2G9	BD Pharmingen
CD62L anti-mouse	BV510	MEL-14	Biolegend

CD200 anti-mouse	BV421	OX-90	BD Horizon
CD160 anti-mouse	PE/Cy7	7H1	Biolegend
CD317 anti-mouse	APC	927	Biolegend

2.7.2 Human reactive antibodies

Table 2. 5 List of antibodies used for staining of human cells

Antibody	Fluorochrome	Clone	Company
CD11b anti-mouse/human	BV605	M1/70	Biolegend
CD1c anti-human	AF700	L161	Biolegend
CD4 anti-human	BV650	OKT4	Biolegend
CD3 anti-human	BV421	SK7	BD Biosciences
CD56 anti-human	BV421	NCAM16.2	BD Biosciences
CD19 anti-human	BV421	H1B19	BD Biosciences
CD20 anti-human	BV421	2H7	BD Biosciences
PD-L1 anti-human	BV605	29E.2A3	Biolegend
CD270 anti-human	APC	122	Biolegend
CD14 anti-human	BV510	M5E2	Biolegend
CD16 anti-human	PE/Dazzle	3G8	Biolegend

2.8 Fluorochromes

The antibody-coupled fluorochromes and their absorption and emission

Table 2.6 Characteristics of fluorochromes

Fluorophore	Abbreviation	Absorption(nm)	Emission (nm)
Alexa fluor 488	AF488	488	519
Alexa fluor 647	AF647	650	647
Alexa fluor 700	AF700	633	723
Allophycocyanin	APC	633	660

APC-Cyanine7	APC/Cy7	650	774
Brilliant violet 421	BV421	407	421
Brilliant violet 521	BV510	405	510
Brilliant violet 605	BV605	405	605
Brilliant violet 650	BV650	407	650
Brillint ultraviolet 395	BUV395	348	395
eFluor 650	eF650	407	650
eFluor 780	eF780	633	780
eFluor 450	eF450	405	450
Fluorescein isothiocyanate	FITC	488	518
mWasabi	wasabi	493	509
PE-cyanine5	PE-Cy5	660	670
Peridinin-chlorophyll-protein complex	PerCP	488	675
Phycoerythrin	PE	488	575
Phycoerythrin-Cy7	PE-Cy7	488	785

2.9 MHC tetramer and F-MulV specific peptide

2.9.1 MHC I tetramer

PE labelled MHC class-I H-2Db tetramer loaded with the peptide AbuAbuLAbuLTVFL (DbGagL tetramer, FV gag CD8+ epitope gPr80gag85-93) recognized by DbGagL specific CD8+ T cells. The MHC class-I tetramer was purchased from MBL International Corporation (Woburn, MA, USA).

2.9.2 CD8 peptide

The F-MuLV CD8+ T cell peptide was synthesized by Pan Tecs (Tübingen, Germany) and reconstituted in 100% sterile DMSO. Peptide name: FMR-H-2DbGagL CD8 epitope. Sequence: AbuAbuLAbuLTVFL.

2.10 Staining reagents

Table 2.7 Staining reagents

Staining reagent	Manufacturer
FVD eF780	eBioscience
CFSE	Invitrogen
Violet tracer	Invitrogen

2.11 Standard kits

Table 2.8 Standard kits

Kit	Manufacturer
Cytofix/cytoperm intracellular staining kit	BD Pharmingen, Heidelberg, Germany
FoxP3 staining set	eBiosceinces, San Diego, USA
Mouse CD8a (Ly-2) isolation kit	Miltenyi Biotec, Bergisch Gladbach, Germany
Myeloid derived suppressor cell isolation kit (mouse)	Miltenyi Biotec, Bergisch Gladbach, Germany

2.12 Depletion antibodies

CD270-CD272 blocking	Anti- CD270 antibody, Clone 6C9/2E10/2B8, rat IgG2a, 0.90 mg/ml (received from collaborator)
CD270-CD160 blocking	Anti- CD160 antibody, Clone 6E7a/1C4, mIgG1, 1mg/ml (received from collaborator)
***InVivo*MAb polyclonal mouse IgG**	IgG antibody, Clone N/A, purchased from BioXcell
***InVivo*MAb a-PD-L1**	PD-L1 antibody, Clone 10F.9G2 purchased from BioXcell
Diphtheria Toxin (DT)	Diptheria toxin, Corynebacterium diphtheria – calbiochem, purchased from Merck
***InVivo*MAb a-Tim3**	Tim3 antibody, Clone RMT3-23 purchased from BioXcell
***InVivo*MAb a-Ly6G**	Ly6G antibody, clone 18A, purchased from BioXcell

3. Methodology

3.1 Animal trials

The animal experiments were conducted according to the guidelines of the Federation of European Laboratory Animal Science Association (FELASA).

3.2 Virus preparation and titre determination

3.2.1 Friend virus

3.2.1.1 *In vivo* production of FV

To obtain a FV stock, susceptible BALB/c mice were infected intra venous (i.v.) with 3,000 spleen focus forming units (SFFU) of FV. On 9 days post infection the mice were sacrificed and the spleens removed. A 15 % spleen homogenate was prepared in PBBS with 1 mM EDTA. The homogenate was then aliquoted and stored at -80°C until use.

3.2.1.2 Titer determination of a FV stock

Titration of a FV stock was done by infecting Y10A mice i.v. with different amounts of virus stock. The spleens were removed 14 days post infection. During the course of FV infection, malignant cell populations develop on the surface of the spleen. These foci can be visualized by incubation of the whole spleens in Boulin´s solution which enhances the visual contrast of foci on the spleen surface. SFFUs can be determined by counting these foci.

3.2.1.3 Construction of FV m-Wasabi

The construction of fluorescently labelled virus was performed by fusing mWasabi to the envelope (Env) open reading frame (ORF) in the F-MuLV. Although direct fusion to the Env R peptide did allow for viral particle formation, the construct was very unstable, and fluorescence was lost after a few passages in cell culture. However, additional introduction of a self-cleaving 2A peptide from porcine teschovirus lent stability to the construct, and fluorescence of the recombinant virus was maintained for more than 15 passages in vitro. After reconstitution of the FV complex comprising F-MuLV-mWasabi and wild-type SFFV, C57BL/6 mice were infected and bone marrow, lymph nodes, and spleens were isolated at different time points. Analysis of the viral loads by using conventional immunocytochemistry-based focal infectivity assay confirmed that the replication

kinetics of the mWasabi-labeled FV was unimpaired and indeed comparable to that of wild-type FV, with the highest virus loads observed in bone marrow and spleen samples at day 7 and low but stable virus loads in the late phase of infection. Of note, none of the mice were able to completely clear the infection, as virus was detected in all bone marrow samples on day 42, but the viral loads in the lymph nodes of half of the mice were below the detection limit at this time point, and again half of these mice also had undetectable viral loads in spleens (174).

3.2.1.4 Infection with FV

Mice were i.v. infected into the lateral tail vein using a 27G-hollow needle. For this the virus stock was thawed, centrifuged at 8000 rpm for 10 minutes and the supernatant was diluted with PBS to reach the required concentration. Usually $2x10^4$SFFU of FV in 300 were used for acute infection experiments.

3.2.2 HIV

3.2.2.1 Production of HIV

293T cells were harvested and seeded at a concentration of 1x105 cells per well of a 24-well plate. At 50 % confluence, the cells were transfected with the HIV-1 JRFL-iGFP plasmid. For transfection the following mixture was prepared with the reagents added in the order they appear in the list. The mixture was incubated for 15 min at room temperature and 50µL were then added drop by drop to each well of the 24-well plate. The cells were then incubated for the next three days at 37 °C and 5 % CO2. To harvest the virus, the supernatant was collected three days later and centrifuged at 600xg for 7 min at 4 °C to clear any cell debris. The virus containing supernatant was concentrated using Amicon Ultra 100 MW filter tubes. For this the supernatant was added to the upper chamber of the tube and centrifuged at 4000xg for 10 to 20 min at 4 °C. This step was repeated until the whole supernatant containing the virus was concentrated. The virus preparation was then aliquoted into 20 to 50µL aliquots and stored at -20 °C until use.

Table 3.1 Transfection mix for HIV-1 JRFL-iGFP virus synthesis

Reagent	Volume
DMEM serum-free	45.205µL
FUGENE ®	3.375µL
1µg HIV-1 JRF-iGFP (700ng/µL)	1.4µL
0.125 µg pAdVAntage™ vector (5836 ng/µl)	0.02µL
Final volume	50µL

3.2.2.2 Titre determination of HIV-1 JRFL-iGFP virus stock

To titrate the virus, TZM-bl cells were harvested and seeded into 12 wells of a 96-well plate at a concentration of 1x104 cells per 200µL complete DMEM. The cells were left to incubate at 37 °C and 5% CO2 until they were 50-60 % confluent. An aliquot of the frozen HIV-1 JRFL-iGFP virus stock was thawed and a 5-fold dilution series (1:5-to-1:3125) was prepared in complete DMEM with additional 2µg/mL dextran in each tube. The media was removed from the cells and replaced by 50µL of the virus dilutions. All infections were performed in duplicates. As a negative control, two wells were challenged with complete DMEM and dextran. The cells were incubated with the virus for 1 hour in the incubator and an additional 50µL of complete DMEM was added to each well followed by incubation for another two days under the same conditions. After two days the supernatant was removed and the cells were rinsed with PBS. The fixation was carried out with 2 % formaldehyde for 20 min at 4 °C followed by two washes with PBS. To stain the cells 100µL of HIV-1 titration staining solution (0.5 mg/mL X-gal, 4mM potassium ferrocyanide, 4mM potassium ferricyanide, 2mM MgCl2 in PBS) was added to each well and left to incubate for 2 hours at 37 °C and 5% CO2. To determine the virus concentration the number of blue cells were counted in each well using a light microscope. The mean number of blue cells for each virus dilution was calculated and multiplied by the dilution factor. The calculated values indicate the number of infectious viral particles per 1µL.

3.3 Intraperitoneal injection (i.p)

The *in vivo* antibodies for treatment or depletion (a-CD270, a-CD160, DT, a-Ly6G, and a-PD-L1/a-Tim-3) were administered via intraperitoneal (i.p) injection. Mice were held by the skin at the back of the neck and the tail was held back. Mice were held with the ventral side exposed and tense, therefore internal organs are not harmed by the injection. The injection was done in a 45° angle into the lower abdomen and slowly administered.

3.4 *In vivo* depletion of cell populations

To deplete gMDSCs in vivo, 100µg per mouse of a-Ly6G (Clone 1A8) antibody diluted in PBS and were administered i.p three times in every two days after a week post infection (Fig. 4.23A). Regulatory T cells were depleted using 0.5µg per mouse diphtheria toxin (DT). 1 µl/mouse of DT solution was diluted in 499 µl of PBS. DEREG mice were administered i.p with DT, treatment was started one week post FV infection and mice were treated three times every three days (Fig. 4.16A).

For blockade of the PD-1 pathway in acute FV-infected mice, 200µg rat anti-mouse PD-L1 Ab (10F.9G2; BioXCell) was administered intraperitoneally every third day for 3 times (Fig. 4.16A). To block the Tim-3 pathway, 100µg rat anti-mouse Tim-3 Ab (RMT3-23; BioXCell) was administered intraperitoneally every other day for 4 times (Fig. 4. 16A). The T cell responses and viral loads were analyzed one day post treatments or 4 days post treatments (Fig. 4.16B, C, D).

For blocking the interaction between CD270 and its inhibitory receptors CD160 and CD272. Mice were injected i.p with 300µl of a-CD270 antibodies and 300µl of a-CD160 antibodies Blocking started after a week post FV infection and mice were treated three times every second day (Fig. 4. 12A).

3.5 Sample preparation

3.5.1 Dissection of mice

Before sacrificing the mice, the mice were anesthetized with isoflurane and blood withdrawn with capillary (behind the eye). Mice were sacrificed by dislocating the cervix and were moistened with ethanol and then fixed with 23G-hollow needles and the fur was cut open carefully not to destroy any internal organs. Initially the cervical, axillary and inguinal lymph node were removed. The

peritoneal cavity was opened and the spleen was removed with tweezers and was cut loose from the fatty tissue by excising both blood vessels. To isolate the bone marrow, both hind legs were cut loose and the flesh was removed. All the organs isolated were stored in PBBS on ice until further processed.

3.5.2 Preparation of spleen cell single suspensions

Spleens were weighed initially and were grinded through a 70 µm cell strainer using the plunger of a syringe. Cells were washed through the strainer using PBBS. From the cell suspensions an aliquot was taken for cell count. Cells were centrifuged at 1200 rpm for 10 minutes and the supernatant was discarded. Based on the cell number, cells were re-suspended in an appropriate volume of PBBS buffer for further downstream application.

3.5.3 Preparation of Bone marrow

A bone marrow cell suspension was achieved by flushing the femur and tibia of each hind leg with a 23G-hollow needle with PBBS. An aliquot for counting the cells was pipetted out. The cells were subsequently centrifuged at 1200 rpm for 10 minutes and the supernatant was discarded. Based on the cell number the cells were re-suspended in an appropriate volume of buffer suitable for down-stream applications.

3.5.4 Preparation of Bone marrow derived dendritic cells

For generating mouse DCs, the bone marrow from a naïve mouse was prepared as described above and re-suspended in 50 mL mouse DC media supplemented with 1 ng/mL mouse recombinant interleukin 4 (mrIL4) and 5 ng/mL mouse recombinant granulocytes monocytes colony stimulating factor (mrGM-CSF). 10 mL of medium with cell suspension were then seeded into a 10 cm cell culture dish and incubated at 37 °C and 5 % CO2 for seven days. After 24 hours an additional 10 mL of supplemented mouse DC media was added to the culture. Five days after seeding, the cells were washed once by centrifuging the cell culture media at 1100 rpm for 6 min (these cells are non-adherent). The cells were then re-suspended in 15 mL supplemented mouse DC media and cultured for another two days. Seven days after initially seeding the bone marrow cells, the differentiated DCs could be used for other applications.

3.5.5 Cell counting

To count cells, an aliquot of the cell suspension was mixed with 0.4 % trypan blue. Dead cells are more permeable than live cells to trypan blue and these cells stain blue. An appropriate dilution

was chosen to count the cells and only live cells were counted for the determination of cell numbers. The cells were counted using either: a disposable haemocytometer, a CellometerTM Auto T4 counting chamber or a Neubauer counting chamber. The counting was performed using a light microscope (haemocytometer and Neubauer chamber) or the CellometerTM Auto T4 cell counter with the appropriate settings. The Cellometer automatically displayed the absolute cell count and dead cells were excluded. For manual cell counting the cell number was determined by counting four squares of a big 16-square field in the chamber. The absolute cell number was then calculated by multiplying the average cell count with the chamber factor ($1x10^4$), the dilution applied to the sample and the volume of the cell suspension.

3.6 Cell culture of cell lines

Adherent cells were grown in a monolayer using the appropriate culture medium. For *Mus dunni* cells normally RPMI 1640, along with 10 % FCS and 1 % Pen-Strep was used. All cells lines were maintained at 37 °C and 5 % CO^2 and checked regularly. Depending on the cell line, the cells were passaged as soon as they grew to ~95% confluence. To passage cells, the medium was discarded and cells were washed once with PBS. Trypsin-EDTA (3mL) was then added and the cells checked frequently for their morphology under a light microscope. When the cells appeared round they were carefully re-suspended in 7 mL of complete cell culture media to inhibit the trypsin. To wash the cells, they were transferred into a 50 mL tube and centrifuged at 520xg for 7 min. Cells were then counted (if required) and seeded into a fresh tissue culture flask followed by incubation at 37 °C and 5 % CO^2 until ready for use.

3.7 Infectious centre assay (IC Assay)

To detect the number of infectious centres of FV-infected cells, $2x10^4$ *Mus dunni* cells in 2 mL complete RPMI were seeded into each well of a 6-well plate. The cells were then incubated over night at 37 °C with 5 % CO2. The following day mouse cell suspensions (derived from spleen or bone marrow of FV-infected mice) were prepared, a 10-fold dilution series formed (starting with $1x10^8$ cells) and 1mL of each dilution was added to a single well of the 6-well plate. The plate was then incubated for three days under the same conditions. During this incubation period, infected cells spread the infection to the *Mus dunni* cells via cell-cell contacts. Cell division of the *Mus dunni* transfers the provirus to their daughter cells and an infected cell colony forms. To visualize the infected cell clones, the media on the *Mus dunni* cells was discarded and the cells were fixed

by overlaying them with 95 % ethanol for 15 min. The ethanol was discarded and the plates washed twice with PBS plus 0.1 % BSA. The cells were then incubated for 2 hours at room temperature or in refrigerator for overnight with 700µL of culture supernatant of an AB720 producing hybridoma cell line. AB720 antibody specifically binds to the Env-protein of F-MuLV recognizing FV-infected cells. After two hours the plates were washed twice with PBS plus 0.1 % BSA. 700µL of a 1:400 dilution (into PBS) of secondary antibody conjugated to HRP (goat-α-mouse- IgG2b-HRP (0.05mol/L)) was added to the cells for 90 min. After the incubation, the antibody was discarded and the plates were washed twice with PBS. The cells were then incubated for 20 min in the dark with 2 mL of fresh AEC substrate solution. A red precipitate is formed by conversion of the soluble substrate AEC in the substrate solution into an in-soluble precipitate catalyzed by the HRP coupled to the secondary antibody. The substrate solution was discarded and the plates were washed twice with H2O. After the plates had dried over night the red spots in each well were counted and calculated for $1x10^6$ added cells. To determine the IC count per $1x10^6$ spleen or bone marrow cells the mean off all dilutions was formed. The appearance of red dots after developing the assay indicated functionality.

3.8 Stimulation of freshly isolated mouse spleen cells for cytokine production

For the intracellular staining of cytokines (like TNFα, IFNγ and IL-2), freshly isolated mouse spleen cells were stimulated *in vitro*. The wells of a Nunc MaxiSorp 96- well plate were coated with 50µL purified αCD3 antibody (10µg/ml) in sodium carbonate coating buffer. The coating of the plate was performed for overnight at 4°C. After α-CD3 coating, the plate was washed three times with PBS. For stimulation of freshly isolated mouse cells, $1x10^7$ cells were added to each well in duplicates. The cells were re-suspended in complete RPMI medium supplemented with 50µM beta mercaptoetanol (β-ME), 2µg/ml purified α-CD28 and 2µg/ml brefeldin A (BFA) and incubated for 5 hours at 37°C. After stimulation, the cells were transferred into new wells and stained for surface molecules and intracellular cytokines. For controls, a sample was left unstimulated but stained with intracellular antibodies and a stimulated sample did not get stained with the intracellular antibodies.

3.9 Multicolor Flow cytometry

3.9.1 Principle of flow cytometry

Flow cytometry is a method to determine and characterize the physical and chemical features the particles in the suspension which pass thought a laser. Usually, for the characterization of cells in the single cell suspension, cells were previously stained with antibodies conjugated with fluorochrome. By excitation with light of a specific wavelength, the electrons in the fluorochrome are shifted to a higher energy level. When they fall back, energy is released as photons with a specific wavelength. The optic system of flow cytometers is composed of lasers of different wavelengths, mirrors and filters (Fig. 3.1). Cells in a heterogeneous single-cell suspension pass a laser beam through a nozzle in a stream of sheath fluid. Passing cells scatter the light of the laser. A forward scatter (FSC) detector detects the scatter in the axis of the light, measuring the size of the cell. A side scatter (SSC) detector detects the light which is scattered in a 90° angle to the light axis and measures the cell granularity. Antibodies coupled to a fluorochrome target intracellular proteins or proteins on the cell surface and the intensity of the every fluorochrome excitation can be measured by flow cytometer.

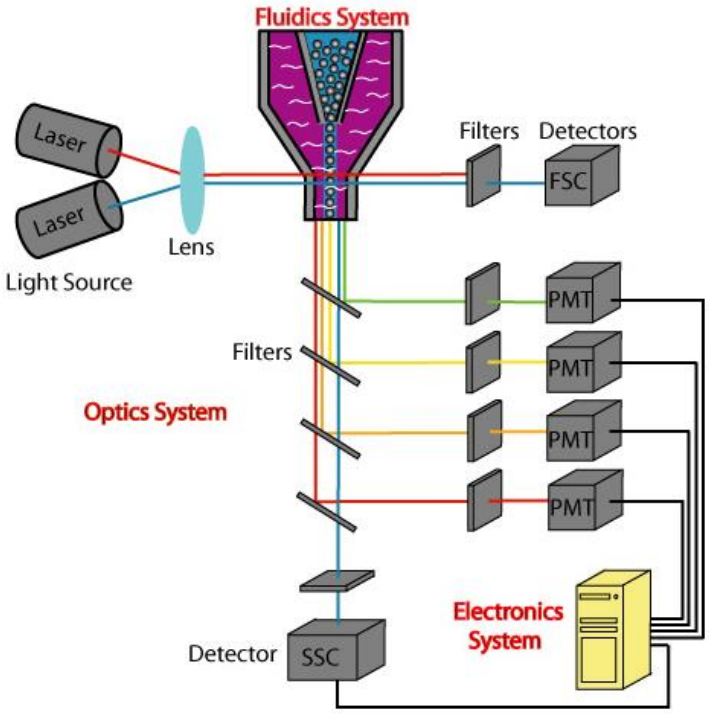

Figure 3.1 Schematic overview of a typical flow cytometer setup

Two lasers send light through the sample. The light emitted by the sample is then isolated by different filters and sent to the different PMT detectors. The PMT detectors transform and enhance the optional signal into an electric signal, which can then be visualized in the analysis software on a computer. (Adapted from www.flowjo.com)

These properties can be used to distinguish different cell populations. The emitted light passes certain filters and mirrors. Sensors detect light only of a specific wavelength. Thus, cells provide signals for certain detectors, depending on the fluorochrome bound to the antibody. The emitted fluorescence allows the characterization of individual cell populations by means of the protein/marker expression. After measurement, cells can be displayed in dot plot diagrams reflecting the intensity of fluorescent signals received by the detectors. Gates can be set in the diagram including the cells of interest for the characterization of certain cell populations due to size, granularity or fluorescent properties.

3.9.2 Staining of mouse cells for flow cytometry

For flow cytometry cell staining of mouse cells usually 3-7x10^6 cells per sample of freshly isolated mouse cells were transferred into a well of a 96-well U-bottom plate and washed with the additional 150µl FACS buffer at 1400rpm for 4 min at 4 °C. The supernatant was discarded by flicking the plate.

3.9.2.1 Cell surface staining

In case of staining of myeloid cells FC blocker was added to prevent the unspecific binding of antibodies. In prior to performing the surface staining, cells were re-suspended in 50µl FC block diluted in FACS buffer and incubated in dark for 15 min at room temperature (RT). After incubation time an antibody mix was prepared in 50µl FACS buffer and added to the cells. The cells were re-suspended in the antibody mix and incubated for 15 min at room temperature or 20 min at 4 °C. After incubation, the cells were washed by addition of 150µl FACS buffer per well and centrifuged at 1400rpm for 4 min. The cells were then either re-suspended in FACS buffer for further processing or directly transferred into FACS tubes for measurement on the LSRII or fixed as described below.

3.9.2.2 Fixation and permeabilization for intracellular staining

Depending on the localization of intracellular antigens different protocols of cell fixation and permeabilization were performed. Cells were either fixed with Cytofix/Cytoperm (BD Biosciences) if only cytoplasmic molecules were to be detected or with Foxp3 staining kit (Invitrogen (by Thermo Fischer Scientific)) for the detection of cytoplasmic and nuclear antigens. For the detection of cytoplasmic antigens cell were re-suspended in 100µL fixing buffer of Cytofix/Cytoperm kit and incubated for 10 minutes at room temperature. Next the cells were washed with addition of 100µLCytofix/Cytoperm wash buffer and centrifuged at 1200rpm for 3 min and proceeded for intracellular staining's.

If nuclear molecules were to be stained, the Foxp3 staining kit was used. The cells were re-suspended in 100µL Foxp3 Fix/Perm fixing solution which was prepared according to the manufacturer's instructions (1:4 of Foxp3 Fix/Perm concentrate into diluent). The cells were left to fix for 2 to 4 hours or overnight at 4 °C. To stop the reaction 100µL of Foxp3 Fix/Perm wash buffer was added to each well and the cells were centrifuged at 1200rpm for 3 minutes at RT. The

cells were then subsequently washed with the addition of 150µl of FACS buffer and centrifuged at 1200rpm for 3 minutes at RT. Subsequently the cells were resuspended in FACS buffer for this application and acquired immediately on the LSRII.

3.9.2.3 Intracellular and intranuclear staining

For intracellular and intranuclear staining, an antibody mix was prepared in 50µl of either Cytofix/Cytoperm wash buffer or Fix/Perm wash buffer (Foxp3 staining set). The cells were re-suspended in the antibody mix and stained for 30 min at 4 °C and, after addition of 100µl of the appropriate buffer, centrifuged at 1200rpm for 3 minutes. The cells were re-suspended in 150 µl of FACS buffer and washed and later transferred into 200 µl of FACS tubes for acquisition on the LSRII.

3.9.2.4 Live dead staining

The exclusion of dead cells and cellular debris in flow cytometry was performed using the dye propidium iodide (PI) or fixable viability dye (FVD). In healthy cells, the cell membrane prevents access of PI to DNA. However, in damaged, apoptotic or dead cells, the membrane is not intact and unable to play its preventing function, allowing rapid PI access into the cell nucleus and DNA with which it interacts. This dye is useful for the DNA analysis and the dead cell exclusion during flow cytometric analysis. 0.5µl of PI was added to the stained cells in 300µl FACS buffer to the sample and immediately acquired.

Discrimination of dead cells in intracellular staining was performed with help of Fixable Viability Dye (FVD). FVD is a viability dye that can be used to label dead cells prior to fixation and/or permeabilization procedures. FVD stain is based on the reaction of a fluorescent reactive dye with cellular proteins (amines). These dyes cannot penetrate live cell membranes, so only cell surface proteins are available to react with the dye, resulting in dim staining. The reactive dye can infuse the damaged membranes of dead cells and stain both the interior and exterior amines, resulting more intense staining. FVD eF780 was added in amount of 1µl per 1 mL of cells together with the surface staining antibodies.

3.9.2.5 Tetramer class I staining

For the detection of Db-GagL-specific CD8+ T cells, spleen cells were stained with PE labelled MHC class I H2-Db (Beckman Coulter, Marseille, France) tetramers specific for FV GagL peptide (Chen et al., 1996; Schepers et al., 2002) as described previously (Zelinskyy et al., 2009).

3.9.3 Staining of human PBMCs

Human PBMCs were thawed and stimulated with PHA (1µg/ml) and IL-2 (10ng/ml) at 37°c and 5 % CO2 for two days. After two days cells were washed and cell count was performed. To infect the cells an MOI of 0.005 wild type HIV-1 virus stock was used. Infected cells were resuspended into wells and then transferred to FACS tube. The cells were centrifuged at 1500 rpm for 5 minutes, and supernatant were discarded. The pellets were resuspended into 100µl of antibody mixture and incubated at room temperature for 10 minutes. 300µl of FACS buffer was added to the tube with cells and antibody mixture and spun for 5 minutes at 1500 rpm. Supernatant were discarded and to the tubes 150µl of Biolegends Fix perm was added and incubated at RT for 20 minutes. Cells were washed for 5 minutes at 1500 rpm with 300µl of Biolegend Permwash buffer and supernatants were discarded afterwards. Antibody solution for intracellular staining was added to the cells and incubated at room temperature for 30 minutes. After incubation the cells were washed thrice with 300µl of Biolegend permwash buffer for 5 minutes at 1500 rpm and supernatant was discarded. Later the cells were resuspended into 150µl of FACS buffer. Finally the cells were resuspended in 100µl of 4% paraformaldehyde and incubated at least for 2hr at RT and the cells were ready to be acquired.

3.10 Statistical analysis

Statistics comparing the two groups were done using the unpaired non-parametric t-test or Mann-Whitney t-test. When more than two groups were compared, a one-way ANOVA was used with a Tukey post-test. (GraphPad Prism software; GraphPad Software Inc., San Diego, USA).

4. Results

Previous studies have shown that the expression of PD-L1 was increased on myeloid cells (Gr1+) during the acute phase of FV (175). Myeloid cells are composed of different subpopulations, and apart from PD-L1 there are other inhibitory ligands expressed on the surface of myeloid cells. The main aim of this study was to determine which myeloid subpopulations are the targets of FV infection and how infection changes the expression of different inhibitory ligands as well as functional properties of myeloid subpopulations.

4.1 Characterization of myeloid cells during acute FV infection

Myeloid cells originate from hematopoietic stem cells in the bone marrow and are comprised of functionally and morphologically different cell populations. Granulocytes and monocytes are the most abundant populations of cells in the spleen. The monocytes further differentiate into macrophages and myeloid dendritic cells (mDCs). For the following phenotypic and functional analysis it was necessary to differentiate each of these myeloid subpopulations from other non-myeloid cells in spleens of infected animals. A combination of conjugated antibodies was designed for the determination of subpopulations of myeloid cells by multicolor flow cytometry (176, 177). The definition of myeloid subpopulations was performed using the following steps of FACS gating. Initially the whole leucocytes were separated from erythrocytes and debris (Fig. 4.1A). Clumps were removed by gating on single cells (singlets) (Fig. 4.1B). Later, myeloid subpopulations (CD11b+) were separated from non-myeloid and dead cells. For the exclusion of non-myeloid cells the lineage markers of T cells (CD3), B cells (CD19), NK cells (NK1.1) and erythroblasts (Ter119) were used (Fig. 4.1C). Myeloid CD11b+ cells were further divided into granulocytes (CD11b+Ly6G^{high}Ly6C^{low}) and monocytes (CD11b+Ly6C^{high}Ly6G^{low}) (Fig. 4.1D). CD11b+ cells, which were double negative for Ly6G and Ly6C but expressed CD11c, were defined as myeloid dendritic cells (mDCs) (CD11b+CD11c+Ly6G-Ly6C) and as macrophages (CD11b+F4/80+CD11c-Ly6G-Ly6C-) accordingly to their expression of F4/80 (Fig. 4.1E).

Mice were infected with FV for 6, 8, 10, or 12 days and splenocytes were isolated to perform a kinetic analysis of FV infection in myeloid cells. Using flow cytometry, enumeration of the different myeloid subpopulations was done. A decline in the number of granulocytes was seen on 10 and 12 days after infection, but this was not statistically significant in comparison to naïve mice (day 0) (Fig. 4.2 A). A statistically significant decrease in the frequencies of monocytes (Fig. 4.2B)

was observed on day 8, 10, and 12 after infection in comparison to naïve mice. A significant drop in the frequencies of macrophages was also seen on 10 and 12 days after infection in comparison to the naïve mice (Fig. 4.2C). Frequencies of mDCs showed a statistically significant decline on 6, 8, 10, and 12 days after FV infection in comparison to the naïve animals (Fig. 4.2D). The data suggests that FV infection resulted in a reduction of all subpopulations of myeloid cells at day 10 and 12 after infection.

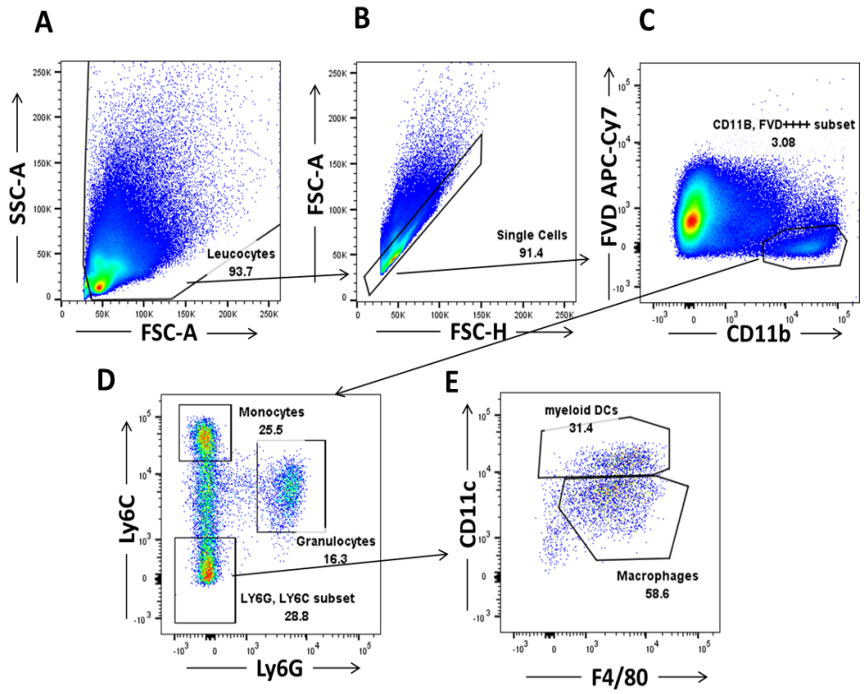

Figure 4.1 Gating strategy for the definition of myeloid subpopulations

Multi-parameter flow cytometry analysis was used to determine the myeloid subpopulations in a mouse spleen. Dot plots of a representative mouse are shown for the gating strategy to define the main myeloid subpopulations. The gating of whole leucocytes (FSC/SSC) (A), singlets (FSC-H/FSC-A) (B), and CD11b-positive/ lineage negative cells (CD3, CD19, NK1.1, and Ter119) was performed for detection of live myeloid cells (C). Myeloid CD11b positive cells were divided into granulocytes ($Ly6G^{high}$ $Ly6C^{low}$) and monocytes ($Ly6C^{high}$ $Ly6G^{low}$) (D). The population of Ly6C-Ly6G- cells was defined as mDC ($CD11c^{high}F4/80^{low}$) and macrophages ($F4/80^{high}$ $CD11c^{low}$) (E).

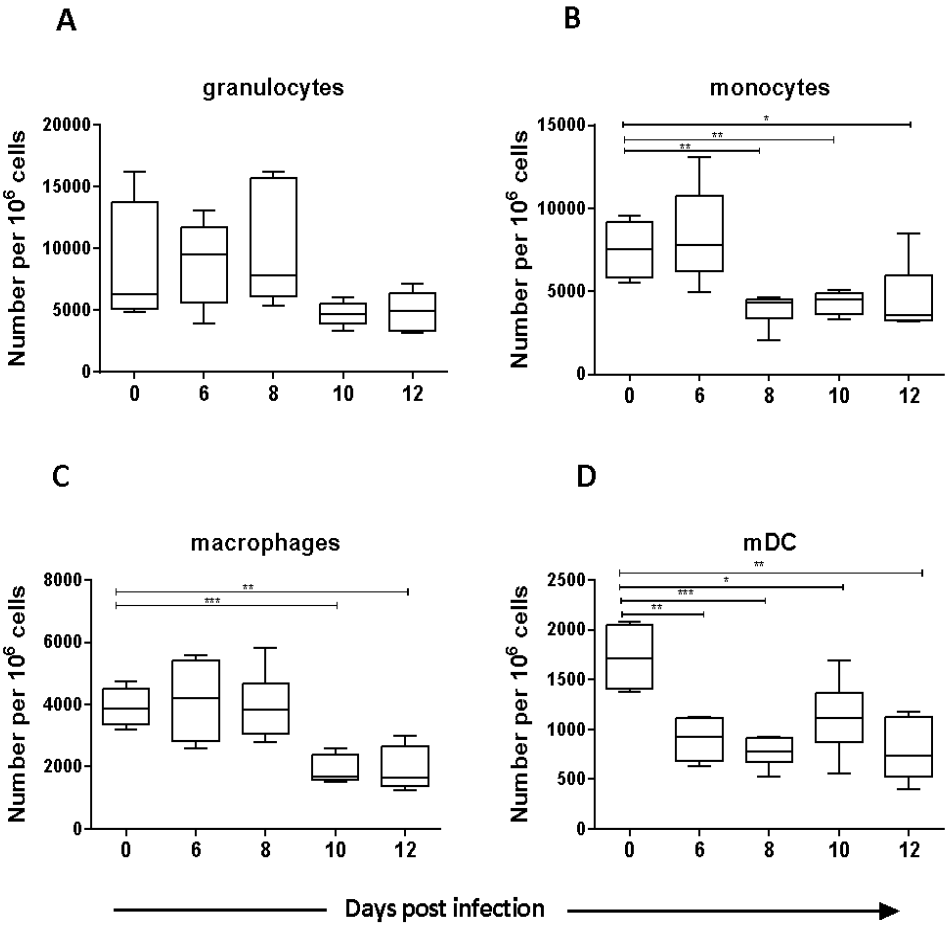

Figure 4.2 Frequencies of myeloid subpopulations during acute FV infection in the spleen

C57BL/6 mice were infected with FV and splenocytes were isolated at different time points after infection. Multi-parameter flow cytometry analysis was used to determine the numbers of different myeloid subpopulations. Frequencies of granulocytes (CD11b+ Ly6G^{high} Ly6C^{low}) (A), monocytes (CD11b+ Ly6C^{high} Ly6G^{low}) (B), macrophages (CD11b+ Ly6G^{low} Ly6C ^{low} F4/80+ CD11c^{low}) (C), and mDC (CD11b+ Ly6G^{low} Ly6C ^{low} F4/80^{low} CD11c+) (D) per one million of nucleated cells in the spleen at different time points after infection were calculated. Each bar represents the mean number plus SEM per one million nucleated cells for a group of 5 - 9 mice. Data were pooled from three independent experiments with similar results. Differences between naïve (day 0) and 6, 8, 10, and 12 days infected mice were analyzed using one-way ANOVA with a Tukey post-test (*$p<0.05$, **$p<0.005$, ***$p<0.0005$, ****$p<0.0001$).

Our next step was to comprehend which myeloid subpopulation serves as target for virus infection. In order to determine the cells with replicating FV, mice were infected with FV encoding m-Wasabi, which is a green fluorescent dye. Cells which expressed m-Wasabi were defined as FV infected and the remnant as non-infected. For the characterization of infection of myeloid cells, the numbers of m-Wasabi expressing cells per one million spleen cells were determined. Also percentages of infected cells for each myeloid subpopulation are shown. High frequencies of infected cells were observed for granulocytes (Fig. 4.3A) and monocytes (Fig. 4.3C) on 6 days post infection, whereas a strong reduction in infected granulocytes and monocytes number was observed on 10 and 12 days post infection. Similar results were obtained for percentages of infected cells, with infected granulocytes (Fig. 4.3B) reaching 4.36% on day 6 and 2.68% on day 8 post infection, but dropped on 10 (0.42%) and 12 (0.19%) days post infection. Also monocytes (Fig. 4.3D) had higher infection rates on 6 (5.19%), and 8 (4.07%) days post infection, with a drop on 10 (0.88%) and 12 (0.29%) days post infection. The frequency of infected macrophages and mDCs showed similar kinetics, however the total numbers (Fig. 4.3E and 4.3G) and percentages (Fig. 4.3F and 4.3H) of infected cells were much lower than for granulocytes or monocytes. Considering the frequencies of infected cells in the spleen, granulocytes and monocytes were the main reservoir of FV in the myeloid subpopulations during the acute phase of infection.

To determine the expression of different inhibitory ligands on FV infected myeloid cells during the acute phase of FV infection, a kinetic analysis of the mean fluorescent intensity of PD-L1, PD-L2, CD270 (HVEM), CD80, CD86, CD200, and CD48 on infected and non-infected myeloid cells was performed. The expressions of inhibitory ligands on the surface of infected myeloid cells (m-Wasabi+) were compared with the expressions of the same ligand on the non-infected myeloid subpopulation (m-Wasabi-) and both infected and non-infected cells were compared with the same subpopulation of myeloid cells from naïve mice (day 0). PD-L1 is one of the two ligands for PD-1 and plays crucial role in regulating T cell activation and tolerance (157). The expression of PD-L1 on infected granulocytes was significantly increased on 10 (MFI 4150) and 12 (MFI 3299) days after infection, whereas no such differences were observed on 6 and 8 days after infection in comparison to the expression of PD-L1 on granulocytes from naïve mice (MFI 1718). The expression of PD-L1 on infected granulocytes was also significantly enhanced when compared to non-infected granulocytes from infected mice on 10 (MFI 1495) and 12 (MFI 1030) days post infection, but not on 6 and 8 days post infection. No differences were observed between the

granulocytes from naïve mice and non-infected granulocytes from infected mice on 6 (MFI 1414), 8 (MFI 1684), 10 (MFI 1495) and 12 (MFI 1030) days after infection (Fig. 4.4A).

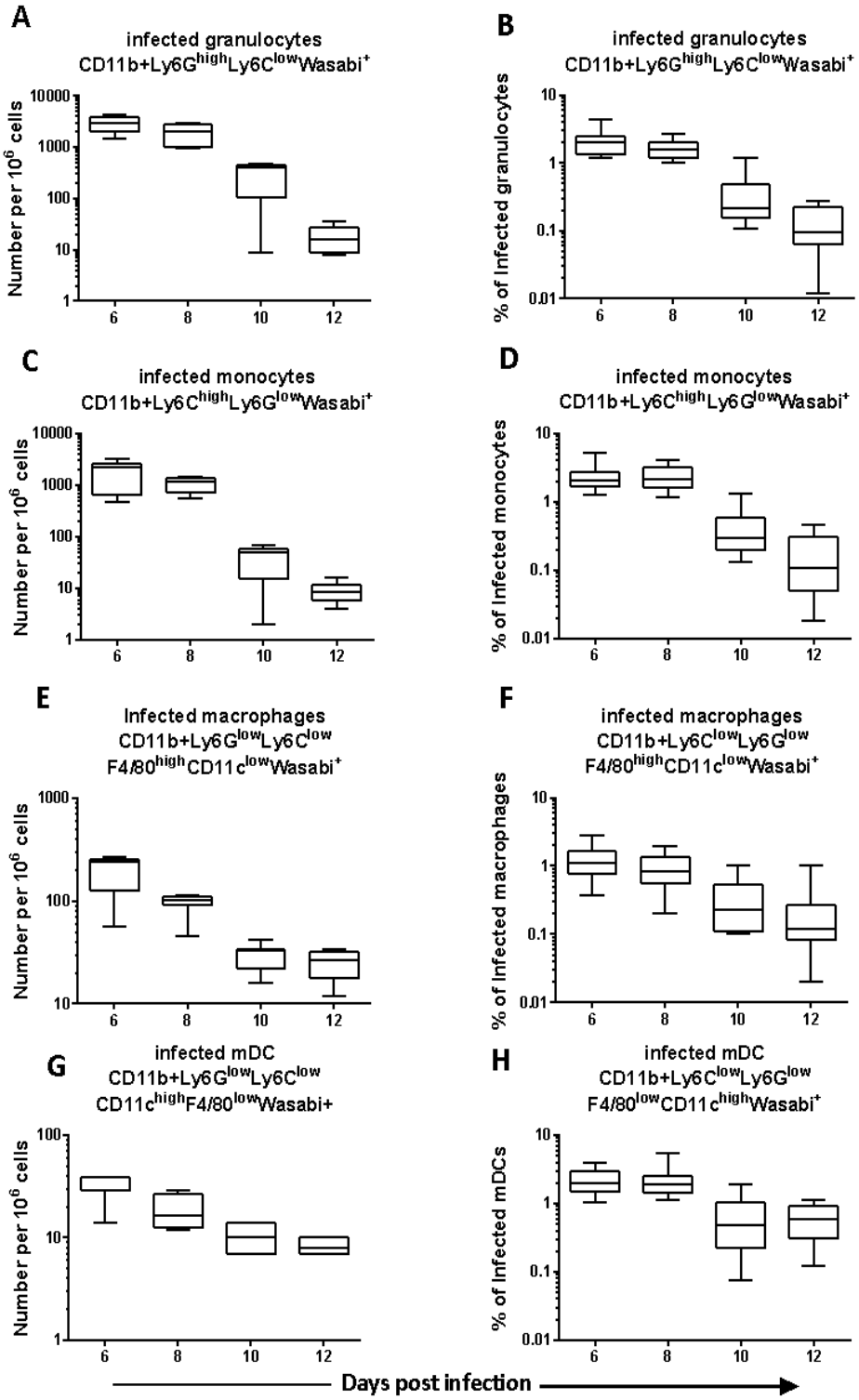

Figure 4.3 Frequencies of FV infected Wasabi+ subpopulations of myeloid cells

C57BL/6 mice were infected with FV encoding mWasabi and splenocytes were isolated at different time points after infection. Multi-parameter flow cytometry analysis was used to analyze the kinetics of different infected (Wasabi+) myeloid subpopulations. A bar plot showing the frequencies per 1 million cells of infected granulocytes (CD11b+ $Ly6G^{high}$ $Ly6C^{low}$ $Wasabi^{+}$) (A), infected monocytes (CD11b+ $Ly6C^{high}$ $Ly6G^{low}$ $Wasabi^{+}$) (B), infected macrophages (CD11b+ $Ly6G^{low}$ $Ly6C^{low}$ F4/80+ $CD11c^{low}$ $Wasabi^{+}$) (C), and infected mDC (CD11b+ $Ly6G^{low}$ $Ly6C^{low}$ $F4/80^{low}$ CD11c+ $Wasabi^{+}$) (D). A bar plot showing the percentage of infected granulocytes (CD11b+ $Ly6G^{high}$ $Ly6C^{low}$ $Wasabi^{+}$) (E), monocytes (CD11b+ $Ly6C^{high}$ $Ly6G^{low}$ $Wasabi^{+}$) (F), macrophages (CD11b+ $Ly6G^{low}$ $Ly6C^{low}$ F4/80+ $CD11c^{low}$ $Wasabi^{+}$) (G), and mDC (CD11b+ $Ly6G^{low}$ $Ly6C^{low}$ $F4/80^{low}$ CD11c+ $Wasabi^{+}$) (H).

PD-L1 expression on infected monocytes was significantly increased on 6 (MFI 3226), 10 (MFI 4099) and 12 (MFI 3234) days after infection in comparison to the monocytes from naïve mice (MFI 1573) and on day 10 (MFI 1822) and 12 (MFI 1434) when compared to the non-infected monocytes from infected mice. No differences were observed between the non-infected monocytes from infected mice and monocytes from naïve mice (Fig. 4.4B). The expression of PD-L1 on infected macrophages was significantly increased on 6 (MFI 3132), 8 (MFI 3231), 10 (MFI 4071), and 12 (MFI 3583) days after infection in comparison to the macrophages from naïve mice (MFI 1040). The expression of PD-L1 was significantly increased on infected macrophages in comparison to the non-infected macrophages from infected mice on 10 (MFI 1539) and 12 (MFI 1173) days post infection, whereas no difference was found on 6 and 8 days post infection. No differences were observed between the non-infected macrophages from infected mice and macrophages from naive mice (Fig 3.4C). The expression of PD-L1 on infected mDCs was significantly increased on 6 (MFI 3853), 8 (MFI 4281), 10 (MFI 5071), and 12 (MFI 3411) days after infection in comparison to the naïve mDCs (MFI 1121) and on 6 (MFI 2144), 10 (MFI 1764), and 12 (MFI 1579) days post infection compared to the non-infected cells. No differences were observed between the non-infected mDCs from infected mice and mDCs from naïve mice (Fig. 4.4D). Thus, all analyzed subpopulations of infected myeloid cells strongly enhanced the expression of PD-L1 on their cell surface upon FV infection. The highest values of PD-L1 MFI

for infected myeloid cells were seen on day 10 and day 12 after FV infection. The expression of PD-L1 on different subpopulations of non-infected myeloid cells in infected mice showed only a tendency of enhancement. Thus, mainly virus infection on a single cell level drives upregulation of PD-L1 in myeloid cells.

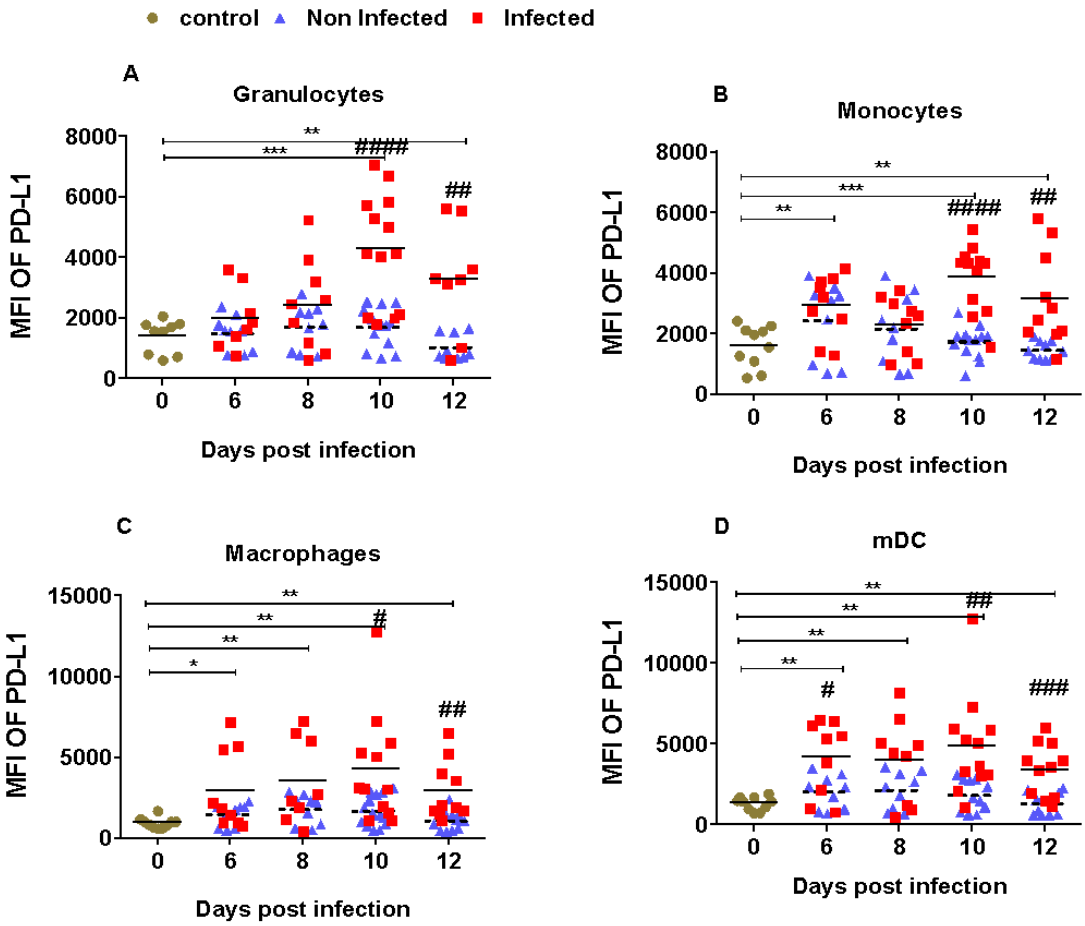

Figure 4.4 Expression of PD-L1 on different myeloid subpopulations after FV infection

C57BL/6 mice were infected with FV-mWasabi and splenocytes were isolated at different time points after infection. Multi-parameter flow cytometry analysis was used to compare the mean fluorescent intensity (MFI) of PD-L1 on the surface of infected (wasabi+; red), non-infected (wasabi-; blue) and naive (day 0; brown) granulocytes (CD11b+ $Ly6G^{high}$ $Ly6C^{low}$) (A), monocytes (CD11b+ $Ly6C^{high}$ $Ly6G^{low}$) (B), macrophages (CD11b+ $Ly6G^{low}$ Ly6C ^{low} F4/80+ $CD11c^{low}$) (C), and mDC (CD11b+ $Ly6G^{low}$ $Ly6C^{low}$ $F4/80^{low}$ CD11c+) (D). Each dot represents an individual mouse, the mean MFI of PD-L1 are indicated. Data were pooled from three

independent experiments with similar results. Differences between 0 and 6, 8, 10, and 12 days were analyzed using one-way ANOVA was used with a Tukey post-test (*$p<0.05$, **$p<0.005$, ***$p<0.0005$, ****$p<0.0001$). Differences between infected and non-infected cells were analyzed using unpaired t-test and are indicated in the figure ($^{\#}p<0.05$, $^{\#\#}p<0.005$, $^{\#\#\#}p<0.0005$, $^{\#\#\#\#}p<0.0001$).

PD-L2 is the other ligand of PD-1. PD-L1 is expressed on APCs and can be induced on various immune cells in response to inflammatory factors (157, 178). The expression of PD-L2 on infected granulocytes was significantly increased on 10 (MFI 4159) and 12 (MFI 5257) days after infection, whereas no differences were observed on 6 and 8 days after infection in comparison to the granulocytes from naïve mice (MFI 190). The expression of PD-L2 on infected granulocytes was strongly enhanced in comparison to the non-infected granulocytes from infected mice on 10 (MFI 326) and 12 (MFI 175) days post infection, but not on 6 and 8 days post infection. No differences in the expression of PD-L2 were observed between the granulocytes from naïve mice and non-infected granulocytes from infected mice (Fig. 4.5A). On monocytes, the expression of PD-L2 on infected cells was significantly increased on 10 (MFI 2558) and 12 (MFI 2681) days after infection in comparison to the monocytes from naïve mice (MFI 160), but not on the 6 and 8 days post infection. The expression of PD-L2 on infected monocytes was significantly enhanced when compared to the non-infected monocytes from infected mice on 10 (MFI 157) and 12 (MFI 146) days post infection, whereas no differences were observed on 6 and 8 days post infection. No differences were observed between the non-infected monocytes and the monocytes from naïve mice (Fig. 4.5B). On macrophages, the expression of PD-L2 on infected cells was significantly increased on 8 (MFI 2001), 10 (MFI 4537) and 12 (MFI 4159) days after infection in comparison to the macrophages from naive mice (MFI 198). The expression of PD-L2 on infected macrophages was significantly increased when compared to non-infected macrophages on 8 (MFI 253), 10 (MFI 273), and 12 (MFI 266) days after infection, but no differences were observed on day 6 post infection. No differences were either observed between the macrophages from naïve mice and non-infected cells from infected macrophages (Fig. 4.5C). On mDCs, the expression of PD-L2 on infected cells was significantly increased on 6 (MFI 2387), 8 (MFI 1633), 10 (MFI 4008), and 12 (MFI 3626) days after infection in comparison to the mDCs from naive mice (MFI 232). The expression of PD-L2 on infected cells was significantly higher when compared to non-infected mDCS from infected mice on 6 (MFI 293), 8 (MFI 111), 10 (MFI 269), and 12 (MFI 246)

days post infection. No differences in the expression of PD-L2 were observed between the non-infected mDCs from infected mice and mDCs from naïve mice (Fig. 4.5D).

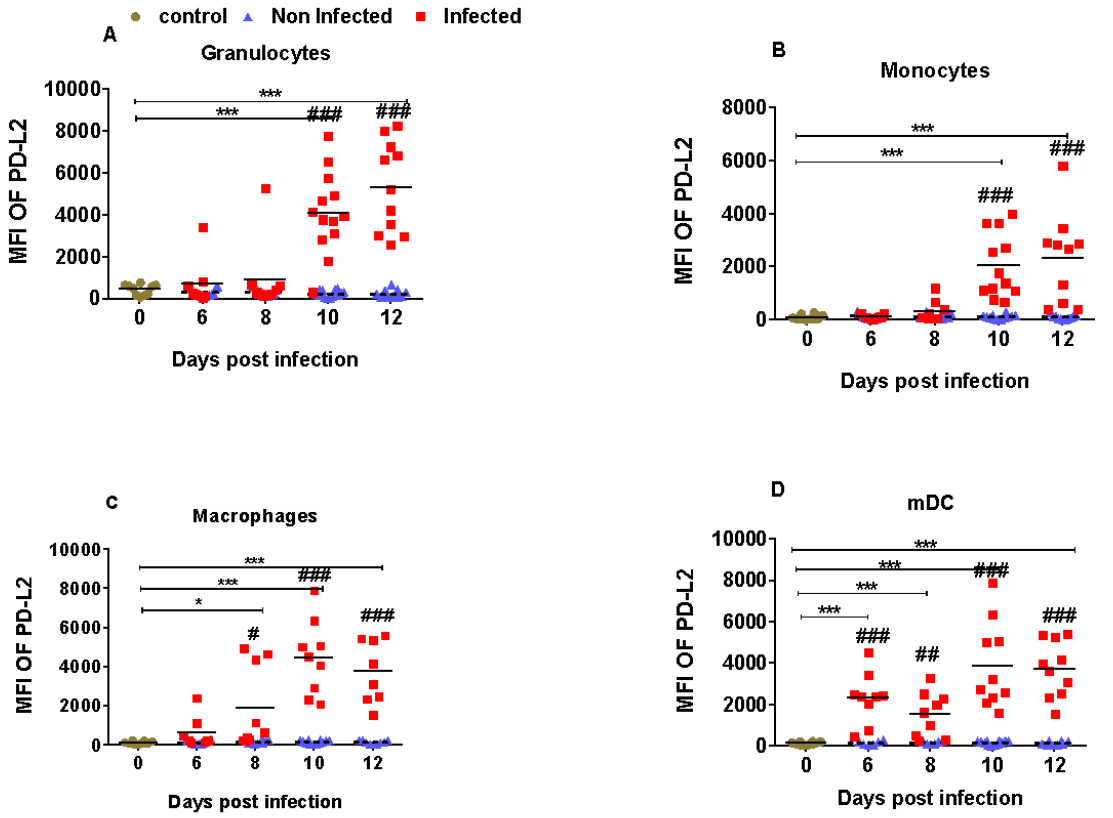

Figure 4.5 Expression of PD-L2 on different myeloid subpopulations after FV infection.

C57BL/6 mice were infected FV-mWasabi and splenocytes were isolated at different time points after infection. Multi-parameter flow cytometry analysis was used to compare the mean fluorescent intensity (MFI) of PD-L2 on the surface of infected (Wasabi+; red), non-infected (Wasabi-; blue) and naive (day 0; brown) granulocytes (CD11b+ Ly6G^{high} Ly6C^{low}) (A), monocytes (CD11b+ Ly6C^{high} Ly6G^{low}) (B), macrophages (CD11b+ Ly6G^{low} Ly6C ^{low} F4/80+ CD11c^{low}) (C), and mDC (CD11b+ Ly6G^{low} Ly6C^{low} F4/80^{low} CD11c+) (D). Each dot represents an individual mouse, the mean MFI of PD-L2 are indicated. Data were pooled from three independent experiments with similar results. Differences between 0 and 6, 8, 10, and 12 days were analyzed using one-way ANOVA was used with a Tukey post-test (*p<0.05, **p<0.005, ***p<0.0005, ****p<0.0001).

Differences between infected and non-infected cells were analyzed using unpaired t-test and are indicated in the figure ($^{\#}p<0.05$, $^{\#\#}p<0.005$, $^{\#\#\#}p<0.0005$, $^{\#\#\#\#}p<0.0001$).

Thus it can be summarized that infected myeloid cells strongly enhanced the expression of PD-L2 on the cell surface. Infected granulocytes and infected monocytes enhanced the PD-L2 expression on 10 and 12 days post infection, whereas infected macrophages and infected mDCs enhanced PD-L2 expression at earlier time points of infection.

CD270 or HVEM (TNFRSF14) is a protein of the TNF superfamily that serves as a common ligand for the costimulatory (LIGHT and LTα) and co-inhibitory (CD272 and CD160) receptors on T and B cells (179). The expression of CD270 on infected granulocytes was significantly increased on 10 (MFI 2837) and 12 (MFI 3619) days after infection, whereas no differences were observed on 6 and 8 days after infection between the infected granulocytes and granulocytes from naïve mice (MFI 1211). The expression of CD270 on infected granulocytes was significantly increased in comparison to the non-infected granulocytes on 10 (MFI 1392) and 12 (MFI 1159) days post infection, however no significant change on 6 and 8 days post infection was observed. No differences were observed between the non-infected granulocytes from infected mice and granulocytes from naïve mice (Fig. 4.6A). On monocytes, the expression of CD270 on infected cells was significantly increased on 10 (MFI 2755) and 12 (MFI 2911) days after infection. No difference between infected monocytes and naïve monocytes (MFI 1368) was observed on 6 and 8 days after infection. The expression of CD270 on infected monocytes was significantly increased when compared to non-infected monocytes of the same mice on 10 (MFI 1392) and 12 (MFI 1440) days post infection. No CD270 upregulation was observed between the monocytes from naive mice and non-infected monocytes from infected mice (Fig. 4.6B). On macrophages, the expression of CD270 on infected cells was significantly increased on 6 (MFI 1280), 8 (MFI 1761), 10 (MFI 3400), and 12 (MFI 2549) days after infection in comparison to the cells from naive mice (MFI 564). The expression of CD270 on infected macrophages was significantly increased in comparison to the non-infected macrophages on 6 (MFI 502), 8 (MFI 407), 10 (MFI 577), and 12 (MFI 622) days post infection from the same mice. No changes were observed between the macrophages from naïve mice and non-infected macrophages from infected mice (Fig. 4.6C). On mDCs, the expression of CD270 on infected cells was significantly increased on 6 (MFI 1761), 8 (MFI 2099), 10 (MFI 3279), and 12 (MFI 2301) days after infection in comparison to the cells

from naive mice (MFI 593). The expression of CD270 on infected mDCs was highly significant in comparison to the non-infected mDCs on 6 (MFI 673), 8 (MFI 647), 10 (MFI 576) and 12 (MFI 496) days post infection from the same mice. Whereas no significant difference in the expression of CD270 between the non-infected mDCs and mDCs of naive mice was observed (Fig. 4.6D). Thus, very similar pattern to PD-L1 and PD-L2 expression was observed for the CD270 expression on infected myeloid cells.

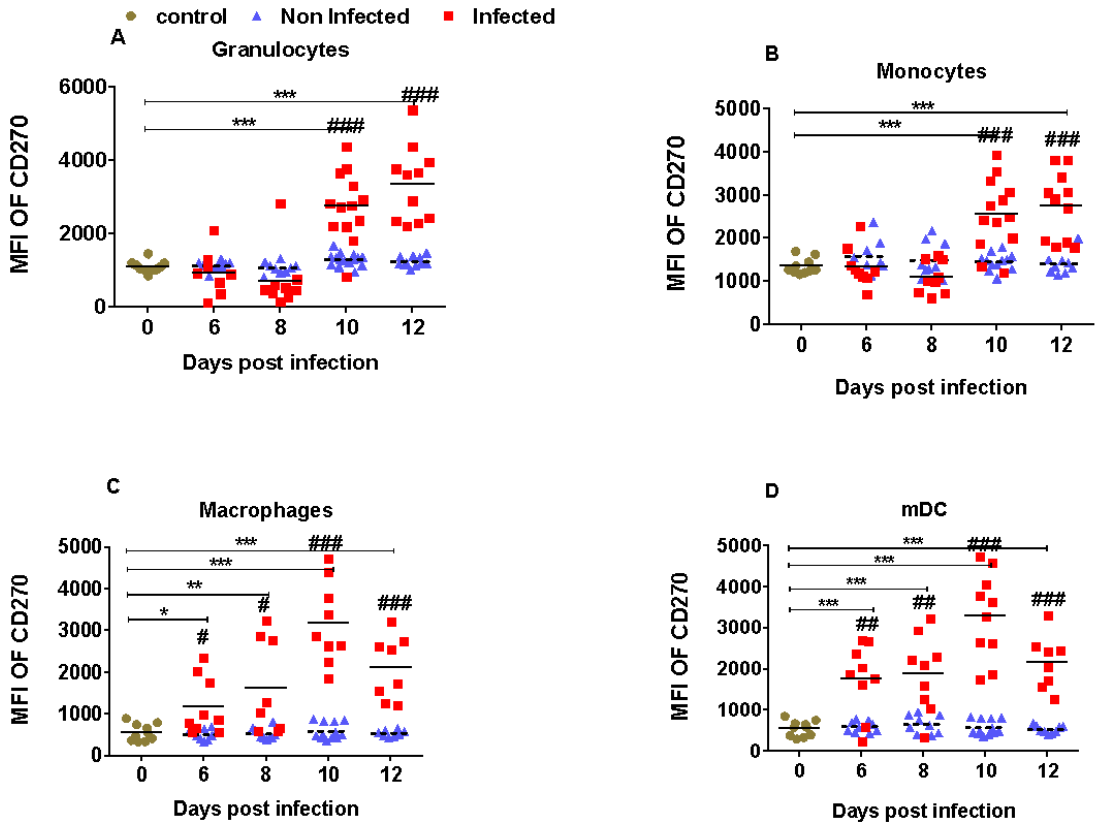

Figure 4.6 Expression of CD270 on different myeloid subpopulations after FV infection.

C57BL/6 mice were infected FV-mWasabi and splenocytes were isolated at different time points after infection. Multi-parameter flow cytometry analysis was used to compare the mean fluorescent intensity (MFI) of CD270 on the surface of infected (Wasabi+; red), non-infected (Wasabi-; blue) and naive (day 0; brown) granulocytes (CD11b+ Ly6G^{high}Ly6C^{low}) (A), monocytes (CD11b+ Ly6C^{high} Ly6G^{low}) (B), macrophages (CD11b+ Ly6G^{low} Ly6C ^{low} F4/80+ CD11c^{low}) (C), and mDC (CD11b+ Ly6G^{low} Ly6C^{low} F4/80^{low} CD11c+) (D). Each dot represents an individual mouse, the mean MFI of CD270 are indicated. Data were pooled from three independent experiments with

similar results. Differences between 0 and 6, 8, 10, and 12 days were analyzed using one-way ANOVA was used with a Tukey post-test (*p<0.05, **p<0.005, ***p<0.0005, ****p<0.0001). Differences between infected and non-infected cells were analyzed using unpaired t-test and are indicated in the figure ($^{\#}$p<0.05, $^{\#\#}$p<0.005, $^{\#\#\#}$p<0.0005, $^{\#\#\#\#}$p<0.0001).

Infected cells enhanced the expression of CD270 on granulocytes and monocytes during late acute phase of infection, whereas the expression on macrophages and mDCs were already enhanced at early time points of infection.

CD80 belongs to the B7 ligand family and are a part of the Ig gene superfamily. CD80 is a regulatory ligand expressed on the surface of antigen presenting cells and interacts with CD28 or CTLA4 (180). The expression of CD80 on infected granulocytes was significantly increased on 8 (MFI 1410), 10 (MFI 2313), and 12 (MFI 2076) days after infection in comparison to granulocytes from naïve mice (MFI 800), but no difference was observed on day 6 post infection. No significant differences were observed between infected and non-infected mice on 6, 8, 10, and 12 days post infection, nor were any changes seen between the granulocytes from naïve mice and non-infected granulocytes from infected mice (Fig. 4.7A). On monocytes, the expression of CD80 on infected cells was significantly increased on 6 (MFI 2385) and 10 (MFI 4283) days after infection in comparison to the monocytes from naive mice (MFI 843), whereas no significant changes were observed on 8 and 12 days post infection. The expression of CD80 on infected monocytes was significantly increased when compared to non-infected monocytes from infected mice on 6 (MFI 780), 8 (MFI 703), 10 (MFI 875), and 12 (MFI 1358) days post infection, whereas no differences were observed between the monocytes from naïve mice and non-infected monocytes from infected mice (Fig. 4.7B). The expression of CD80 on infected macrophages was significantly increased on 10 (MFI 4296) and 12 (MFI 3894) days post infection in comparison to macrophages from naïve mice (MFI 274), whereas no changes were observed on infected granulocytes in comparison to the granulocytes from naïve mice on 6 and 8 days post infection. The expression of CD80 on infected macrophages was significantly increased in comparison to the non-infected macrophages from infected mice on 10 (MFI 1220) and 12 (MFI 1199) days post infection, but no changes were observed on 6 and 8 days. No differences were observed between macrophages of naïve mice and non-infected macrophages from infected mice (Fig. 4.7C). On mDCs, the expression of CD80 on

infected cells was significantly increased on 6 (MFI 3526), 8 (3554), 10 (MFI 4352) and 12 (MFI 4824) days post infection in comparison to the mDCs of naïve mice (MFI 960). The expression of CD80 on infected mDCs was significantly increased in comparison to the non-infected mDCs from infected mice on 10 (MFI 2280) and 12 (MFI 2323) days post infection, whereas no differences were observed between the mDCs of naïve mice and non-infected mDCs of infected mice (Fig. 4.7D). Infected cells enhanced the expression of CD80 during the early phase of infection on granulocytes and monocytes, whereas the expression on macrophages and mDCs was enhanced during late acute phase of infection. Interestingly, the expression of CD80 was enhanced at 10 days post infection on monocytes.

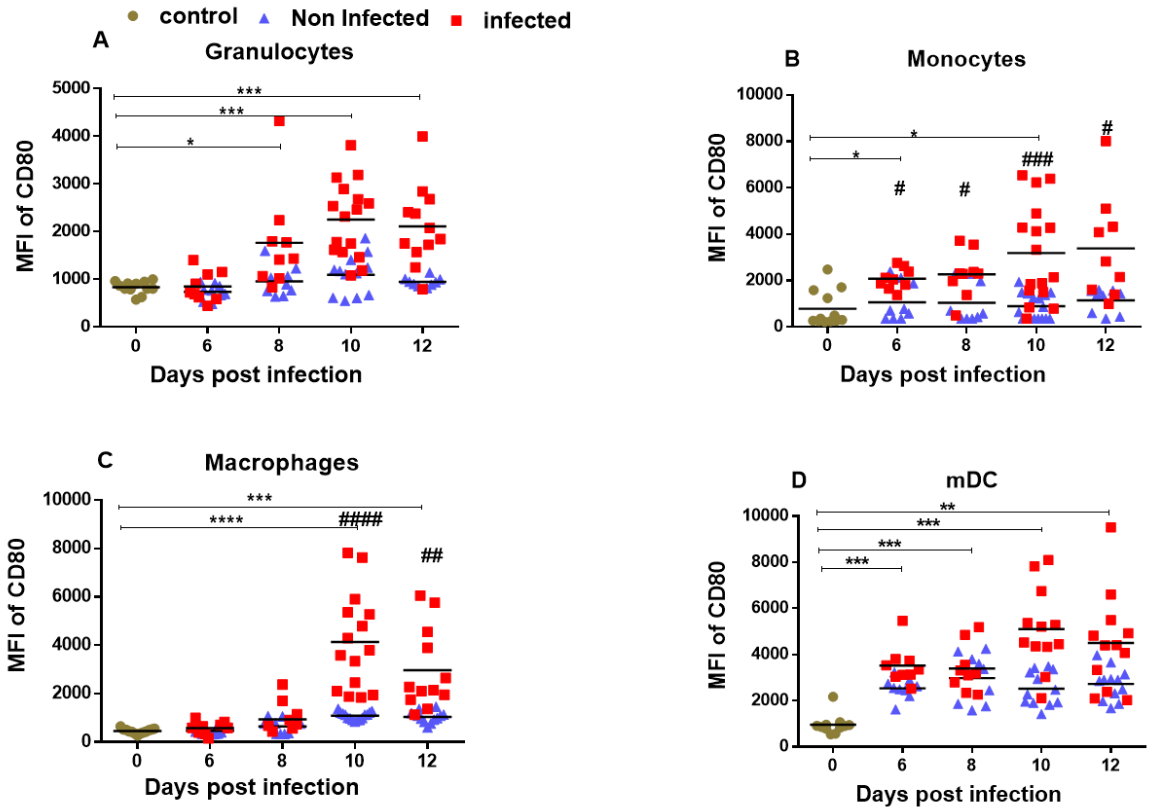

Figure 4.7 Expression of CD80 on different myeloid subpopulations in the spleen.

C57BL/6 mice were infected with FV-mWasabi and splenocytes were isolated at different time points after infection. Multi-parameter flow cytometry analysis was used to compare the mean fluorescence intensity (MFI) of CD80 on the surface of infected (wasabi +; red), non-infected (wasabi-; blue) and naive (day 0; brown) granulocytes (CD11b+ Ly6G^{high} Ly6C^{low}) (A),

monocytes (CD11b+ Ly6C^{high} Ly6G^{low}) (B), macrophages (CD11b+ Ly6G^{low} Ly6C ^{low} F4/80+ CD11c^{low}) (C), and mDC (CD11b+ Ly6G^{low} Ly6C^{low} F4/80^{low} CD11c+) (D). Each dot represent an individual mouse, the mean MFI of CD80 are indicated. Data were pooled from three independent experiments with similar results. Differences between 0 and 6, 8, 10, and 12 days were analyzed using one-way ANOVA was used with a Tukey post-test (*p<0.05, **p<0.005, ***p<0.0005, ****p<0.0001). Differences between infected and non-infected cells were analyzed using unpaired t-test and are indicated in the figure (#p<0.05, ##p<0.005, ###p<0.0005, ####p<0.0001).

CD86 engages with CTLA4, which results in the attenuation of T cell responses or it engages with CD28 for the stimulation of T cells (181). The expression of CD86 on infected granulocytes was significantly increased on 6, 8, 10, and 12 days after infection in comparison to the granulocytes from naive mice. A significant increase in the expression of CD86 was observed on the infected granulocytes in comparison to the non-infected granulocytes from infected mice on 8, 10 and 12 days post infection. No differences were detected between the granulocytes from naïve mice and non-infected granulocytes from infected mice (Fig. 4.8A). On monocytes, increased expression of CD86 was observed on infected calls on 6, 8, 10 and 12 days post infection in comparison to the monocytes from naïve mice. A significant increase in the expression of CD86 was observed on infected monocytes when compared to the non-infected monocytes on 6 and 8 days post infection, whereas no changes were observed between the monocytes from naïve mice and non-infected monocytes from infected mice (Fig. 4.8B). The expression of CD86 on infected macrophages was significantly increased on 6, 8, and 10 days in comparison to the macrophages from naïve mice, but no difference was observed on day 12 post infection. Increased expression of CD86 was observed on infected macrophages in comparison to the non-infected macrophages from the infected mice on day 8 post infection. Again, no differences were observed between the macrophages from naïve and non-infected macrophages from infected mice (Fig. 4.8C). Similar to the other myeloid cells, increased expression of CD86 was observed upon infection of mDCs on 6, 8, 10, and 12 days post infection. A significant increase in the expression of CD86 was observed on infected mDCs in comparison to the non-infected mDCs from infected mice on 8 and 10 days post infection. No differences between mDCs from naïve mice and non-infected mDCs from infected mice were observed (Fig. 4.8D). Taken together, infection enhanced the expression

of CD86 on granulocytes, monocytes, macrophages and mDCs starting at the early phase of infection.

CD200 is the member of Ig supergene family, like CD80 and CD86, and CD200 interaction with its ligand leads to immunoregulatory functions (182). The expression of CD200 on infected granulocytes was significantly increased on 8 (MFI 762), 10 (MFI 1058), and 12 (MFI 1058) days after infection in comparison to the granulocytes from naive mice (MFI 215). No significant differences were observed on 6 (MFI 474) days post infection on infected granulocytes when compared to granulocytes of naïve mice. A significant increase in the expression of CD200 on infected granulocytes in comparison to the non-infected granulocytes from infected mice was observed on 6 (MFI 164), 8 (MFI 283), 10 (MFI 283), and 12 (MFI 144) days post infection, however no differences were seen between the granulocytes from naïve mice and non-infected granulocytes from infected mice (Fig. 4.9A).

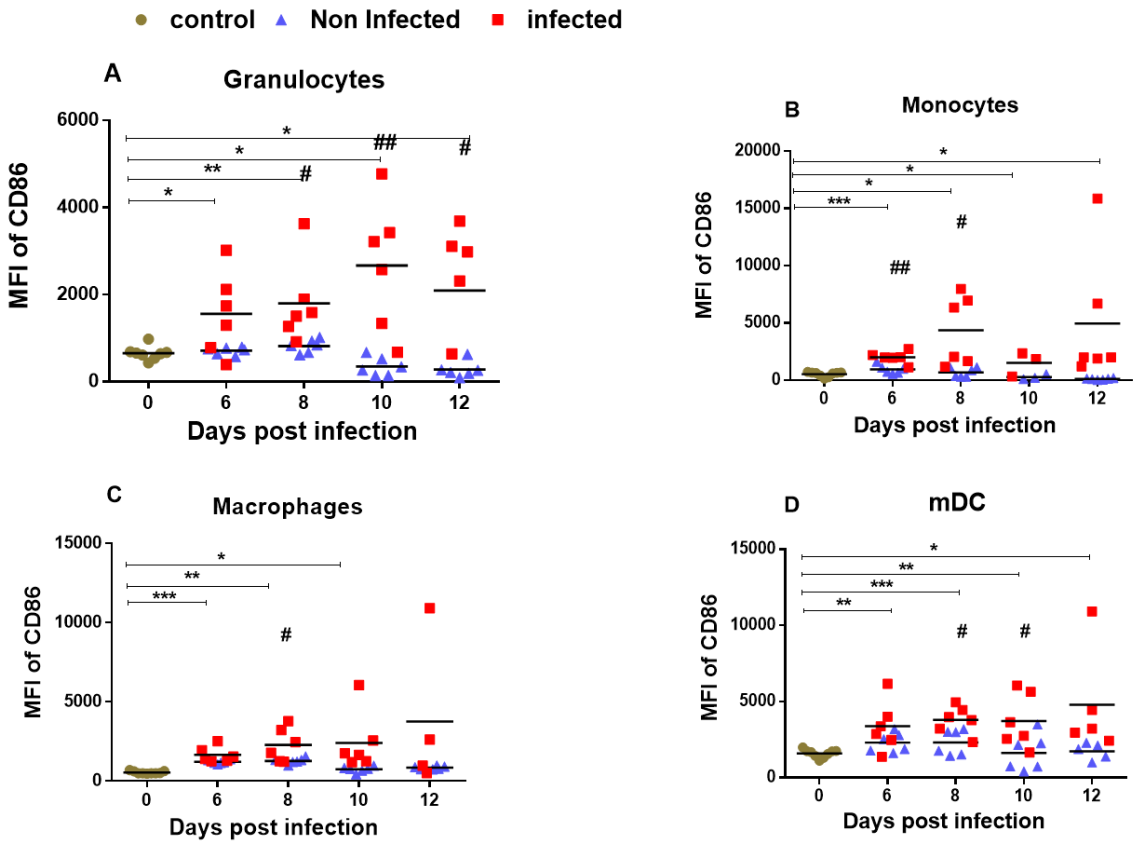

Figure 4.8 Expression of CD86 on different myeloid subpopulations in the spleen.

C57BL/6 mice were infected with FV-mWasabi and splenocytes were isolated at different time points after infection. Multi-parameter flow cytometry analysis was used to compare the mean fluorescence intensity (MFI) of CD86 on the surface of infected (wasabi +; red), non- infected (wasabi-; blue) and naive (day 0; brown) granulocytes (CD11b+ $Ly6G^{high}$ $Ly6C^{low}$) (A), monocytes (CD11b+ $Ly6C^{high}$ $Ly6G^{low}$) (B), macrophages (CD11b+ $Ly6G^{low}$ Ly6C ^{low} F4/80+ $CD11c^{low}$) (C), and mDC (CD11b+ $Ly6G^{low}$ $Ly6C^{low}$ $F4/80^{low}$ CD11c+) (D). Each dot represent an individual mouse, the mean MFI of CD86 are indicated. Data were pooled from three independent experiments with similar results. Differences between 0 and 6, 8, 10, and 12 days were analyzed using one-way ANOVA was used with a Tukey post-test (*p<0.05, **p<0.005, ***p<0.0005, ****p<0.0001). Differences between infected and non-infected cells were analysed using unpaired t-test and are indicated in the figure (#p<0.05, ##p<0.005, ###p<0.0005, ####p<0.0001).

On monocytes, the expression of CD200 on infected cells was increased in some mice on 10 and 12 days after infection in comparison to the monocytes from naïve animals, however these differences were not significant. The expression of CD200 was significantly increased on infected monocytes in comparison to the non-infected monocytes on day 10 post infection. No changes were observed between the monocytes from naïve mice and non-infected monocytes from infected mice (Fig. 4.9B). On macrophages, the expression of CD200 on infected cells was increased on 10 and 12 days after infection in comparison to the macrophages from naive mice. The differences were not statistically significant, and no changes were observed between the infected and non-infected macrophages from same mice and also between non-infected and naïve mice (Fig. 4.9C). On mDCs, the expression of CD200 on infected cells was significantly increased on 6 (MFI 1022) and 8 (MFI 1230) days after infection in comparison to the mDCs from naive mice (MFI 336), no differences were observed on day 10 and 12. The expression of CD200 was significantly increased on infected mDCs in comparison to the non-infected mDCs from infected mice on 6 (MFI 387), 10 (MFI 484) and 12 (MFI 328) days post infection. No differences were observed between the mDCs from naïve mice and non-infected mDCs from infected mice (Fig. 4.9D). The expression of CD200 on infected granulocytes was strongly increased at every analyzed time point. Infected mDCs cells enhanced the expression of CD200 during the early phase of infection and the expression of CD200 on infected monocytes and on infected macrophages was enhanced at day 10 in comparison to non-infected cells.

CD48 is the ligand for CD244 (2B4) and is expressed on hematopoietic cells. Interaction of CD48-CD244 plays a crucial role in regulating target cell lysis of NK cells and cytotoxic T lymphocytes (183). An enhanced expression of CD48 on infected and non-infected granulocytes from infected mice was observed at day 6 (MFI 1016), 8 (MFI 1385) and 10 (MFI 1016) in comparison to the granulocytes from naïve mice (MFI 301). No differences were observed between the infected and non-infected granulocytes from the infected mice (Fig. 4.10A). Infected monocytes significantly enhanced the expression of CD48 on 6 (MFI 8953) and 12 (MFI 10723) days after infection in comparison to the monocytes from naïve mice (MFI 7562), no differences were observed on 8 and 10 days after infection. No differences were observed between the infected and non-infected monocytes from infected mice (Fig. 4.10B). Increased expression of CD48 was observed on infected macrophages on 6 (MFI 3831), 8 (MFI 4472), and 10 (MFI 4071) days after infection in comparison to macrophages from naïve mice (MFI 2963). No differences were observed between the infected and non-infected macrophages from infected mice (Fig. 4.10C). Infected mDCs significantly increased the expression of CD48 on day 10 (MFI 9729) post infection in comparison to the mDCs from naïve mice (MFI 7871), no changes were detected on 6, 8 and 12 days after infection. No difference in the expression of CD86 was observed between the infected and non-infected mDCs from infected mice (Fig. 4.10D). Similar to other ligands with inhibitory function, infected myeloid cells enhanced the expression of CD48 on their cell surface.

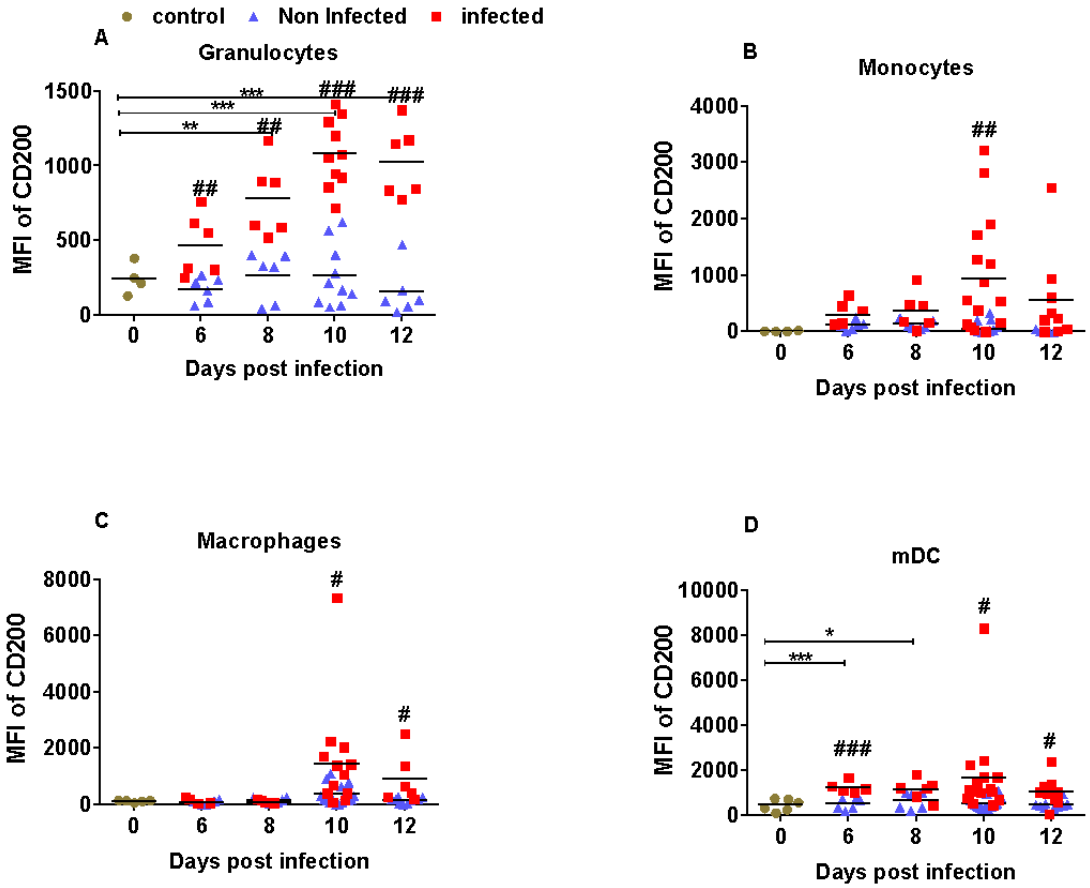

Figure 4.9 Expression of CD200 on different myeloid subpopulations after FV infection.

C57BL/6 mice were infected FV-mWasabi and splenocytes were isolated at different time points after infection. Multi-parameter flow cytometry analysis was used to compare the mean fluorescent intensity (MFI) of CD200on the surface of infected (wasabi +; red), non-infected (wasabi-; blue) and naive (day 0; brown) granulocytes (CD11b+ Ly6G^{high} Ly6C^{low}) (A), monocytes (CD11b+ Ly6C^{high} Ly6G^{low}) (B), macrophages (CD11b+ Ly6G^{low} Ly6C ^{low} F4/80+ CD11c^{low}) (C), and mDC (CD11b+ Ly6G^{low} Ly6C^{low} F4/80^{low} CD11c+) (D). Each dot represents an individual mouse, the mean MFI of CD200 are indicated. Data were pooled from three independent experiments with similar results. Differences between 0 and 6, 8, 10, and 12 days were analyzed using one-way ANOVA was used with a Tukey post-test (*p<0.05, **p<0.005, ***p<0.0005, ****p<0.0001). Differences between infected and non-infected cells were analyzed using unpaired t-test and are indicated in the figure ($^{\#}$p<0.05, $^{\#\#}$p<0.005, $^{\#\#\#}$p<0.0005, $^{\#\#\#\#}$p<0.0001).

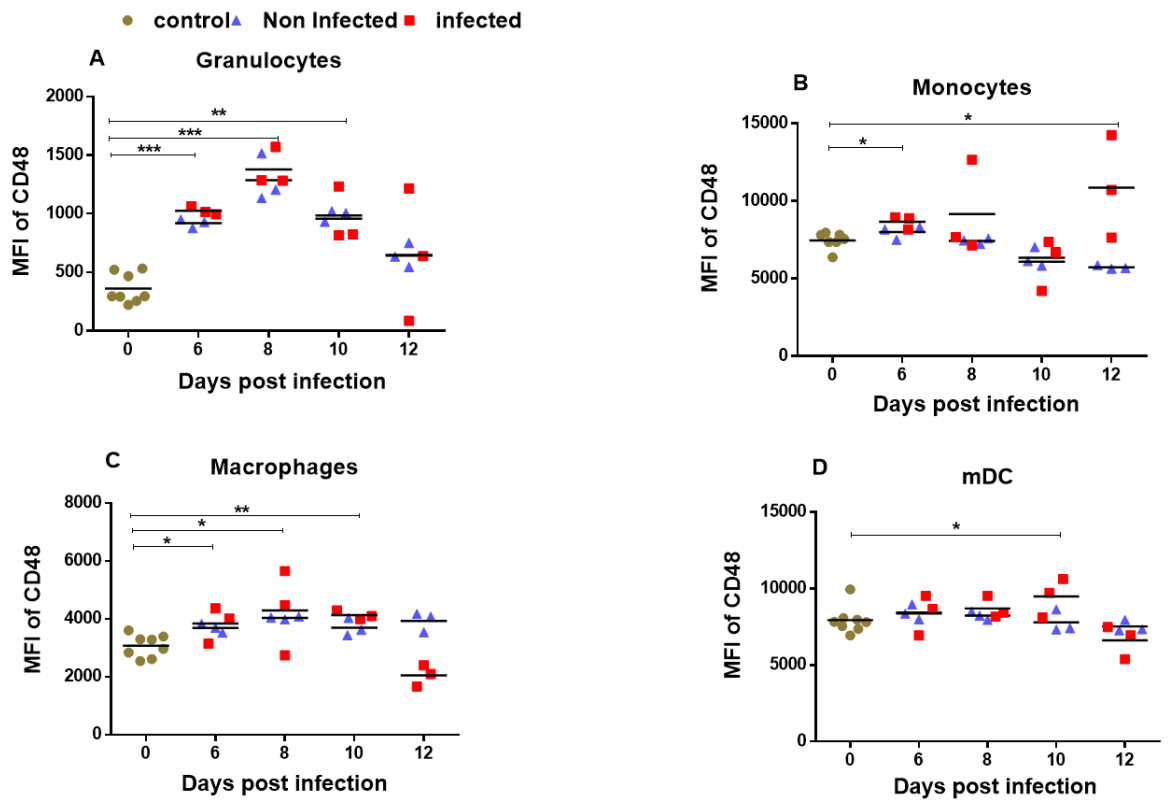

Figure 4.10. Expression of CD48 on different myeloid subpopulations in the spleen.

C57BL/6 mice were infected with FV-wasabi complex and splenocytes were isolated at different time points after infection. Multi-parameter flow cytometry analysis was used to compare the mean fluorescence intensity (MFI) of CD48 on the surface of infected (wasabi +; red), non- infected (wasabi-; blue) and naive (day 0; brown) granulocytes (CD11b+ Ly6G^{high} Ly6C^{low}) (A), monocytes (CD11b+ Ly6C^{high} Ly6G^{low}) (B), macrophages (CD11b+ Ly6G^{low} Ly6C ^{low} F4/80+ CD11c^{low}) (C), and mDC (CD11b+ Ly6G^{low} Ly6C^{low} F4/80^{low} CD11c+) (D). Each dot represent an individual mouse, the mean MFI of CD200 are indicated. Data were pooled from two independent experiments with similar results. Differences between 0 and 6, 8, 10, and 12 days were analyzed using one-way ANOVA was used with a Tukey post-test (*p<0.05, **p<0.005, ***p<0.0005, ****p<0.0001). Differences between infected and non-infected cells were analyzed using unpaired t-test and are indicated in the figure (#p<0.05, ##p<0.005, ###p<0.0005, ####p<0.0001).

FV infected myeloid subpopulations enhanced the expression of PD-L1, PD-L2, CD270, CD80, CD86, and CD48 during acute phase of FV infection. The pattern of these expression was different on every subpopulation for every individual molecule. The immuno-regulatory ligands provided signals to effector cells after getting in contact. Here, we speculate that simultaneous expression of different inhibitory ligands on infected myeloid subpopulations may provide the negative signals for CTL and prevent the infected cells from elimination.

4.2 Expression of inhibitory receptors on FV-specific CD8+ T cells

In the experiments described above, an enhanced expression of immunoregulatory ligands on different populations of infected myeloid cells was shown during FV infection. The main objective of the following experiments was to analyze FV-specific effector CD8+ T cells for the expression inhibitory receptors binding the inhibitory ligands observed on infected myeloid cells. Mice were sacrificed on 8, 10, and 12 days post infection and kinetic analysis of different inhibitory receptors (PD-1, CD272 (BTLA), CD160, CD244 (2B4), Tim3, Lag3) was performed with CD8+ T cells specific for the H-2D^{b}–restricted Friend murine leukemia virus–glycosylated immundominant gag epitope (tetramer+) (184). The CD8+ T cells from naïve mice (day 0) were used as reference population of CD8+ T cells.

PD-1 is the receptor for PD-L1 and PD-L2 (157). The percentages of virus specific tetramer+CD8+ T cells expressing PD-1 were significantly increased on 8, 10, and 12 days post infection when compared with the CD8+ T cells from naïve mice. These increased percentages of virus specific tetramer+CD8+ T cells expressing PD-1 on 10 and 12 days (Fig. 4.11A), were associated with increased expression of PD-L1 and PD-L2 on infected myeloid cells at same time points (Fig. 4.4 & Fig. 4.5). CD272 (BTLA) and CD160 are the inhibitory receptors of the ligand CD270 (HVEM), which belongs to the tumor necrosis factor (TNF) receptor superfamily (185). An increase in the percentages of the virus-specific CD8+ T cells which expressed CD272 (Fig. 4.11B) and CD160 (Fig. 4.11C) on 8, 10 and 12 days post infection was observed. This increase in the percentage of virus specific CD8+ T cells expressing inhibitory receptors CD272 and CD160 on day10 and 12 were directly associated with the increased expression of CD270 (HVEM) on infected myeloid cells (granulocytes, monocytes, macrophages and mDCs) on day 10 and 12 post infection (Fig. 4.6) .

2B4 is also known as CD244.2, which provides an inhibitory signal after binding to CD48 (153). 2B4 is mainly expressed on NK cells but some reports have also reported their expression on T cells. Infection with FV resulted in a significant increase in the percentage of virus-specific CD8+ T cells expressing 2B4 at 8, 10 and 12 days post infection (Fig. 4.11D). Tim-3 is an inhibitory receptor, which binds to 4 different ligands (Galectin-9, phosphatidylserine, Caecam-1 and HMGB1) (147), and is specifically expressed on IFN-g producing CD4 and CD8 T cells. Apart from its expression on T cells it is also expressed by Tregs and innate immune cells. FV infection significantly increased the percentage of virus specific CD8+ T cells expressing Tim-3 on 10 and 12 days post infection (Fig. 4.11E). CD200R is the inhibitory receptors for CD200 (182). FV infection significantly enhanced the percentage of virus specific CD8+ T cells expressing CD200R mainly on day 8, but the percentage declined on day 10 and 12 post infection (Fig 3.11F). The increase in the percentage of virus-specific CD8+ T cells expressing CD200R on day 8 was associated with the increased expression of CD200 on infected granulocytes (Fig. 4.9A). Lag3 is a receptor for MHC II molecules on infected cells. Infection with FV resulted in a significant increase in the percentage of virus specific CD8+ T cells expressing Lag3 on 8, 10 and 12 days post infection (Fig. 4.11G).

To summarize, activation of CD8+ T cells induced by FV infection leads to an expansion of these virus-specific cells, which simultaneously upregulate PD-1, CD272, CD160, CD244, Tim-3, CD200R and Lag3 on their surface. CD8+ T cells mainly expand on day 10 and 12 post infection (Zelinskyy et al., 2006), which resulted in increased frequencies of PD-1, CD272, CD160 and CD244 positive cells.

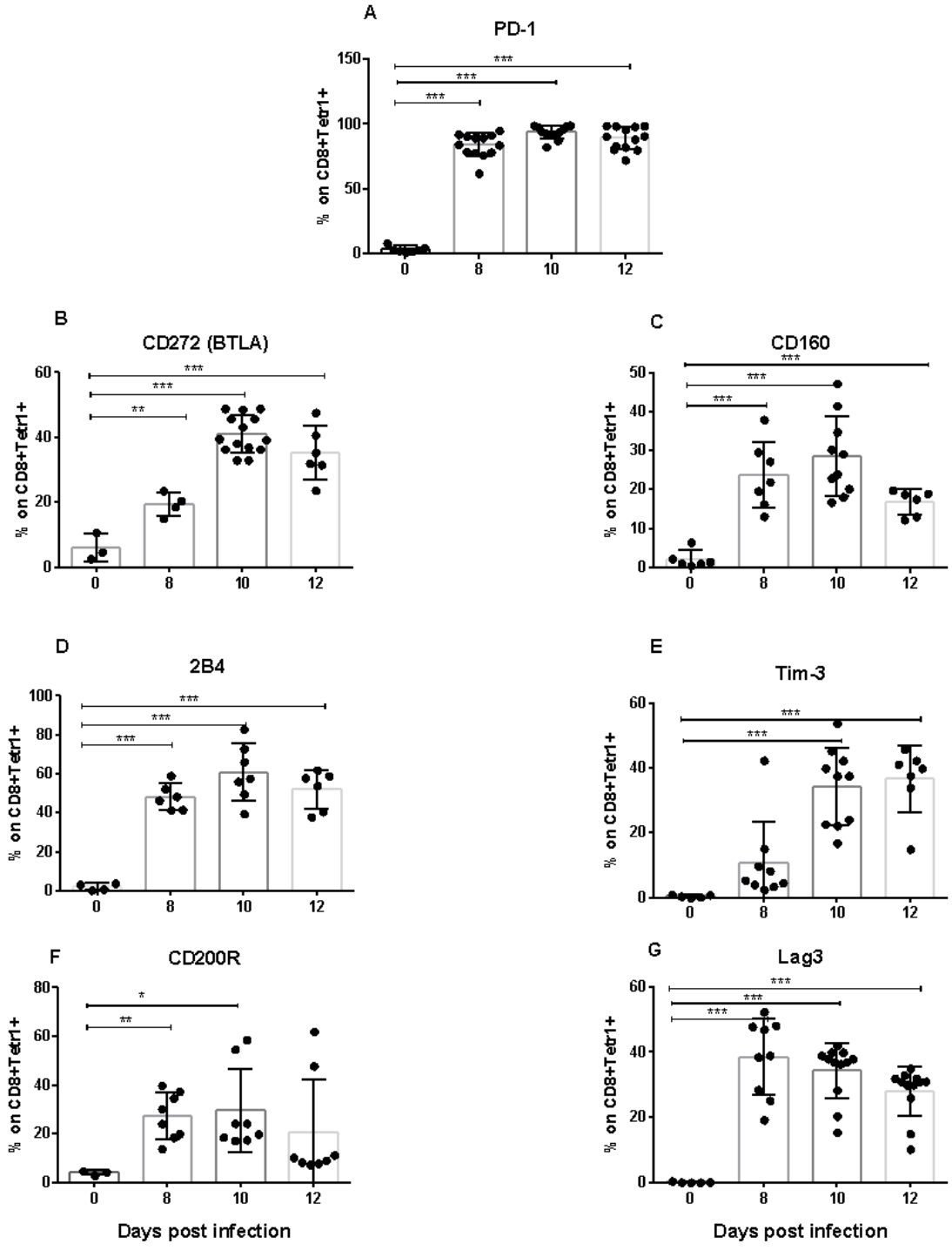

Figure 4.11. Expression of inhibitory receptors on virus -specific CD8 T cells after FV infection

C57BL/6 mice were infected with FV complex and splenocytes were isolated at different time points after infection. Multi-parameter flow cytometry analysis was used to compare the percentage of cells positive for the inhibitory receptors PD-1 (**A**), CD272 (BTLA) **(B)**, CD160 (**C**), 2B4 (CD244.2) (**D**), Tim3 (**E**), CD200R **(F)** and Lag3 **(G)** among CD8+ T cells specific for the H-2Db–restricted Friend murine leukemia virus–glycosylated immundominant gag epitope (tetramer+) with the percentage of CD8+ T cells in naïve mice (day0). Data were pooled from three independent experiments with similar results. Each dot represents an individual mouse and the percentage of PD-1, CD272, CD160, 2B4, Tim-3, CD200R and Lag3 and their SD is indicated. Differences between 0 and 8, 10, and 12 days were analyzed using one-way ANOVA was used with a Tukey post-test (*p<0.05, **p<0.005, ***p<0.0005, ****p<0.0001).

Since several inhibitory receptors are expressed on CD8+ T cells during FV infection at the same time when inhibitory ligands appear on infected myeloid cells, it is likely that their interactions might contribute to T cell exhaustion and impaired virus control. This was investigated in the following experiments.

4.3 Blocking CD270 interaction with its receptor CD160 and CD272 in FV infected mice

Infected monocytes and infected granulocytes enhanced the expression of CD270 at 10 and 12 days post infection (Fig. 6A, B). The expression of CD270 also increased, on macrophages and mDCs during infection. The CD270/CD272/CD160 co-inhibitory pathway has emerged as a potential target for the development of therapeutic interventions (179). The increased expression of CD270 on infected myeloid cells on day 10 and 12 (Fig. 4.6) was associated with increased percentages of virus specific CD8+ T cells expressing the ligands CD160 and CD272 (Fig. 4.11B, C). The main aim of our next experiment was to determine if these molecules have an inhibitory effect on cytotoxic CD8+ T cells. Two different anti-CD270 antibodies that selectively prevents the interaction of CD270 with its inhibitory receptors CD160 or CD272 respectively were used for the treatment of FV infected mice (Fig 4.12A). Treatments were performed with individual antibodies or in combination of the two, and as read out the CD8+ T cell response was characterized. Blockage of the CD270/CD272 and CD270/CD160 interaction individually and the combined blocking of the interaction of CD270 to both inhibitory receptors CD160 and CD272 showed a tendency to increase the percentage of CD43+CD8+ effectors (Fig. 4.12B) and tetramer+CD43+CD8+ T cells (Fig. 4.12C). The combined blocking of both inhibitory receptors

resulted in a significant increase in the percentage of effector CD43+CD8+ T cells producing GzmB in comparison to FV infected non treated mice (Fig. 4.12D). Although virus-specific tetramer+CD43+CD8+ T cells producing GzmB also showed a tendency to increase after combination therapy the difference were not significant in comparison to FV infected non treated mice (Fig. 4.12E). Importantly, the level of FV replication was significantly reduced after treatment with antibodies, which prevent the binding of CD270 to the CD160 receptor or after combination of both anti-CD270 blocking antibodies (Fig. 4.12F). Thus, the combination treatment with antibodies preventing the binding of CD270 to both of its inhibitory receptors expressed on CD8+ T cells and resulted in enhanced numbers of GzmB producing effector CD8+ T cells and improved elimination of FV. This immunomodulatory therapeutic strategy directed on CD270 maybe a new option for the treatment of viral infections.

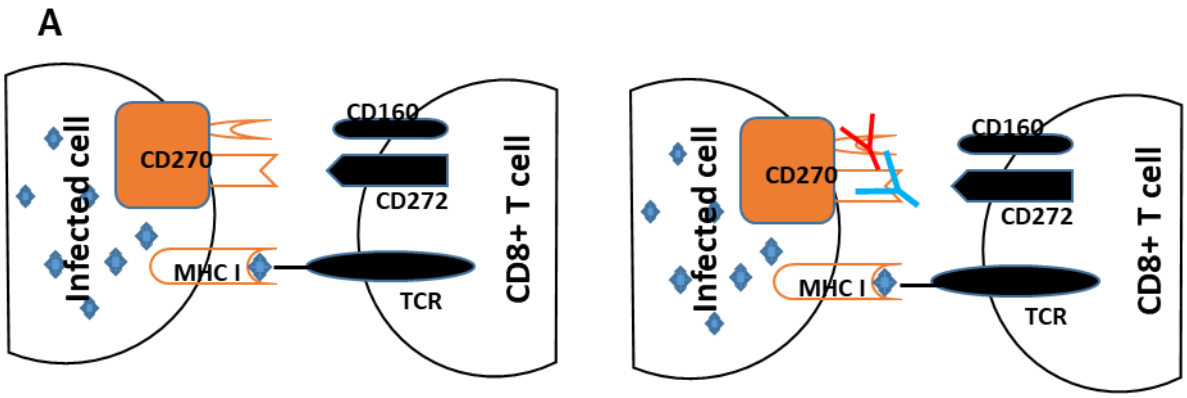

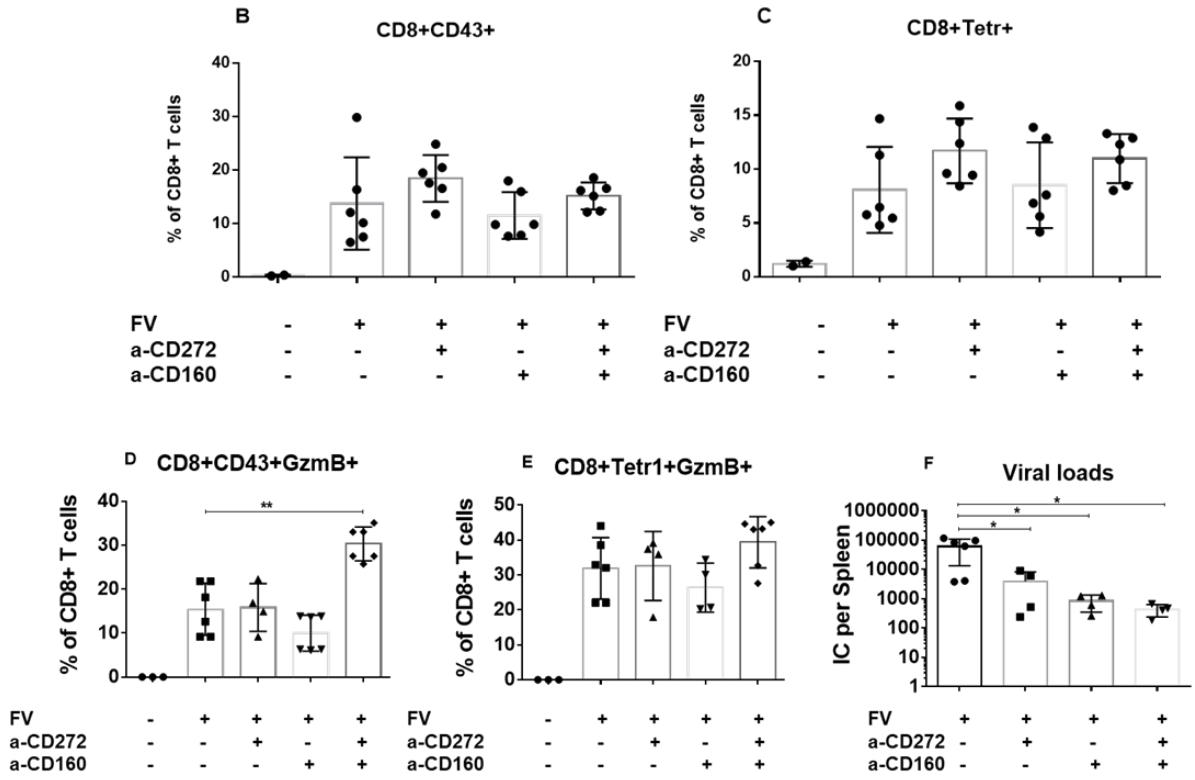

Figure 4.12 Influence of blocking the CD270 interaction with CD160 and CD272 on FV-induced effector CD8+ T cells

C57BL/6 mice were infected with FV and selective blocking of CD270 interaction with antibodies against CD160 and CD272 was performed. Splenocytes were isolated 12 days after infection and used for multi-parameter flow cytometry and quantifying infectious center (IC) levels. Interaction between CD270 and its receptors (A), selective blocking of interaction between CD270 and its inhibitory receptors CD272 and CD160 is shown. The percentages of effector CD43+CD8+ T cells (B), and virus-specific tetramer+ CD8+ T cells (C), the percentage of effector CD43+CD8+ T cells producing GzmB (D), and virus-specific tetramer+ CD8+ T cells producing GzmB (E) and the FV load in the spleen (F) are shown. Data were pooled from two independent experiments with similar results.

FV infection lead to enhanced expression of CD270 on infected granulocytes, monocytes, macrophages, and mDCs during acute phase of infection. The enhanced expression of ligands were associated with increased percentage of virus specific tetramer+ CD8+ T cells expressing CD272 and CD160. The blocking with antibodies against the interaction of CD270 with its both inhibitory

receptors resulted in reduced viral load and showed tendency towards increased percentage of effector CD8+CD43+ T cells producing GzmB and. No changes were observed on the percentage of effector and virus-specific CD8+ T cells. Hence, we speculate here that other cell population maybe involved in the regulation of interaction between CD270 and its inhibitory receptors.

4.4 Characterization of human myeloid cells after HIV-1 infection

The detailed characterization of infected subpopulations of myeloid cells in the FV model showed the enhanced expression of different inhibitory ligands (Fig. 4.4-10). Our further aim was to determine if similar inhibitory ligands were also upregulated on human myeloid cells infected with HIV-1. PBMCs from healthy volunteers were stimulated with PHA and IL-2 for two days before infection with HIV-1 and the frequency of infected cells that expressed HIV capsid protein P24 were determined by flow cytometry. The previously proposed gating strategy was again performed for the definition of the main human myeloid subpopulations (186, 187). Initially, the whole leucocytes were separated from erythrocytes and debris (Fig. 4.13A). Clumps were removed by gating on single cells (Fig. 4.13B) and dead cells were separated (Fig. 4.13C). Myeloid subpopulations were divided from the live non-myeloid cells by using the lineage markers of T cells (CD3), B cells (CD20), NK cells (CD56). Live cells were divided into monocytes (CD14+) (Fig. 4.13D), macrophages (CD11b+) (Fig. 4.13E), and mDCs (CD1c+) (Fig. 4.13F). A kinetic analysis of HIV P24 was performed in CD4+ T cells, monocytes, macrophages, and mDCs. Cells were analyzed on 3, 5, and 7 days post HIV infection. A detectible infection of all investigated cell populations was observed on day 3 after infection. The percentage of HIV-1 infected cells was highest (around 20%) in the CD4+ T cells (Fig. 4.14A) on day 7 post infection. Monocytes showed around 7.5% (Fig. 4.14B), macrophages around 5% (Fig. 4.14C) and mDCs around 9% (Fig. 4.14D) HIV-1 infected cells on day 7 post infection. The *in vitro* infection of human PBMCs indicated that myeloid cells, additionally to the main targets for HIV, could also be infected. This data correspond with *in vivo* studies which revealed monocytes and macrophages as the reservoir of HIV during chronic infection (188, 189).

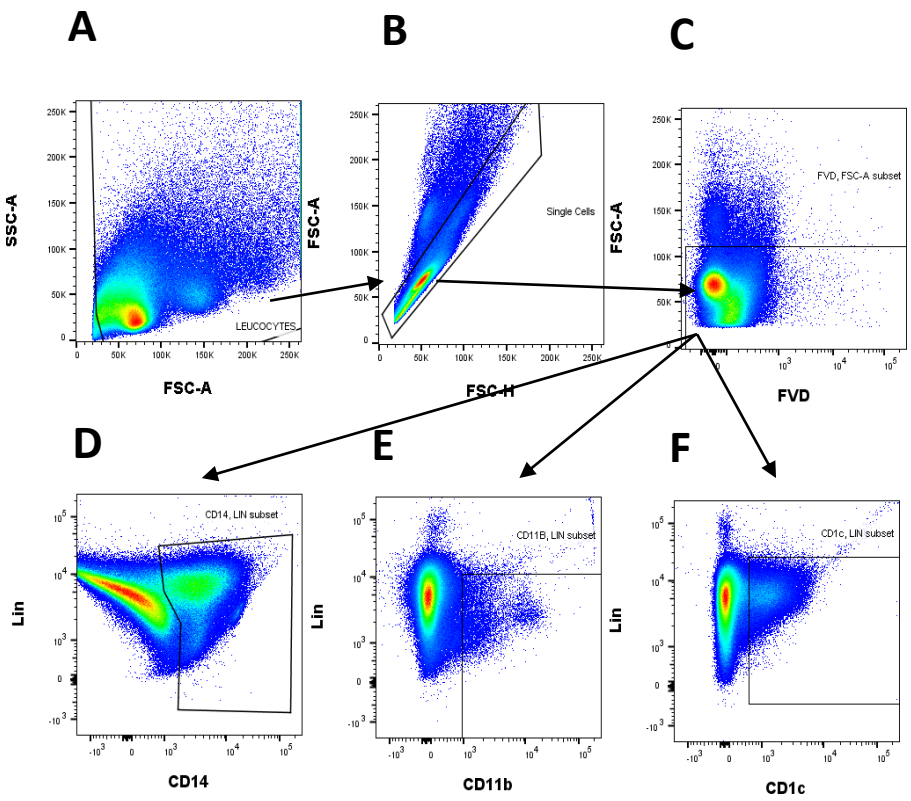

Figure 4.13 Gating strategy for the definition of myeloid subpopulations in human PBMC

Multi-parameter flow cytometry analysis was used to determine the myeloid subpopulations in human PBMCs. Dot plots of a representative human PBMCs are shown to explain the gating strategy to define the main myeloid subpopulations. The gating of whole leucocytes (FSC/SSC) (A), single cells (FSC-H/FSC-A) (B), and live cells (FVD/FSC-A) (D), and lineage (CD3, CD19, CD56) negative (Lin-) monocytes (CD14+Lin-), macrophages (CD11b+Lin-) (E), and mDCs (CD1c+Lin-) (F).

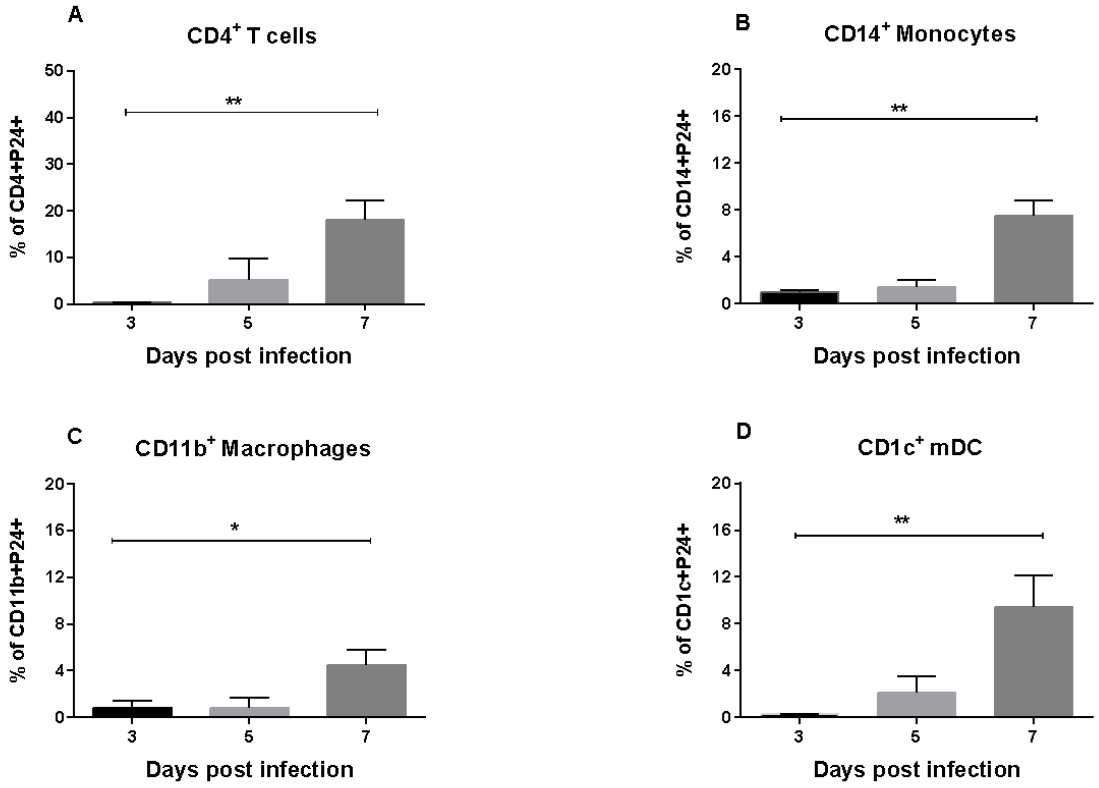

Figure 4.14 HIV in vitro infection of CD4+ T cells and myeloid subpopulations from human PBMCs

Human PBMCs were stimulated with PHA and IL-2 prior to infection with HIV-1 and were analyzed on day 3, 5, 7 after infection. Multi-parameter flow cytometry analysis was used to compare the percentage of p24 on different subpopulations of infected cells. Percentages of infected CD4+P24+ T cells (**A**), infected CD14+P24+ Monocytes (**B**), infected CD11b+P24+ Macrophages **(C)**, and infected CD1cP24+ mDCs **(D)**. Data were pooled from two different experiments. Difference between day 3, 5 and 7 were analyzed using one-way ANOVA was used with a Tukey post-test and are indicated in the figure ((*p<0.05, *p<0.005).

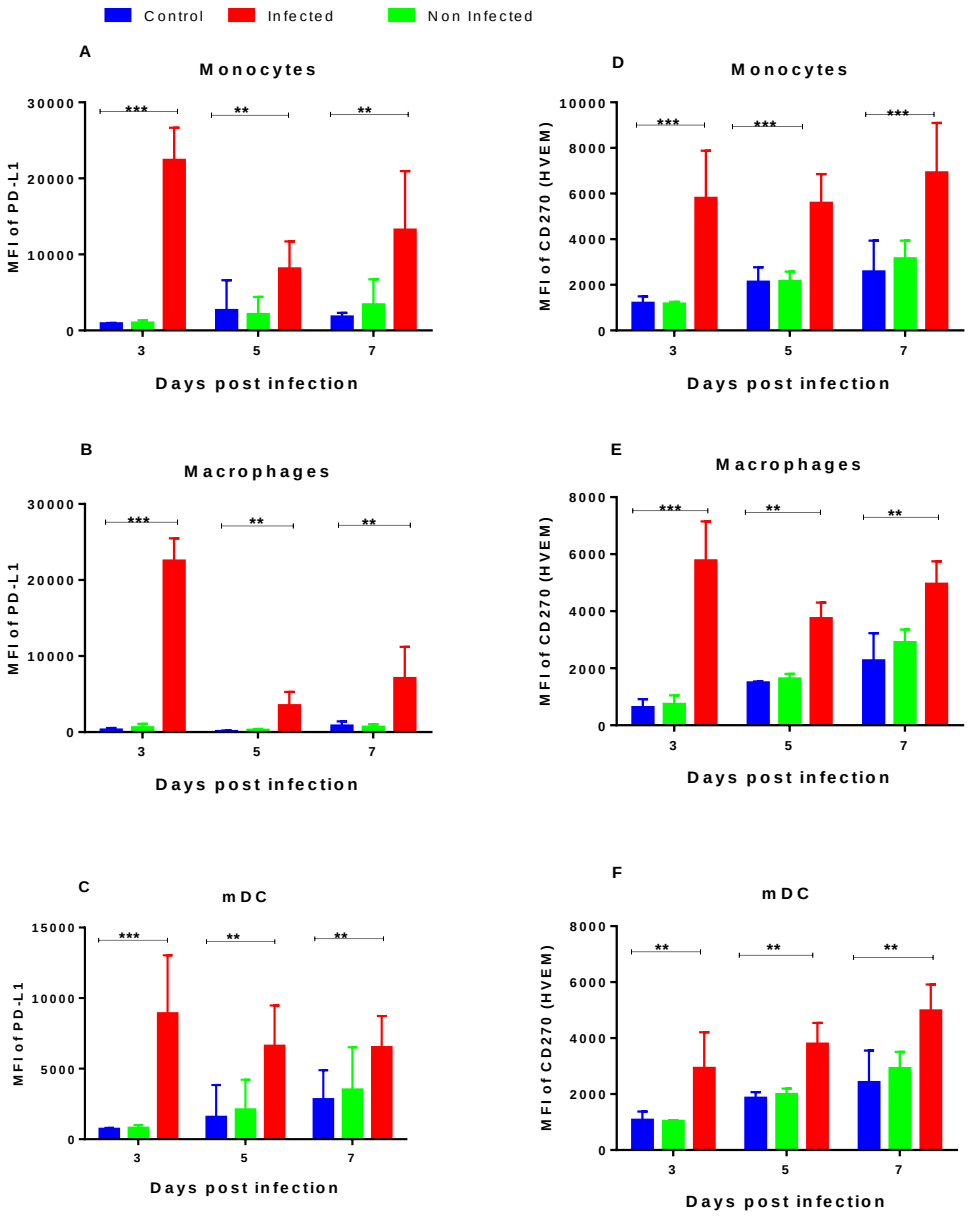

Figure 4.15 Expression of inhibitory ligands on different myeloid subpopulations in human PBMCs

Human PBMCs were stimulated with PHA and IL-2 for two days and infected with HIV-1. Multi-parameter flow cytometry analysis was used to compare the expression (MFI) of inhibitory ligands on the surface of infected (P24+), non- infected (P24-) and control (stimulated PBMCs without HIV-1 infection) myeloid cell subpopulations at 3, 5 and 7 days after infection. Mean fluorescent intensity (MFI) of PD-L1 on monocytes (A), macrophages (B) and mDCs (C). Mean fluorescent

intensity (MFI) of CD270 on monocytes (D), macrophages (E) and mDCs (F) are presented. Data were pooled from two different experiments. Difference between day 3, 5 and 7 were analyzed using one-way ANOVA was used with a Tukey post-test and are indicated in the figure ((*$p<0.05$, *$p<0.005$).

An analysis of the PD-L1 and CD270 expression on human monocytes, macrophages and mDCs after HIV-1 infection was performed. The expression of inhibitory ligands on the surface of HIV-1 infected myeloid cells (P24+) was compared with the expressions of the same ligands on the non-infected myeloid subpopulation (P24-) and both infected and non-infected cells were compared with the same subpopulation of myeloid cells from uninfected cells (control). The expression of PD-L1 on monocytes was significantly higher in the infected cells (P24+) in comparison to the non-infected (P24-) and uninfected cells on 3, 5, and 7 days post in vitro infection, and no differences were observed between the non-infected monocytes and control cells (Fig. 4.15A). On macrophages a significantly higher expression of PD-L1 was observed on infected cells (P24+) on 3, 5, and 7 days post infection in comparison to the non-infected (P24-) and control macrophages. No differences in the expression of PD-L1 were observed between the non-infected and uninfected macrophages (Fig. 4.15B). On mDCs, the expression of PD-L1 was also significantly upregulated upon HIV infection (P24+). No differences in the expression of PD-L1 was observed between the non-infected and uninfected mDCs (Fig. 4.15C).

The expression of CD270 was significantly higher in the infected monocytes (P24+) in comparison to non-infected (P24-) and control monocytes. No differences in the expression of CD270 was observed between the non-infected and control monocytes (Fig. 4.15D). On macrophages, the expression of CD270 was also significantly higher in infected cells (P24+) in comparison to the non-infected (P24-) and uninfected control monocytes (Fig. 4.15E). On mDCs, the expression of CD270 on infected cells (P24+) was again significantly higher in comparison to the non-infected (P24-) and control mDCs on 3, 5, and 7 days post infection (Fig. 4.15F).

Taken together, human myeloid cells infected with HIV-1 enhance the expression of PD-L1 and CD270 on their cell surface. Highest expression of PD-L1 was observed during early points of infection, whereas peak CD270 expression levels varied between different myeloid subpopulations. From this data, it can be speculated that HIV infection of myeloid cells induces

an increased expression of inhibitory ligands in patients, which may help the virus to evade antiviral CTL responses.

4.5 Combination treatment during acute FV infection with anti-PD-L1/anti-Tim-3 antibodies and depletion of regulatory T cells

The combination of two or more therapeutic treatments to specifically target malignancies is a cornerstone of cancer therapy (190), but also for chronic virus infections like HIV, HBV and HCV (191, 192). The combined immunotherapy targeting Tregs and inhibitory receptors previously showed high efficacy in the treatment of chronic FV (193) and LCMV infections. The following idea was to investigate if similar treatment during acute FV infection may result in complete elimination of the virus and thus preventing the establishment of viral chronicity. For the current experiments the DEREG strain of mice on C57BL/6 background was used, since these animals express the diphtheria toxin (DT) receptor under the control of the Foxp3 promoter (194). Injection of DT resulted in the specific elimination of Tregs, which was combined with an injection of blocking antibodies against PD-L1 and Tim-3. Mice were treated with either treatment alone (Treg depletion or inhibitory receptor block with the two antibodies) or a combination of both treatments. The treatment was performed during the second week of FV infection (day 7 to 13) and the spleens were analyzed directly after treatment on day 14 after infection (Fig. 4.16A).

CD8+ T cells contain granules with cytotoxic molecules, like the serine protease granzyme B (GzmB). Percentages of CD8+ GzmB+ T cells were significantly enhanced in mice receiving combination immunotherapy in comparison to any monotherapy (Fig. 4.16B). Moreover, we also analyzed whether immunotherapy induced cytotoxic CD4+ T cells. Previous studies reported that during acute FV infection virus-specific CD4+ T cells develop a Th1 or TfH-like phenotype with no signs of cytotoxic activity (195, 196). Accordingly, GzmB expression in CD4+ T cells was not detected in FV-infected mice or animals receiving either Treg or inhibitory receptor therapy, but approximately 10% of the CD4+ T cells from mice on combination therapy started to produce GzmB (Fig. 4.16C). The augmented cytotoxic T cell responses after combination treatment were expected to result in reduced viral loads in these mice. Indeed, it was associated with a dramatic reduction of FV loads (Fig. 4.16D) and in some mice of this group (about 25%) infectious virus was no longer detectable with an infectious center assay. This data suggests that combination

immunotherapy may be a promising approach for the treatment of acute virus infections, which may even prevent the establishment of viral chronicity.

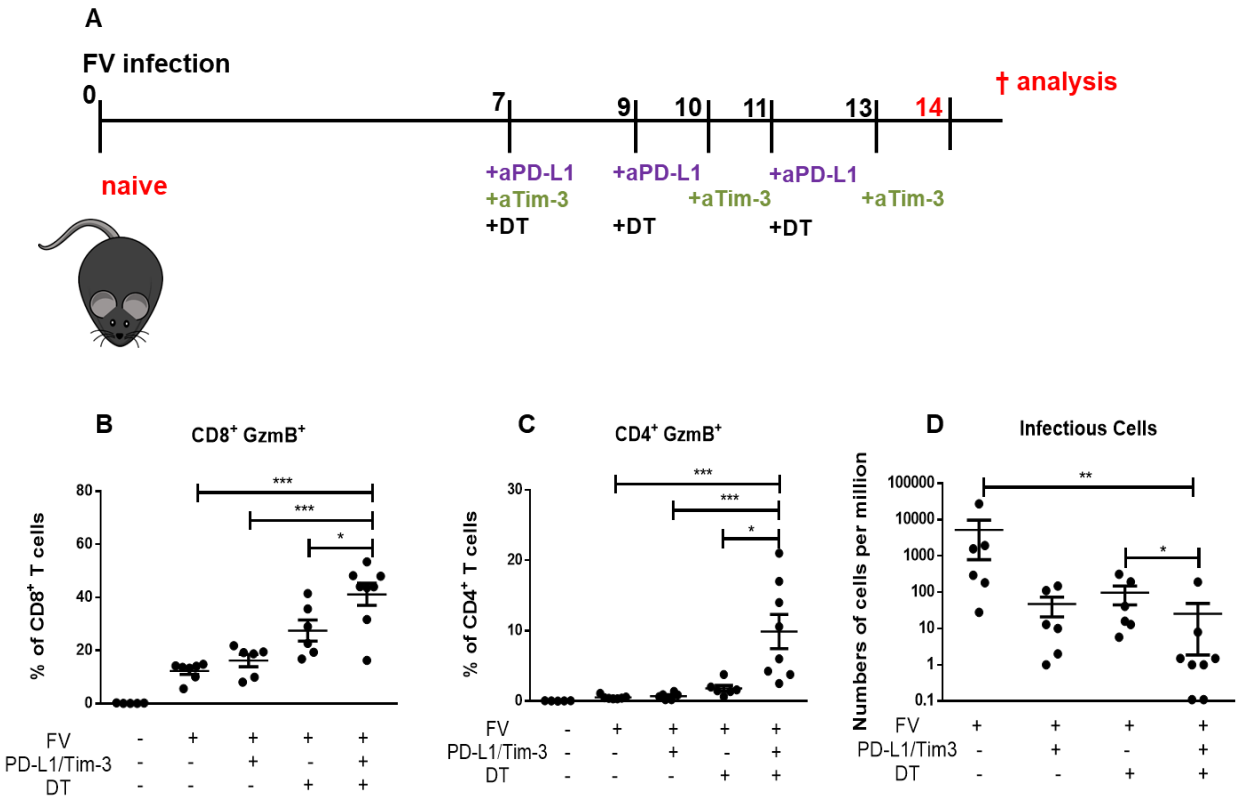

Figure 4.16. Effect of combination therapy on the production of GzmB in CD8+ and CD4+ T cells and on the replication of FV in acutely infected mice.

DEREG mice were infected with FV and treated with DT and/or blocking antibodies against PD-L1 and TIM-3 as indicated (A). Percentages of CD8+ T cells which produce the GzmB (B) and the percentages of CD4+ T cells producing the GzmB (C) were detected by flow cytometry. Spleens of FV-infected mice from the different treatment groups were analyzed for viral loads by infectious center assays one day after termination of treatment (D). Each dot represents an individual mouse. Data were pooled from 3 independent experiments with similar results. Statistically significant differences are indicated by asterisks (* < 0.05; ** < 0.005; *** < 0.0005; Non-parametric Mann-Whitney test).

4.6 Expansion of MDSCs after combination therapy

Myeloid derived suppressor cells (MDSC) are a small population (less than 3%) of cells in the myeloid colony having similarities with myeloid progenitors and precursors. Along with Tregs and inhibitory checkpoint ligands/receptors, MDSCs also have a crucial role in regulating the adaptive immune response. Suppression of immune cells is the main feature of MDSCs and T cells are their main targets (104). After analyzing the expansion of GzmB producing CD8+ and CD4+ T cells after Treg depletion and/or inhibitory pathway blockage in acutely infected mice, the next aim was to analyze the effect of combination treatment on MDSCs. Reports suggest that expansion of MDSC (109) and Tregs (197) leads to the suppression of cytotoxic CD8+ T cells. FV infection expanded the numbers of granulocytic myeloid derived suppressor cells (gMDSC) and monocytic myeloid derived suppressor cells (mMDSC) in comparison to naïve animals. Treatment with a-PD-L1/a-Tim-3 and DT alone had no significant impact on MDSC numbers. However, mice which underwent combined therapy with PD-L1/Tim-3 and depletion of Tregs presented with a significant expansion of granulocytic MDSC (gMDSC) (Fig. 4.17A) and monocytic MDSC (mMDSC) (Fig. 4.17B).

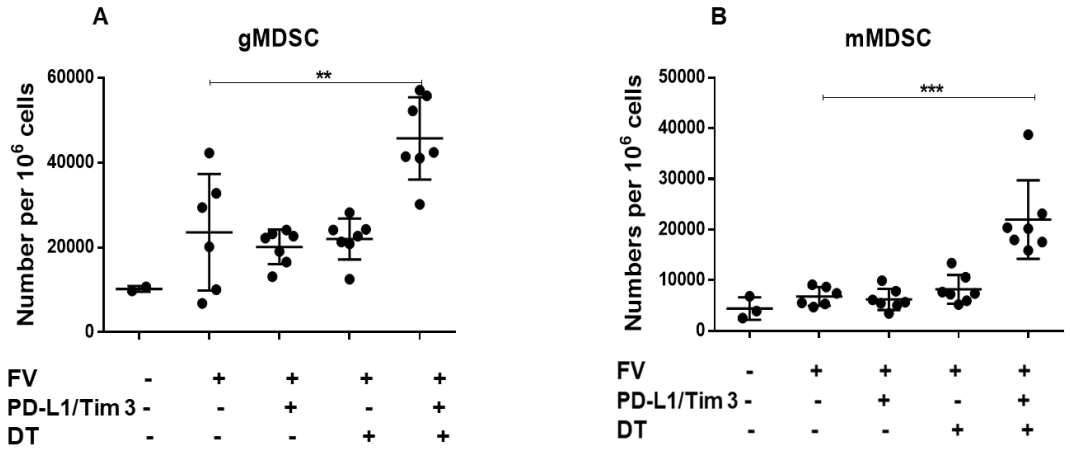

Figure 4.17. Expansion of MDSCs subset after combination therapy

DEREG mice were infected with FV and/or treated with a-PD-L1, a-Tim3 and DT. Multi-parameter flow cytometry analysis was used to determine the numbers of granulocytic myeloid derived suppressor cells (gMDSCs) (**A**), and monocytic myeloid derived suppressor cells (mMDSCs) (**B**). MDSCs per one million nucleated cells in the spleens of the naïve, FV infected,

and treated mice. Data were pooled from three independent experiments with similar results. Each dot represents an individual mouse. Differences between FV-infected and treated were analyzed using one-way ANOVA was used with a Tukey post-test and are indicated in the figure (*p<0.05, **p<0.005, ***p<0.0005).

The expression of inhibitory molecules on MDSCs is one possible mechanism of the suppression mediated by these cells. In the next step, the expression of PD-L2, CD270, MHC II, CD80, and CD86 (PD-L1 was not analyzed because it was blocked by antibody) on the surface of gMDSC and mMDSC was analyzed after combination therapy. A further aim was to analyze the role of inhibitory ligands on both subsets of gMDSC and mMDSC after treatment with a-PD-L1/a-Tim-3 and depletion of Treg alone as well as in combination. There was no difference observed in the frequency of gMDSCs, which expressed PD-L2 on their surface between treated, FV-infected non-treated and naïve mice (Fig. 4.18A). On mMDSC, a significant rise in frequencies of mMDSCs expressing PD-L2 was observed in infected mice, which increased further after combination treatment, but this was not significant (Fig. 4.18B). Treatment of FV infected mice with a-PD-L1/a-Tim-3 or depletion of Tregs alone significantly reduced the numbers of mMDSCs expressing PD-L2 on their cell surface, whereas treatment with a-PD-L1/a-Tim3 or depletion of Tregs alone or in combination had no influence on the frequencies of gMDSCs expressing PD-L2.

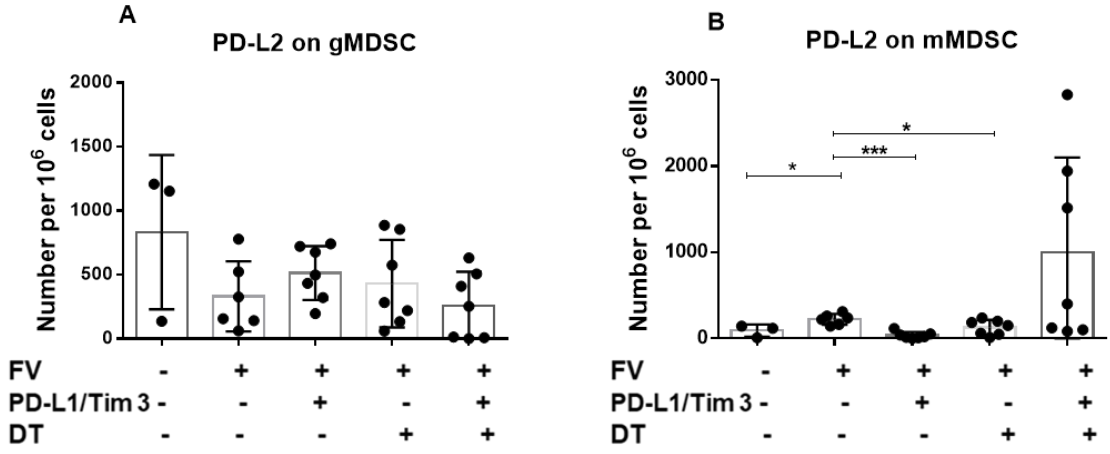

Figure 4.18 Numbers of MDSCs expressing PD-L2 on their cell surface after immune therapy

DEREG mice were infected with FV and/or treated with a-PD-L1, a-Tim3 and DT. Multi-parameter flow cytometry analysis was used to determine the numbers of gMDSCs (A) and mMDSCs (B) expressing PD-L2 per one million nucleated cells in the spleens of naïve, FV infected, and treated mice. Data were pooled from three independent experiments with similar results. Each dot represents an individual mouse. Differences between FV-infected and treated were analyzed using one-way ANOVA was used with a Tukey post-test and are indicated in the figure (*p<0.05, **p<0.005, ***p<0.0005).

Then, numbers of gMDSCs and mMDSC expressing CD270 per million spleen cells after treatment with a-PD-L1/a-Tim-3 and depletion of Tregs were analyzed. No difference in the numbers of gMDSCs expressing CD270 was observed between groups of naïve and infected animal, as well as in animals that underwent single treatment with a-PD-L1/a-Tim-3 antibodies. A significant increase in the numbers of gMDSCs expressing CD270 was observed after depletion of Tregs as well as after combined depletion of Tregs and PD-L1/Tim-3 in comparison to FV-infected non-treated animals (Fig. 4.19A). FV infected non-treated animals showed a significant increase in mMDSCs expressing CD270 in comparison to the naïve animals, and no differences were observed after single treatment with a-PD-L1/a-Tim-3 antibodies or depletion of Tregs. However, combined treatment led to a significant increase in the numbers of mMDSCs expressing CD270 (Fig. 4.19B) in comparison to FV-infected non-treated animals. Combined immunotherapy directed on Tregs and regulatory molecules PD-L1 and Tim-3 enhanced the numbers of gMDSCs and mMDSCs expressing CD270 on their cell surface.

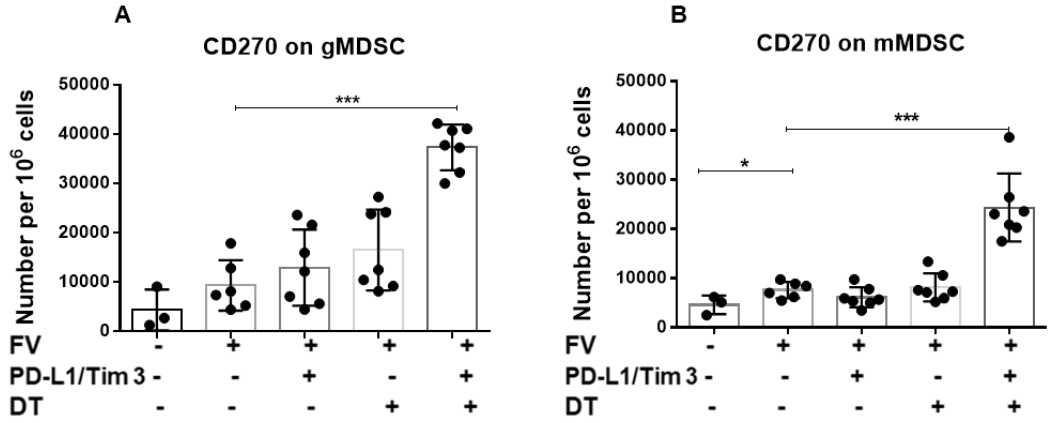

Figure 4.19 Numbers of MDSCs expressing CD270 on their cell surface after immune therapy

DEREG mice were infected with FV and/or treated with a-PD-L1, a-Tim3 and DT. Multi-parameter flow cytometry analysis was used to determine the numbers of gMDSCs (A) and mMDSCs (B) expressing CD270 per one million nucleated cells in the spleens of naïve, FV infected, and treated mice. Data were pooled from three independent experiments with similar results. Each dot represents an individual mouse. Differences between FV-infected and treated were analyzed using one-way ANOVA was used with a Tukey post-test and are indicated in the figure (*$p<0.05$, **$p<0.005$, ***$p<0.0005$).

Studies indicated the upregulation of MHC II within solid tumors (198, 199). MHC II suppresses the functionality of effector T cells after binding to the Lag-3 inhibitory receptor (200, 201). No differences were observed in the numbers of gMDSCs expressing MHC II in naïve mice and FV-infected non-treated mice as well as in the mice that underwent single treatment with a-PD-L1/a-Tim-3 antibodies or depletion of Tregs. Mice, which underwent combination treatment with a-PD-L1/a-Tim-3 and DT, had significantly higher numbers per million gMDSCs expressing MHC II than the FV-infected non-treated animals (Fig. 4.20A). A significant increase in numbers of mMDSC expressing MHC II were also observed in mice that were FV-infected non-treated in comparison to naïve mice, but no differences were observed in mice which underwent single treatment with depletion of Tregs, whereas a significant decrease in numbers of mMDSCs expressing MHC II was observed in mice treated with a-PD-L1/a-Tim3 antibodies in comparison to FV-infected non-treated mice. Mice that underwent combined treatment with a-PD-L1/a-Tim-3 antibodies and depletion of Tregs had significantly higher numbers of mMDSCs expressing MHC II in comparison to naïve mice (Fig. 4.20B).

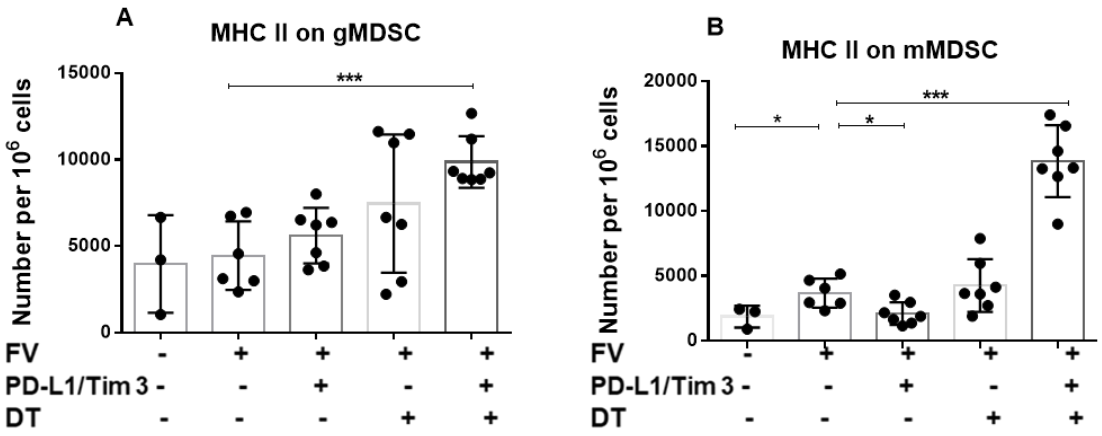

Figure 4.20 Numbers of MDSCs expressing MHC II on their cell surface after immune therapy

DEREG mice were infected with FV and/or treated with a-PD-L1, a-Tim3 and DT. Multi-parameter flow cytometry analysis was used to determine the numbers of gMDSCs (A) and mMDSCs (B) expressing MHC II per one million nucleated cells in the spleens of naïve, FV infected, and treated mice. Data were pooled from three independent experiments with similar results. Each dot represents an individual mouse. Differences between FV-infected and treated were analyzed using one-way ANOVA was used with a Tukey post-test and are indicated in the figure (*$p<0.05$, **$p<0.005$, ***$p<0.0005$).

Along with CD270, CD80 is also one of the functional molecule linked with the activation of MDSCs. CD80 is the inhibitory ligands of CTLA-4 and is located on the surface of myeloid cells. The numbers of gMDSCs expressing CD80 on naïve mice, FV-infected non-treated mice and mice which underwent single treatment with a-PD-L1/a-Tim-3 or depletion of Tregs did not show any differences. The mice that underwent combined treatment showed significant increase in the number of gMDSCs expressing CD80 in comparison to the FV-infected non-treated mice (Fig. 4.21A).The pattern of mMDSC expressing CD80 were similar to gMDSCs, no differences were observed between naïve, FV-infected non-treated and mice which underwent single treatment with a-PD-L1/a-Tim-3 antibodies and depletion of Tregs. However, the mice which underwent combination treatment had significantly higher frequencies of mMDSC expressing CD80 in comparison to the FV-infected non-treated mice (Fig. 4.21B). Combined depletion of Tregs and

treatment PD-L1/Tim3 enhanced the frequency of MDSCs subsets expressing CD80 on the cell surface.

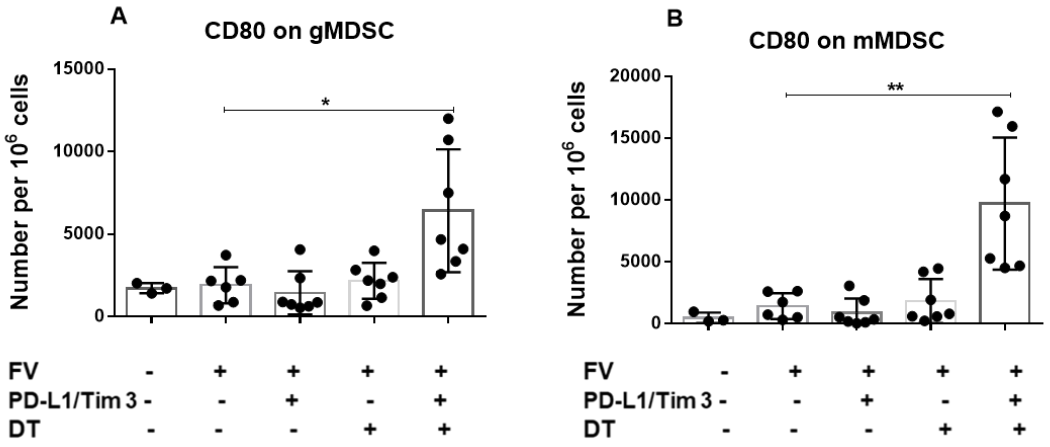

Figure 4.21 Numbers of MDSCs expressing CD80 on their cell surface.

DEREG mice were infected with FV and/or treated with a-PD-L1, a-Tim3 and DT. Multi-parameter flow cytometry analysis was used to determine the numbers per million cells of gMDSCs (A) and mMDSCs (B) expressing CD80 per one million nucleated cells in the spleens of naïve, FV infected, and treated mice. Data were pooled from three independent experiments with similar results. Each dot represents an individual mouse. Differences between FV-infected and treated were analyzed using one-way ANOVA was used with a Tukey post-test and are indicated in the figure (*$p<0.05$, **$p<0.005$, ***$p<0.0005$).

CD86 similar to CD80 binds to CTLA-4 and negatively regulates the activation of T cells (202). No differences in the number of gMDSC expressing CD86 was observed between the naive, FV-infected non-treated and treated animals (Fig. 4.22A). Similar pattern was seen in the numbers per million cells of mMDSCs expressing CD86 on their surface, however the mice which underwent combined treatment with a-PD-L1/a-Tim-3 antibodies and depletion of Tregs had significantly higher numbers of mMDSCs expressing CD86 in comparison to the naïve and treatment control mice (Fig. 4.22B). Combination treatment with a-PD-L1/a-Tim-3 and depletion of Tregs led to the enhanced mMDSCs which expressed CD86 on their cell surface.

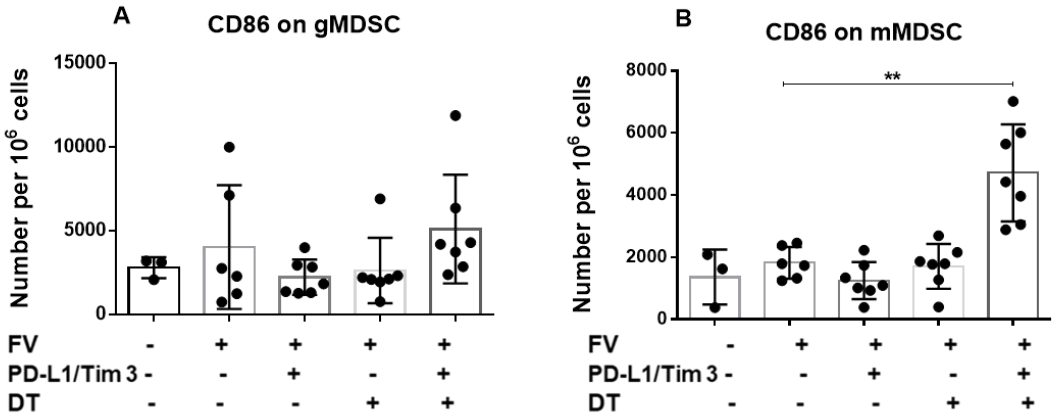

Figure 4.22 Numbers of MDSCs expressing CD86 on their cell surface

DEREG mice were infected with FV and/or treated with a-PD-L1, a-Tim3 and DT. Multi-parameter flow cytometry analysis was used to determine the numbers of gMDSCs (A) and mMDSCs (B) expressing CD86 per one million nucleated cells in the spleens of naïve, FV infected, and treated mice. Data were pooled from three independent experiments with similar results. Each dot represents an individual mouse. Differences between FV-infected non-treated and treated were analyzed using one-way ANOVA was used with a Tukey post-test and are indicated in the figure (*p<0.05, **p<0.005, ***p<0.0005).

4.7 Combination treatment directed towards checkpoint ligand/receptors and gMDCS during acute FV infection

MDCSs suppress the functionality of CD8+ T cells and interfere with the elimination of chronic FV infection (109). Thus, a therapy directed towards PD-L1/Tim3 together with targeting Ly6G for the elimination of gMDSCs is a possible strategy for the treatment of retroviral infection. We started treatment with a-PD-L1/a-Tim-3 and depletion of gMDSC at one week post FV infection (Fig. 4.23A). Mice underwent treatment with a-PD-L1/a-Tim-3 or with a-Ly6G antibodies individually or in combination during second week of infection. Treatment with a-Ly6G depleted 98% of the gMDSCs (Fig. 4.23B). Spleens from different groups of mice were weighed and the numbers of infectious centers were calculated. FV infection led to an increase in spleen weights compared to naïve mice. The single treatment with a-Ly6G or a-PD-L1/a-Tim-3 significantly decreased spleen weights and also reduced the numbers of infectious spleen cells. The combination

therapy had no additional effect on spleen weights (Fig. 4.23C) and the numbers of infectious cells were similar to the animals, which received either monotherapy (Fig. 4.23D).

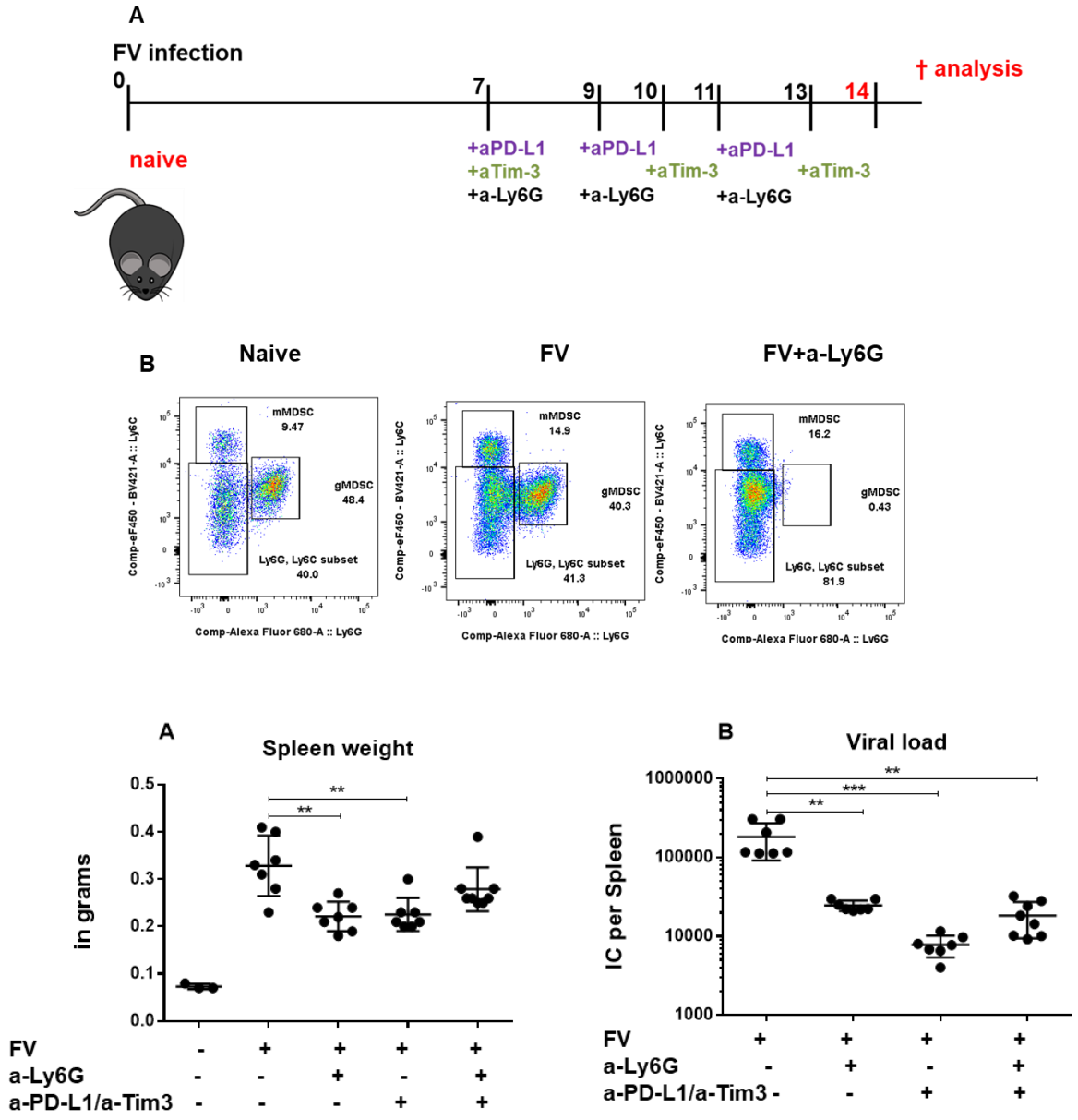

Figure 4.23 Effect of combination therapy directed towards MDSCs and PD-L1/Tim3 on FV replication

Mice were infected with FV and treated with a-PD-L1/a-Tim3 and a-Ly6G alone or in combination. Spleen weight and numbers of infectious cells in the spleen were determined after 14 days of infection. (**A**) Experimental design of FV infection and treatment with α-PD-L1/α-Tim-

3 and α-Ly6G antibodies. (B) Representative dot plots of MDSC after treatment with α-PD-L1/α-Tim-3 and α-Ly6G antibodies, (C) the spleen weights, (**D**) infectious centers per spleen are presented. Differences between FV-infected non-treated and treated mice were analyzed using one-way ANOVA was used with a Tukey post-test and are indicated in the figure (*$p<0.05$, **$p<0.005$, ***$p<0.0005$).

gMDSCs suppress the functionality of cytotoxic CD8+ T cells during FV infection (109). Thus, a combination therapy targeting gMDSCs and inhibiting receptors may promote the expansion of virus-specific effector CD8+ T cells. In order to test this, the CD8+ T cell population was analyzed after treatment with a-PD-L1/a-Tim-3 and depletion of gMDSC. FV infection leads to virus induced activation of cytotoxic CD8+ T cells, which can be detected at one week post infection (Fig. 4.24A) and results in decline of viral loads (Fig. 4.23B). Treatment with a-PD-L1/a-Tim-3 enhanced the immune response by expanding virus specific effector CD8+ T cells and also enhanced the production of cytotoxic molecules by these cells. Treatment with a-Ly6G showed no additional effect on effector CD43+CD8+ or virus specific tetramer+ CD8+ T cells. (Treatment with a-PD-L1/a-Tim-3 enhanced the expansion of effector CD43+CD8+ (Fig. 4.24A) and virus-specific tetramer+ CD8+ T cells (Fig. 4.24B). Treatment with a-PD-L1/a-Tim-3 antibodies enhanced the frequencies of CD43+CD8+ effector cells producing GzmA (Fig. 4.24C) and GzmB (Fig. 4.24D).

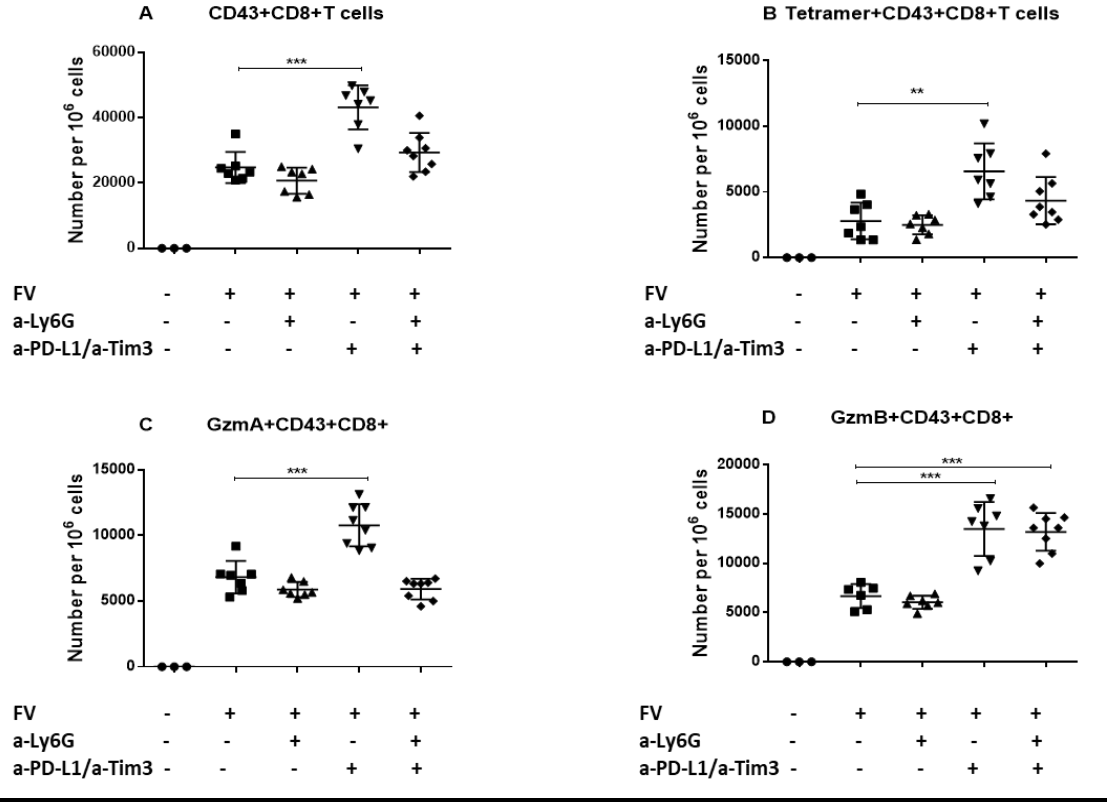

Figure 4.24 Numbers of CD8$^+$ T cells expressing cytotoxic molecules during acute FV infection after combination therapy

C57/BL6 mice were infected FV and/or treated with a-PD-L1, a-Tim3 and a-Ly6G. Effector CD43+CD8+ T cells and virus specific tetramer+ CD8+ T cells were detected by flow cytometry and viral loads in spleen were estimated after 14 days of infection. The frequencies of CD8+CD43+ effector T cells (**A**), the frequencies of virus specific Tetramer+CD8+ T cells (**B**), and frequencies of CD8+CD43+ T cells producing GzmA (**C**) and GzmB (**D**) were calculated per one million nucleated cells in the spleen. Differences between FV-infected mice without treatment and treated animals were analyzed using one-way ANOVA with a Tukey post-test and are indicated in the figure (*p<0.05, **p<0.005, ***p<0.0005).

4.8 Proliferation of effector CD8+ T cells after combination treatment during FV infection

The activation of effector CD8+ T cells due to an infection leads to enhanced proliferation of these cells. In order to define the proliferation of CD8+ T cells the intracellular expression of Ki67 was analyzed. Ki67 is a nuclear protein and a marker for cell proliferation (203). Mice depleted of

gMDSC showed enhanced proliferation of effector CD43+CD8+ T cells in comparison to FV-infected non-treated mice. Treatment with a-PD-L1/a-Tim-3 antibodies significantly enhanced proliferation of CD8+CD43+ effector T cells in comparison to the FV-infected non-treated mice. Surprisingly the mice that underwent combination treatment had similar frequencies of proliferating Ki67+ CD43+ CD8+ T cells as FV-infected non-treated mice (Fig. 4.25).

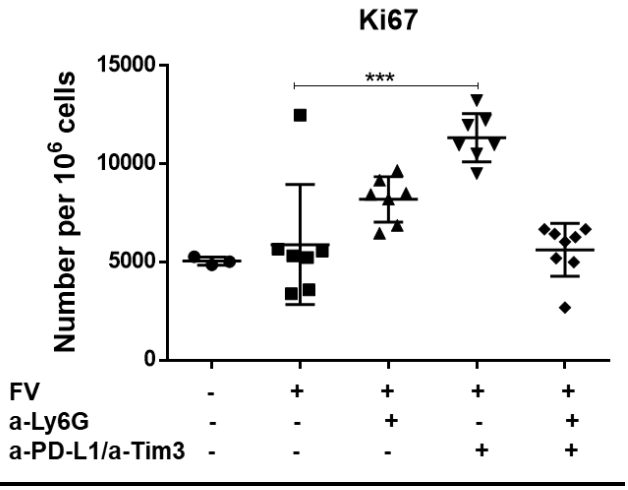

Figure 4.25 Proliferation of effector CD8+ T cells after treatment during acute FV infection

C57/BL6 mice were infected with FV and treated with a-Ly6G, anti-PD-L1/a-Tim-3. The numbers of the CD8+ T cells expressing Ki67 per one million nucleated spleen cells were determined at day 14 after FV infection using flow cytometry. A three independent experiments were performed. Differences between FV-infected non-treated and treated were analyzed using one-way ANOVA was used with a Tukey post-test and are indicated in the figure (*$p<0.05$, **$p<0.005$, ***$p<0.0005$).

IL-2, IFN-γ and TNF-α are inflammatory cytokines produced by activated CD8+ T cells. The effector CD43+CD8+ T cell population producing antiviral cytokines was analyzed after treatment with a-PD-L1/a-Tim-3 and/or depletion of gMDSC during FV infection. FV infection led to the induction of CD43+CD8+ effector cells producing inflammatory cytokines (Fig. 4.26A, B, and C). Enhanced numbers of effector CD43+CD8+ T cells produced IFN-γ in the absence of gMDSCs (Fig. 4.26A), but depletion of gMDSC showed no effects on the production of IL-2 (Fig. 4.26B) or TNF-α (Fig. 4.26C). Treatment with a-PD-L1/a-Tim-3 significantly increased the numbers of CD43+CD8+ T cells producing IFN-g (4984 cells/10^6) and TNF-α (28396 cells/10^6) in comparison

to FV-infected non-treated mice. However, no significant differences were observed for IL-2 producing cells (Fig. 4.26B) on FV-infected non-treated mice in comparison to naïve mice. No difference in the frequencies of effector CD8+ T cells producing IL-2 were detected between FV-infected non-treated mice and the mice which underwent individual and combined treatment with a-Ly6G, a-PD-L1/a-Tim-3. Thus, the combination therapy directed towards gMDSCs and PD-L1/Tim3 had no enhancing effects on the production of inflammatory cytokines in comparison to the treatment with a-PD-L1/a-Tim-3 treatment alone.

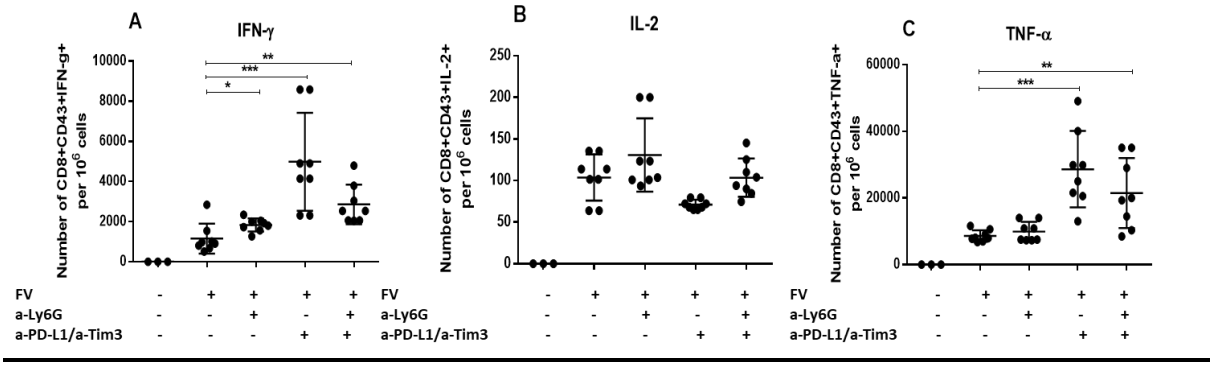

Figure 4.26 Production of cytokines by CD43+CD8+ effector T cells after combination treatment directed towards a-PD-L1/a-Tim-3 and a-Ly6G

C57/BL6 mice were infected with FV and treated with a-PD-L1/a-Tim3 and a-Ly6G. Proinflammatory cytokines produced by CD43+CD8+ effector T cells in spleen were measured using flow cytometry at day 14 after infection. Number of CD8+CD43+ effector T cells per one million nucleated spleen cells producing IFN-γ (**A**), IL-2 (**B**), and TNF-α (**C**) are displayed. Data were pooled from three independent experiments. Differences between FV-infected non-treated and treated mice were analyzed using one-way ANOVA was used with a Tukey post-test and are indicated in the figure (*$p<0.05$, **$p<0.005$, ***$p<0.0005$).

4.9 Expansion of regulatory T cells after treatment with anti-PD-L1/anti-Tim-3 and anti-Ly6G antibodies

In previous experiments it was observed that the depletion of Tregs leads to a strong expansion of MDSCs, which was potentiated by additional treatment directed against inhibitory checkpoint molecules. In order to investigate if depletion of gMDSCs leads to the expansion of Tregs, we analyzed FV infected mice after the combination treatment with a-PD-L1/a-Tim-3 and anti-Ly6G

antibodies at day 14 after infection. FV infection significantly enhanced the percentage of CD4+ T cells expressing FoxP3 in infected spleens in comparison to spleens of naïve mice. Depletion of gMDSC significantly reduced the percentage of CD4+ T cells expressing FoxP3 in comparison to FV-infected non-treated mice. Treatment with a-PD-L1/a-Tim-3 also resulted in a significant reduction in the percentage of Tregs in comparison to FV-infected non-treated. Combined treatment with a-PD-L1/a-Tim-3 and depletion of gMDSC led to a significant decrease in the percentage (Fig. 4.27) of CD4+ T cells expressing FoxP3 in comparison to non-treated FV infected mice.

CD39 and CD73 are ectonucleatidases enzymes (204), which are crucial for the immunosuppressive activity of Tregs (167) and FV infection significantly enhanced the percentage of CD4+FoxP3+ Tregs expressing CD39 and CD73 in comparison to the naive mice. Depletion of gMDSC and treatment with -PD-L1/a-Tim-3 did not have any effect on the expression of CD39 (Fig. 4.28A) or CD73 (Fig. 4.28B) on the surface of CD4+FoxP3+ Tregs. The combination treatment had also no effect on the percentage of Tregs that expressed CD39 or CD73.

TNFR2 is one receptor for TNFα (205). TNFR2 induces nuclear factor kappa B (NF-kB) and leads to the activation of Tregs and proliferation of these cells after binding to TNFα (206). FV infection enhanced the expression of TNFR2 on CD4+Foxp3+ Tregs in comparison to naïve animals (Fig. 4.28C), but depletion of gMDSCs or treatment with a-PD-L1/a-Tim-3 significantly decreased the percentage of CD4+FoxP3+ Tregs expressing TNFR2. The combination of a-PD-L1/a-Tim-3 treatment with depletion of gMDSCs was also associated with a reduced frequency of CD4+FoxP3+ Tregs expressing TNFR2 in comparison to FV-infected non-treated mice (Fig. 4.28C).

Vβ5+ Tregs are specific for the mouse endogenous retrovirus superantigen (MMTV Sag) and become activated and proliferate in response to FV infection (207). FV infection induced a significant increase in the percentage of CD4+FoxP3+ Tregs expressing Vβ5 in comparison to naïve mice. In mice treated with a-Ly6G the expansion of CD4+FoxP3+Vβ5+ Tregs was not augmented. In contrast, treatment with a-PD-L1/a-Tim-3 significantly increased the percentage of CD4+FoxP3+ that expressed Vβ5 in comparison to FV infected non-treated mice. Combined treatment with a-PD-L1/a-Tim-3 and depletion of gMDSC did not show any difference in comparison to the FV infected mice (Fig 4.28D). Thus, the combination therapy during acute retroviral infection directed against gMDSCs and PD-L1/Tim3 checkpoint molecules was

associated with reduced expansion of Tregs. This is an interesting feature, which may be applied for the development of immunomodulation protocols for the therapy of viral infections and malignancies.

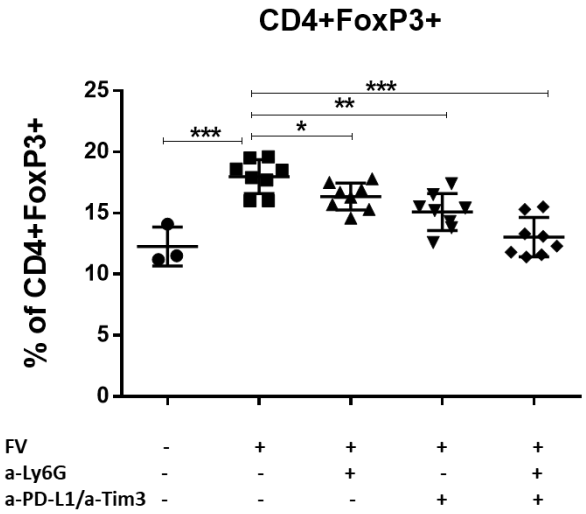

Figure 4.27 Regulatory T cell responses after combination treatment in FV infected mice

C57/BL6 mice were infected with FV and/or treated with a-PD-L1, a-Tim3 and a-Ly6G. Multicolor flow cytometry was used for detection regulatory CD4+ Foxp3+ T cells at day 14 after FV infection. The percentage of CD4+ T cells expressing FoxP3+is presented. Differences between naïve, FV-infected non-treated and treated were analyzed using one-way ANOVA with a Tukey post-test and are indicated in the figure (*$p<0.05$, **$p<0.005$, ***$p<0.0005$).

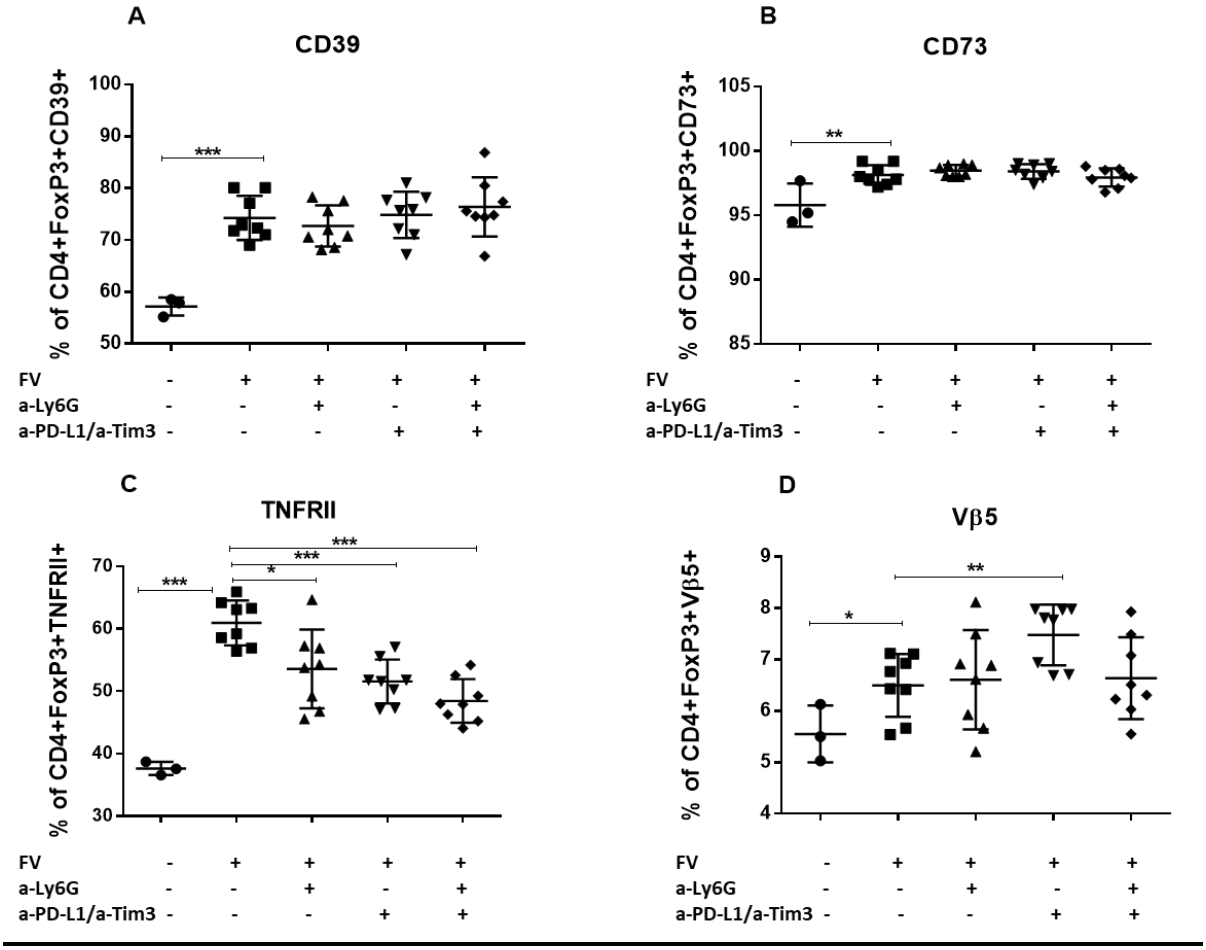

Figure 4.28 Phenotypes of Tregs cells

C57/BL6 mice were infected with FV and/or treated with a-PD-L1/a-Tim3 and a-Ly6G. Multicolor flow cytometry was used for detection and phenotypic characterization of regulatory CD4+ Foxp3+ T cells at day 14 after FV infection. Percentage of CD4+FoxP3+ expressing CD39+ (**A**), +CD73+ (**B**), TNFR II+ (**C**), and Vβ5+ (**D**) on their cell surface are presented. Data were pooled from three identical experiments. Differences between naïve, FV infected non-treated and treated animals were analyzed using one-way ANOVA was used with a Tukey post-test and are indicated in the figure (*p<0.05, **p<0.005, ***p<0.0005).

5. Discussion

Expression of inhibitory ligands on infected myeloid cells during acute retrovirus infection

Myeloid cells are vital part of the innate immune system, as they initiate and regulate the adaptive immune response against viral infections. However, different viruses misuse the myeloid cells as targets cells, which increase viral replication and viral dissemination in the body. Moreover, some subpopulations of myeloid cells promote the enhanced replication of viruses and are important part of viral pathogenesis. For example the infection of CD169 positive macrophages was associated with enforced viral replication vesicular stomatitis virus (VSV) (208) and LCMV (209) . During HIV infection, myeloid cells play an important role in the viral pathogenesis by enabling viral spread during early infection and as the reservoir of virus during chronic phase of infection (reviewed in (210)). Immature mucosal dendritic cells encounter HIV (211-213), migrate to LNs and transmit virus to CD4+ T cells (98, 214, 215). During chronic HIV infection follicular DCs (216-218) and tissue macrophages are an important reservoir for viral persistence (219-221).

Understanding the interactions between infected myeloid cells and antiviral effector cells might be very important for the development of a cure of retroviral infections. The infection of mice with FV is a unique model for the characterization of antiviral innate and adaptive immunity. Earlier studies with FV have shown that erythroid precursor cells (erythroblast) are the main targets for FV during acute infection. However, myeloid cells are part of the viral reservoir during acute and chronic virus infection (4, 175). Adaptive CD8+ T cells are able to efficiently eliminate infected erythroblasts, however myeloid cells escape from killing by expressing PD-L1 and persist during the late phase of infection (175). The current study analyzed the kinetics of FV infection in different myeloid subpopulations and showed that granulocytes and monocytes were the main targets for the virus (Fig. 4.3 A-D). A small part of the macrophages and mDCs were also infected with FV (Fig. 4.3 E-H). FV infection led to a significant decrease of all myeloid subpopulations at day 10 and 12 post infection (Fig. 4.2). Interestingly, reduced granulocyte counts were also observed in 50 % of HIV-1 infected patients and was associated with advanced disease progression including lower CD4+ T cells count and higher HIV-1 RNA levels (79, 222). Decline of neutrophil counts and function has severe impact on HIV-1 infection (223, 224). The expanded cytotoxic CD8+ T cells mediated the elimination of FV infected cells during acute phase of infection (225). Thus, the population of virus-specific CD8+ T cells participated in the significant reduction of

myeloid subpopulations on day 10 and 12 in FV infected spleens (Fig. 4.2). Why the part of infected myeloid cells escape the CD8+ T cell mediated killing and stay the reservoir for viral replication during chronic infection? The answer to this question could provide new ideas for the development of future therapies for acute and chronic retroviral infection.

Inhibitory receptors expressed on the cell surface of virus-specific CD8+ T cells regulates the effector functions of these cells during acute and chronic viral infections (137, 226, 227). Expectedly the expression of inhibitory ligands for these receptors on the infected target cells may protect these cells for the elimination mediated by virus-specific CD8+ T cells. PD-L1 and PD-L2 are the ligands of the most powerful inhibitory receptor PD-1 (228-230). The importance of PD-1/PD-L1 interactions for the regulation of the acute antiviral CD8+ T cell response was demonstrated in the FV model (136, 231).

The accumulation of infected B cells and infected Gr-1+ myeloid cells expressed high level of PD-L1 which was associated with the development of dysfunctional effector cells. In this way myeloid cells become the reservoir for persistent viral replication (175). In order to extend our knowledge about the possible role of inhibitory ligands expressed on individual subpopulations of myeloid cells, we characterized the expression of different inhibitory ligands on subpopulations of infected and non-infected myeloid cells during acute FV infection *in vivo* (Fig. 4.4 - 4.10) and HIV infection *in vitro* (Fig.4.15). The expression of inhibitory ligands on infected and non-infected cells was compared with one another and with a reference to myeloid subpopulation isolated from naïve mice. Subsequently, virus specific CD8+ T cells were also characterized for the expression of different inhibitory receptors. FV infected granulocytes, monocytes, macrophages and mDCs enhanced the expression of PD-L1 in comparison to non-infected subpopulations of myeloid cells and corresponding myeloid cells from naïve mice (Fig. 4.4 A-D). In granulocytes the enhancement of PD-L1 expression was observed on day 10 after infection and also at later time point. On remaining populations of infected myeloid cells the enhanced expression of PD-L1 was observed from day 6 onwards after infection. In previous studies it was shown that the enhanced expression of PD-L1 on infected cells was upregulated directly by virus during early infection. Thus, infected monocytes, macrophages and mDCs enhanced the expression of PD-L1 after FV infection. Interestingly, all *in vitro* HIV infected monocytes, macrophages and mDCs enhanced the expression of PD-L1 (Fig. 4.15 A-C). Thus, we observed the direct effect of retroviral infection of

myeloid cells on the expression of PD-L1. Similar to our results enhanced expression of PD-L1 was also observed on monocytes and DCs during HIV infection (232) and treatment with ART was associated with decreased expression of PD-L1 on monocytes (233) and mDCs (234). Increased expression of PD-L1 was also observed on monocytes from HIV-infected patients, and was regulated by type I IFN (235). HIV *in vitro* data showed that incubation of macrophages with the virus upregulated the expression of PD-L1 and PD-L2 (236). The upregulation of PD-L1 and PD-L2 on mDCs and macrophages was regulated by the HIV accessory protein nef (237), whereas other group showed that the upregulation of PD-L1 on mDCs during chronic HIV infection was induced by HIV-1 tat protein (238) (239). Thus, the infection of myeloid cells with retroviruses enhances PD-L1 expression. In our study of FV infected granulocytes and monocytes, it was observed that the second stage of PD-L1 expression was associated with functionality of effector CD8+ T cells. We also characterized the expression of the second ligand for the PD-1 receptor PD-L2. This molecule is mainly expressed on antigen presenting cells and can be enhanced on various myeloid cells by different inflammatory factors (178). FV infected macrophages and mDCs enhanced the expression of PD-L2 in comparison to non-infected cells from infected mice and cells from naïve mice (Fig. 4.5). The level of PD-L2 expression on all characterized infected myeloid subpopulation was significantly upraised from day 10 after infection. Thus, the effect of cytotoxic CD8+ T cells may also be responsible for the upregulation of PD-L2 on populations of infected cells. The expression pattern of PD-L2 and PD-L1 was similar on infected granulocytes and mDCs but different on monocytes and macrophages. Our data matched the already existing data on PD-L2 expression on myeloid cells. Increased expression of PD-L2 was observed on DCs and macrophages on exposure to IL-10, IL-4, IFN-γ and TLR ligands (236, 240, 241). The upregulation of PD-L2 on different cell populations was previously observed after infection with RSV (242), papilloma virus (243), avian oncovirus Marek's disease virus (244) and hantavirus (245). However, the data about the effects of PD-L2 on T cell response remains controversial. Some studies show that the enhancement of PD-L2 was due to the activation of CD8+ T cells (246, 247). PD-L2 acts as an adjusting molecule that can enhance CTL and Th1 responses (248). Other studies show the opposite effects. The enhanced expression of PD-L2 in human esophageal cancer and hepatocellular carcinoma (HCC) was associated with impaired disease free survival and poor prognosis (249-251). The simultaneous analysis of the expression of inhibitory ligands PD-L1 and PD-L2 on infected myeloid cells and the expansion of CD8+ T cells which expressed PD-1 could

provide us with additional evidence about the interaction of effector T cells and target infected cells during viral infection. The accumulation of infected myeloid cells with high expression of PD-L1 and PD-L2 have strong effect for the development on the dysfunction of CD8+ T cells during late phase of retroviral infection. The effects of the PD-1 signaling on virus-specific CD8+ T cell during acute FV infection was recently characterized in detail by utilizing mice which were deficient of PD-1 or of PD-L1 molecules (231). PD-1 or PD-L1 knockout mice showed increased functionality of virus-specific CD8+ T cells in comparison to wild type animals. The enhanced CD8+ T cell responses were associated with better control of virus replication. The enhanced proliferation and diminished apoptosis of effector CD8+ T cells was observed in PD-1or PD-L1 knockout animals (231). The PD-1 signaling also regulated the production of different Gzm's in the CD8+ T cells and thus determined its cytotoxicity. Thus, the negative signals, which effector CD8+PD-1+ T cells receive after repeated interactions with myeloid cells expressing high level of PD-L1 and PD-L2, contribute to the dysfunction and death of effector cells.

Similar to PD-1 receptor, there are numbers of other checkpoint receptors which are expressed on activated effector lymphocytes and exert inhibitory effects. For example CD272 and CD160 are the inhibitory receptors of CD270 ligand (185). Engagement of CD270 to LIGHT and LTα provides co-stimulatory signaling to effector cells (179, 185, 252). Most of the data about the functional effect of CD270 and its receptors are obtained from different tumor models. The role of this regulatory pathways during viral infections is not completely understood. Enhanced expression of CD270 was observed on colorectal cancer (CRC) cells and is a biomarker of poor prognosis for disease progression. The expression of CD270 acts as a biomarker, which is inversely correlated with numbers of tumor infiltrating T cells (253). The increase of the CD270 expression was observed in melanoma and was related with poor overall survival (254). It was reported that binding of CD272 to CD270 led to the reduction in T cell activation and proliferation (255). CD270 expressed on tumor cells during chronic lymphocytic leukemia (CLL) in cooperation with other inhibitory ligands dysregulated the polarization of effector T cells (256). In this way it impairs the formation of cytotoxic synapses between CTLs and tumor, and malignant cells escaped the elimination. Increased expression of CD160 on CD8+ T cells associated with reduced proliferation and perforin production which finally results in functional impairment of CD8+ T cells (257). The simultaneous analysis of inhibitory ligand CD270 on FV infected subpopulations of myeloid cells and the expression of inhibitory receptors on effector CD8+ T

cells contribute to our understandings of this regulatory mechanisms during adaptive immune response against retroviral pathogen. The enhanced expression of CD270 on infected macrophages and mDCs was observed at every characterized time point of infection (Fig. 4.6 C, D). FV infected granulocytes and monocytes enhanced the expression of CD270 at day 10 and 12 after infection (Fig. 4.6 A, B). The part of expanded virus-specific CD8+ T cells expressed inhibitory receptors CD160 (Fig. 4.11C) and CD272 (Fig. 4.11B). The pattern of the expression kinetics of inhibitory ligand CD270 on infected myeloid subpopulation was very similar to the expression kinetics of PD-L1. Moreover, the expression of inhibitory receptors on virus-specific CD8+ T cells provide the assumption that CD270 have the similar effects on elimination of infected cells and on the development of T cell dysfunction like PD-L1. However the interaction of CD270 with their inhibitory receptors has different effect in different infection models. Upregulation of CD160 on exhausted antigen specific CD8+ T cells was observed during chronic LCMV infection (142, 258). CD8+ T cells upregulate CD160 on cell surface during HIV infection (259). The co-expression of PD-1 and CD160 on population of HIV-specific CD8+ T cells was associated with advanced effector dysfunctionality of T cells (260). However, elite controllers had significantly higher frequencies of CD8+PD1-CD160+ T cells in comparison to naïve and HAART treated HIV patients (155). Interestingly, CD8+ T cell response against malaria was associated with the expression of CD160 and CD272 and lead to dysfunction of cytotoxic CD8+ T cells (254, 261). The deficiency of CD270 or CD272 during vaccinia virus infection impaired the CD8+ T cell response against pathogen and reduced the differentiation of memory cells (262). Thus, the contradictory data obtained from these infection models indicates that it was necessary to perform additional experiments to clarify the functional role of these molecules during immune response against retroviruses.

In order to determine which effects induced the interaction of CD270 with its inhibitory receptors expressed on effector CD8+ T cells, the binding of CD270 with its inhibitory receptors were prevented by treatment with two antibodies. The treatment with both antibodies, which block the interactions between CD270 and its inhibitory receptors, was performed individually and in combination was performed during acute FV infection. Treatment with antibodies which prevented the interaction of CD270 with CD272 or CD160 reduced the viral loads in treated mice in comparison to non-treated animals (Fig. 4.12F). This effect was potentiated by the application of both antibodies in combination. The expansion of virus-induced effector CD8+ T cells and virus-

specific CD8+ T cells was not changed after treatment with antibodies. However, the combination of both antibodies led to tendency of the enhanced production of GzmB in population of effector CD8+ T cells. It could be possible that other cells were involved in elimination of FV during the antibody treatment directed on CD270. In the future, in treatment experiments directed on CD270 will be necessary to characterize the expansion of effector CD4+ T cells and on NK cells. Previously it was shown that interaction of CD270 to its inhibitory receptors CD160 and CD272 results in the inhibition of T cells and NK cells functions (179). Some studies analyzed the effects of individual blocking of interactions CD270 with its inhibitory receptors expressed on T cells. Blocking the interaction between CD160 and CD270 restored the proliferative capacity of human CD8+ T cells *in vitro* (257). Moreover, blocking the interaction between CD270 and CD160 rescued CMV and HIV-specific CD8+ T cell proliferation and cytokine production (260). Blockade of CD272 interaction with CD270 promoted survival and memory generation of CD8+ T cells (263). Subpopulations of infected myeloid cells enhanced the expression CD270 (Fig. 4.6), and simultaneously the effector CD8+ T cells expressed both inhibitory receptors for CD270 (Fig. 4.12 B & C). Both the inhibitory receptors of CD270 are associated with inhibition of T cells. CD272 has been described to inhibit T cell responses (255), whereas CD160 is associated with impairment of CD8+ T cell function and is independent of PD-1 expression (257). Thus, blocking the interactions between ligand CD270 and its both inhibitory receptors CD272 and CD160 could possibly be a new strategy for immunotherapy against viral infections and cancers. Moreover, our study provides new insights on the role of this regulation during acute immune response against retroviruses.

CD200 is the ligand for inhibitory CD200R receptor. In our study we performed detailed characterization of CD200 expression on myeloid cells and subsequently its receptor on virus-specific CD8+ T cells. One third of expanded virus-specific CD8+ T cells express CD200R at day 8 after infection. Later the numbers of cells expressed CD200R were declined (Fig. 4.11E). FV infection enhanced the expression of CD200 on infected granulocytes during acute phase of infection. At same time the expressions of CD200 on non-infected granulocytes remain unchanged. From all remaining myeloid subpopulation the enhanced expression of CD200 was observed only on mDCs at day 6 and day 8 after infection (Fig. 4.9A). Previous study showed the CD200 expression on endothelial cells, neurons and lymphocytes (264-266). Some studies have indicated the inhibitory role of CD200/CD200R interactions during T cell exhaustion (267). Our

data suggest that this pathway may also be involved in the regulation of virus-specific CD8+ T cells during early acute response against retroviruses. Previously the increased expression of CD200 was observed in mouse EMT6 breast cancer cells and was associated with increase in tumor growth and metastasis. The inhibition of CD200 reduced tumor growth (268). The expression of CD200R was observed on myeloid cells, B and T lymphocytes (266). The interaction between CD200 and CD200R regulates the lung inflammation during influenza infection (267). Further study with a focus on the role of CD200-CD200R interaction during acute and chronic infection may boost our understanding about immune regulation of adaptive T cell response and could provide insights in designing immunomodulatory therapies.

The different inhibitory checkpoint receptors are simultaneously expressed on surface of cytotoxic effector cells. Assumingly, the signals from these receptors may regulate the functionality of these potentially dangerous cells during immune response in infected organs. The detailed analysis of the expression of inhibitory receptors on virus-specific CD8+ T cells can provide a hint about the potential contribution of these molecules in the regulation the functionality of CD8+ T cells. Lag3 is the checkpoint receptor which recognizes the MHC II molecules and provide the inhibitory signals to CD8+ T cells. PD-1^{high} CD8+ T cells also express Lag3 and other inhibitory receptors (136). In our study, we observed that about forty percent of virus-specific CD8+ T cells expressed Lag3 during acute FV infection (Fig. 4.11G). The increase of Lag3 expression is associated with inhibition of memory T cells development during acute LCMV infection (269). During chronic LCMV infection Lag3 expression is correlated with the disease severity. This receptor was co-expressed with PD-1 on exhausted and dysfunctional CD8+ T cells (270). Blockage of Lag3 in combination with PD-L1 resulted in improved CD8+ T cell response and reduction in viral load (271). Thus, the inhibitory effects from Lag3 receptor provided additional downregulation of effector CD8+ T cells during acute response against retroviral infection. Further studies focusing on the regulatory effects mediated by Lag3 may add up to the preexisting knowledge and also in development of immunomodulatory therapies.

2B4 (CD244) is a member of the signaling lymphocyte activation molecule (SLAM) family and binds to CD48 expressed on the APCs (149, 272). In our study increased expression of CD48 was observed on FV-infected granulocytes (6, 8, 10 dpi), monocytes (6, and 12 dpi), macrophages (6, 8, and 10 dpi) and mDCs (10 dpi) (Fig. 4.10). More than fifty percent of virus-specific CD8+ T

cells expressed the 2B4 receptor (Fig. 4.11D). This data provides with the evidence that the regulation mediated by interaction of CD48 with 2B4 has an impact on the functionality of virus-specific D8+ T cells. Increased expression of 2B4 was observed on CD8+ T cells during progression of AIDS (273). Moreover, the co-expression of PD-1, CD160 and 2B4 was observed on exhausted HCV-specific CD8+ T cells (274). However during chronic HIV infection simultaneous expression of 2B4 and CD160 is the phenotypic feature of virus-specific cytotoxic CD8+ T cells. These CD8+ T cells were responsible for the control of HIV infection (275). During LCMV infection blocking the interaction of 2B4 with CD48 led to increased IFN-g production by exhausted CD8+ T cells (142). 2B4 and CD48 are the possible interesting targets for the immunmodulation of the adaptive immune response against pathogens and tumors.

Tim-3 is the receptor of Galectin-9 (Gal-9), carcinoembryonic antigen cell adhesion molecule 1 (Caecam-1), high mobility group protein B1 (HMGB1), and phosphatidylserine (PtdSer) (147). About forty percent of FV-specific CD8+ T cells expressed Tim-3 at day 10 and 12 days post infection (dpi) (Fig. 4.11E). Increased percentage of CD8+ T cells expressing Tim-3 is a characteristic feature of exhausted T cells during chronic virus infection. Interestingly, treatment of FV infected mice with anti-Tim-3 antibodies enhanced the viral replication (136), however the combination of anti-Tim-3 antibodies with anti-PD-L1 treatment led to improved virus-elimination. Similarly, combination treatment used during preclinical tumor models of solid tumors and hematologic cancer which involved antibodies against Tim-3 improved the anti-tumor CD8+ T cell response and led to the reduction in tumor growth (276, 277). During immune response against solid tumor CT26 colon carcinoma, the expression of Tim-3 and PD-1 was associated with exhaustion of CD8+ T cells (276). The combination treatment of patients with advanced metastatic melanoma (278), non-small cell lung cancer (NSCLC) (279), or follicular B cell non-Hodgkin lymphoma (FL) (147) with antibodies against PD-1 and Tim-3 improved anti-tumor CD8+ T cells and enhanced the elimination of tumors.

CD80 and CD86 binds to the receptors CD28 and CTLA-4, which further delivers activating (CD28) or suppressing (CTLA-4) signals to the T cells (280, 281). In the current study, increased expression of CD80 (Fig. 4.7 A-D) and CD86 (Fig. 4.8 A-D) was observed on infected granulocytes, monocytes, macrophages and mDCs during acute FV infection. Similar results were also observed during HIV-1 infection, where increased expression of CD80 and CD86 was

observed on monocytes and CCR5+ T cells (235). The expression of CD80 and CD86 on T cell and dendritic cells in patients with nasopharyngeal carcinoma highlights to be a marker of better prognosis (282). CD80 and CD86 play crucial role in activating TCR signaling as well as in suppressing TCR signaling. More focused study may provide a broad array of information which may prove vital for the development of anti-viral and anti-tumor therapies.

Myeloid cells have the enormous potential for the regulation of adaptive immunity. The phenotypic characterization of infected myeloid cells as targets for virus-specific CD8+ T cells lead to the following conclusion. Infected myeloid cells enhance the expression of different inhibitory ligands. Simultaneously, virus-specific CD8+ cells express the corresponding checkpoint receptors and can be suppressed by infected myeloid cells. This pathway contributes towards the immune escape of virus and for the establishment of the chronicity. On the other hand the immunomodulatory treatments directed on these checkpoint molecules may contribute to future therapies of chronic viral infections.

Combination therapy directed on checkpoint ligands/receptors, Tregs, and MDSCs

Acute virus infection leads to strong activation of immune system and several inhibitory mechanisms are required to counteract this response in infected organs. Tregs, inhibitory receptors and MDSCs are the most powerful controllers of the activation and function of T cells in infectious diseases (109, 227, 283). All these inhibitory mechanisms work independently of each other and suppress the differentiation and expansion of cytotoxic CD8+ T cells. The combined depletion or inhibition of Tregs together with the blockage of inhibitory ligands or receptors enhanced the antiviral T cell responses during chronic FV infection and was proposed as a treatment for chronic virus infections and malignancies (193, 284). Furthermore, treatment with anti-PD-1 and anti-CTLA-4 antibodies has been approved for treatment of patients with melanoma which resulted in the activation of T cells, and also increased the numbers of effector CD8+ T cells in the biopsies of responders to this treatment in comparison to the non-responders (285). The expansion of effector cells after this combination treatment resulted in tumor relapse in melanoma patients (286). The combination therapy directed on CTLA-4 and PD-1 checkpoint receptors of cancer patients has a very similar biological effect to the combination therapy which we performed during acute FV infection in current study (Fig. 4.16 A). It was shown that the anti-CTLA-4 antibodies, currently used for the treatment of melanoma and lung cancer patients, significantly reduces the

number of Tregs (287, 288), and this could act as a mechanism activating the anti-tumor immune response. In the current study, mice were treated with anti-PD-L1/anti-Tim3 antibodies and Tregs were depleted during acute phase of infection. The main aim of this therapy was to eliminate the virus before chronicity of FV was established. Combined treatment with anti-PD-L1/anti-Tim3 antibodies and depletion of regulatory T cells induced the expansion of effector CD8+ and CD4+ T cells producing GzmB. These cells efficiently controlled the virus, in fact in some mice the viral load was non-detectible. However, elimination of Tregs and blockage of checkpoint receptors led to enormous expansion of gMDSCs and mMDSCs. We suppose that this expansion of MDSCs tends to compensate the absence of eliminated inhibitory effects of checkpoint receptors and Tregs. The expanded MDSC expressed of PD-L2, CD270, MHC II, CD80 molecules. Thus, these cells were able to suppress the effector CD8+ T cells which express inhibitory receptors. Thus, the expanded populations of MDSCs may reduce the therapeutic effect arrived after the combination therapy. The depletion of expanded MDSCs may improve the antiviral activity of CD8 and CD4+ T cells. On the other hand the simultaneous elimination of different mechanisms which abrogate the cytotoxic CD8+ and CD4+ T cells may enhance the risk of the development of severe autoimmune pathology. Interestingly, the main complications during the treatment of patients with PD-1/PDL-1 blocking antibodies and with Treg-reducing CTLA-4 antibodies (284, 289) are autoimmune disorders. These disorders are also referred to as immune-related adverse events (irAE), and are the main indication for the termination of treatment with immune checkpoint blockers. In some cases, the immunomodulatory treatments led to irAE with fatal outcome (290). Thus the experimental approval of different immunomodulatory treatments are necessary for the development of safe and efficient therapy against malignancies and viral infections. An alternative immunomodulatory therapy was proposed for the treatment directed on gMDSCs in combination with antibodies against PD-L1/Tim3. Several clinical trials on cancer have targeted MDSCs by inhibiting the mechanisms of MDSC-mediated immunosuppression, blocking the MDSC trafficking, and by depleting MDSC (291). Previous study shows that gMDSCs were preferentially responsible for the immunosuppression during late phase of FV infection. Depletion of all MDSC by 5-fluorouracil and depletion of gMDSC by anti-Ly6G significantly enhanced the number of effector and tetramer+ CD8+ T cells and reduced the virus replication (109). In the current study mice received anti-PD-L1/-Tim-3 antibodies or anti-Ly6G antibodies for depletion of gMDSC individually as well as in combination during acute FV infection. In order to improve the depletion

of gMDSCs the treatment was started at day seven after infection and was repeated every second day. In previous study the treatment with anti-Ly6G antibodies was performed once at day nine after infection (109). Combined treatment with anti-PD-L1/anti-Tim3 antibodies and depletion of gMDSC performed during acute FV infection did not provide any additional benefit for virus control in comparison to individual treatment with anti-PD-L1/anti-Tim3 antibodies. Also no potentiation in expansion of virus-specific CD8+ T cells after combination therapy were observed. These differences in the expansion of effector CD8+ T cells after anti-L6G treatment observed previously shows that the minimal modulation of the treatment protocol may lead to completely different effects of the treatment on the immune response. The individual treatment of animals with anti-PD-L1/anti-Tim3 antibodies and with anti-Ly6G led to the significant reduction in the numbers of CD4+ T cells expressing FoxP3+ (Fig. 4.26). This effect was potentiated in case of combination treatment. Received data evidenced that gMDSCs were involved in the regulation of Tregs expansion. Similar effects of MDSCs on the expansion of Tregs were previously demonstrated in A20 B cell lymphoma model. In this study *in vivo* inhibition of MDSC led to abrogation of Tregs proliferation and tumor induced tolerance in antitumor specific CD4+ T cells (108). Summarizing the current data, we can suppose that the different experimental therapies approved in experimental animal models provides necessary evidences for the understanding of very complex system, regulating the adaptive T cell immune response. All these knowledge are essential for development of efficient and safe immunomodulatory therapy of tumors and viral infections.

6. Summary

Cytotoxic effector CD8+ T cells (CTLs) are responsible for the elimination of viruses and some malignancies. However, during chronic infections with viruses, like HIV, these cells become dysfunctional or exhausted. The dysfunction of CTLs is partly induced by inhibitory receptors up-regulated on these cells during chronic infection. However, effector CD8+ T cells express high levels of inhibitory receptors already during acute viral infections, but remain functional at this time point. This indicates that inhibitory receptors also regulate T cell functionality during the acute phase of infection. In the current study the Friend retrovirus (FV) mouse model was used to define the mechanisms that regulate CD8+ T cell immunity. From previous studies it was known that myeloid cells are targets for FV infection during acute and chronic phase. We performed a detailed characterization of subpopulations of myeloid cells as targets for FV during acute infection. FV preferentially infected granulocytes and monocytes and reduced the frequencies of these myeloid cells significantly in the spleen of infected mice. A few macrophages and mDCs were also infected with FV. A detailed phenotypic characterization of infected myeloid cells showed an up-regulation of the inhibitory ligands PD-L1, PD-L2, CD270 (HVEM), CD80, CD86, CD200, and CD48 in comparison to non-infected myeloid subpopulations. Simultaneously virus-specific CD8+ T cells were analyzed for the expression of the receptors for these ligands. We observed that effector CD8+ T cells expressed many different inhibitory receptors on the cell surface after infection. Thus, infected myeloid cells expressing inhibitory molecules likely escaped the elimination by virus-specific CD8+ T cells positive for inhibitory receptors. In order to determine whether CD270, which was expressed on infected myeloid cells, suppresses CTL responses and interferes with the elimination of virus, we performed blocking experiments. Treatment with anti-CD270 antibodies, which selectively blocked the interaction of CD270 ligand to both its inhibitory receptors CD160 and CD272 was performed. Treated mice significantly reduced viral loads, however, the numbers of effector CD8+ T cells were not changed.

From previous studies it was known that regulatory T cells and myeloid-derived suppressor cells also downregulate the functionality of CTLs during acute FV infection. In order to improve the elimination of FV by enhancing the functionality of CTLs two different combination treatments were performed.

In the first treatment experiment, Tregs were eliminated and the checkpoint receptors/ligands interaction was blocked with antibodies against PD-L1 and Tim-3. This combination treatment led to a strong expansion of CD8+ and CD4+ T cells producing the cytotoxic molecule granzyme B and improved elimination of FV. However, the combination treatment resulted in an expansion of MDSCs as a possible compensatory effect, which was necessary for the control of expanded CTLs. In the second combination treatment experiment, PD-L1 and Tim-3 were blocked and MDSCs were depleted with anti-Ly6G antibodies. While the treatment with PD-L1 and Tim-3 blocking antibodies as well as the depletion of MDSCs resulted in reduced numbers of FV infected cells when applied individually, the combination treatment did not lead to a further improvement of efficacy. This second combination therapy was not associated with the expansion of virus-specific CD8+ T cells and resulted in a reduction of Tregs instead of an increase. The current data allows us to better understand the very complex system that regulates the adaptive T cell response during a virus infection. This knowledge can be essential for the development of efficient and safe immunomodulatory therapies against tumors and infectious diseases.

7. Zusammenfassung

Zytotoxische CD8+ Effektor-T-Zellen (ZTL) sind für die Eliminierung von Virusinfektionen und Tumorerkrankungen verantwortlich. In chronischen Infektionen mit Viren wie zum Beispiel HIV kommt es jedoch zur Erschöpfung und Dysfunktion dieser Zellen. Die Dysfunktion der ZTL wird zum Teil durch eine starke Expression inhibitorischer Rezeptoren in der chronischen Infektion induziert, andererseits exprimieren CD8+ Effektor-T-Zellen auch schon in der akuten Phase viraler Infektionen in einem hohen Maß inhibitorische Rezeptoren, bleiben zu diesem Zeitpunkt aber funktional. Dies deutet darauf hin, dass inhibitorische Rezeptoren auch während der akuten Phase der Infektion die T-Zell-Funktionalität regulieren. In der vorliegenden Studie wurde das Friend Retrovirus (FV) Mausmodell genutzt um Mechanismen zu definieren, welche die CD8+-T-Zell-Immunität regulieren. Aus vorangegangenen Studien war bekannt, dass myeloide Zellen Zielzellen für die FV-Infektion sowohl in der akuten als auch der chronischen Phase darstellen. Es wurde daher detailliert untersucht, welche Subpopulationen myeloider Zellen Zielzellen von FV in der akuten Infektion darstellen. FV infizierte bevorzugt Granulozyten und Monozyten, und die Infektion führte zu einer signifikanten Reduktion in der Frequenz dieser myeloiden Zellen in den Milzen infizierter Mäuse. Auch einige Makrophagen und mDCs wurden durch FV infiziert. Eine detaillierte phänotypische Charakterisierung infizierter myeloider Zellen zeigte eine stärkere Expression der inhibitorischen Liganden PD-L1, PD-L2, CD270 (HVEM), CD80, CD86, CD200 und CD48 im Vergleich mit nicht-infizierten myeloiden Subpopulationen. Es wurde andererseits auch die Expression der Rezeptoren dieser inhibitorischen Liganden auf Virus-spezifischen CD8+ T-Zellen untersucht, hierbei zeigte sich, dass CD8+ Effektor-T-Zellen nach der Infektion zahlreiche Rezeptoren auf der Oberfläche exprimieren. FV-infizierten myeloiden Zellen gelingt es also wahrscheinlich auf Grund der hohen Expression inhibitorischer Liganden, der Eliminierung durch Virus-spezifische CD8+ T-zellen zu entgehen. Um zu untersuchen ob das auf infizierten myeloiden Zellen stark exprimierte CD270 die ZTL-Antwort unterdrückt und die Virus-Eliminierung verhindert, wurden Mäuse mit einem blockierenden Antikörper behandelt, welcher selektiv die Interaktion von CD270 mit den inhibitorischen Rezeptoren CD160 und CD272 inhibiert. Mit dem Antikörper behandelte Mäuse zeigten signifikant reduzierte Viruslasten, allerdings blieb die Zahl an CD8+ Effektor-T-Zellen unverändert.

Aus früheren Studien war bekannt, dass auch regulatorische T-Zellen und myeloide suppressive Zellen (*myeloid-derived suppressor cells*, MDSCs) die Funktionalität von ZTL während der

akuten FV-Infektion herabregulieren. Um die Eliminierung von FV zu verbessern wurden daher zwei verschiedene Kombinations-Therapien eingesetzt, welche die ZTL-Funktionalität steigern sollten. In einem ersten Ansatz wurden Tregs depletiert und blockierende Antikörper gegen PD-L1 und Tim-3 eingesetzt. Diese Kombinations-Therapie führte zu einer starken Expansion von Granzym B-produzierenden CD8+ und CD4+ T-Zellen und verbesserte die Eliminierung von FV. Allerdings führte diese Therapie auch zu einer, möglicherweise kompensatorischen, Expansion von MDSCs, welche vermutlich die expandierte ZTL-Population kontrollierte. In einem zweiten Therapie-Ansatz wurde die Blockade von PD-L1 und Tim-3 mit der Depletion von MDSCs durch einen Ly6G-Antikörper kombiniert. Während sowohl die Applikation von PD-L1- und Tim3-Antikörpern und die Depletion von MDSCs allein zu einer reduzierten Zahl FV-infizierter Zellen führte, wurde durch die Kombinations-Therapie keine weitere Verbesserung der Effektivität erreicht. Auch führte diese Kombinations-Therapie nicht zu einer Expansion Virus-spezifischer CD8+ T-Zellen, jedoch unerwartet zu einer Reduktion der Anzahl von Tregs.

Die vorliegenden Daten ermöglichen uns ein besseres Verständnis der sehr komplexen Mechanismen, welche die adaptive T-Zell-Antwort während einer Virus-Infektion regulieren, und können wichtige Erkenntnisse liefern für die Entwicklung effektiver und sicherer immunmodulatorischer Therapien gegen Infektions- und Tumor-Erkrankung.

References

1. **Bieniasz PD.** 2009. The cell biology of HIV-1 virion genesis. Cell Host Microbe **5:**550-558.
2. **Friend C.** 1957. Cell-free transmission in adult Swiss mice of a disease having the character of a leukemia. J Exp Med **105:**307-318.
3. **Kabat D.** 1989. Molecular biology of Friend viral erythroleukemia. Curr Top Microbiol Immunol **148:**1-42.
4. **Hasenkrug KJ, Brooks DM, Dittmer U.** 1998. Critical role for CD4(+) T cells in controlling retrovirus replication and spread in persistently infected mice. J Virol **72:**6559-6564.
5. **Li JP, D'Andrea AD, Lodish HF, Baltimore D.** 1990. Activation of cell growth by binding of Friend spleen focus-forming virus gp55 glycoprotein to the erythropoietin receptor. Nature **343:**762-764.
6. **Maisel J, Klement V, Lai MM, Ostertag W, Duesberg P.** 1973. Ribonucleic acid components of murine sarcoma and leukemia viruses. Proc Natl Acad Sci U S A **70:**3536-3540.
7. **Troxler DH, Ruscetti SK, Scolnick EM.** 1980. The molecular biology of Friend virus. Biochim Biophys Acta **605:**305-324.
8. **Cmarik J, Ruscetti S.** 2010. Friend Spleen Focus-Forming Virus Activates the Tyrosine Kinase sf-Stk and the Transcription Factor PU.1 to Cause a Multi-Stage Erythroleukemia in Mice. Viruses **2:**2235-2257.
9. **Hasenkrug KJ, Dittmer U.** 2000. The role of CD4 and CD8 T cells in recovery and protection from retroviral infection: lessons from the Friend virus model. Virology **272:**244-249.
10. **Moreau-Gachelin F.** 2008. Multi-stage Friend murine erythroleukemia: molecular insights into oncogenic cooperation. Retrovirology **5:**99.
11. **Chesebro B, Miyazawa M, Britt WJ.** 1990. Host genetic control of spontaneous and induced immunity to Friend murine retrovirus infection. Annu Rev Immunol **8:**477-499.
12. **Ney PA, D'Andrea AD.** 2000. Friend erythroleukemia revisited. Blood **96:**3675-3680.
13. **Hasenkrug KJ, Chesebro B.** 1997. Immunity to retroviral infection: the Friend virus model. Proc Natl Acad Sci U S A **94:**7811-7816.
14. **Deeks SG, Overbaugh J, Phillips A, Buchbinder S.** 2015. HIV infection. Nat Rev Dis Primers **1:**15035.
15. **Novembre FJ, de Rosayro J, Nidtha S, O'Neil SP, Gibson TR, Evans-Strickfaden T, Hart CE, McClure HM.** 2001. Rapid CD4(+) T-cell loss induced by human immunodeficiency virus type 1(NC) in uninfected and previously infected chimpanzees. J Virol **75:**1533-1539.
16. **O'Neil SP, Novembre FJ, Hill AB, Suwyn C, Hart CE, Evans-Strickfaden T, Anderson DC, deRosayro J, Herndon JG, Saucier M, McClure HM.** 2000. Progressive infection in a subset of HIV-1-positive chimpanzees. J Infect Dis **182:**1051-1062.
17. **Simon MA, Brodie SJ, Sasseville VG, Chalifoux LV, Desrosiers RC, Ringler DJ.** 1994. Immunopathogenesis of SIVmac. Virus Res **32:**227-251.
18. **Shanmugasundaram U, Kovarova M, Ho PT, Schramm N, Wahl A, Parniak MA, Garcia JV.** 2016. Efficient Inhibition of HIV Replication in the Gastrointestinal and

Female Reproductive Tracts of Humanized BLT Mice by EFdA. PLoS One **11:**e0159517.

19. **Shultz LD, Brehm MA, Garcia-Martinez JV, Greiner DL.** 2012. Humanized mice for immune system investigation: progress, promise and challenges. Nat Rev Immunol **12:**786-798.
20. **Traggiai E, Chicha L, Mazzucchelli L, Bronz L, Piffaretti JC, Lanzavecchia A, Manz MG.** 2004. Development of a human adaptive immune system in cord blood cell-transplanted mice. Science **304:**104-107.
21. **Thompson MR, Kaminski JJ, Kurt-Jones EA, Fitzgerald KA.** 2011. Pattern recognition receptors and the innate immune response to viral infection. Viruses **3:**920-940.
22. **Beignon AS, McKenna K, Skoberne M, Manches O, DaSilva I, Kavanagh DG, Larsson M, Gorelick RJ, Lifson JD, Bhardwaj N.** 2005. Endocytosis of HIV-1 activates plasmacytoid dendritic cells via Toll-like receptor-viral RNA interactions. J Clin Invest **115:**3265-3275.
23. **Lepelley A, Louis S, Sourisseau M, Law HK, Pothlichet J, Schilte C, Chaperot L, Plumas J, Randall RE, Si-Tahar M, Mammano F, Albert ML, Schwartz O.** 2011. Innate sensing of HIV-infected cells. PLoS Pathog **7:**e1001284.
24. **Heil F, Hemmi H, Hochrein H, Ampenberger F, Kirschning C, Akira S, Lipford G, Wagner H, Bauer S.** 2004. Species-specific recognition of single-stranded RNA via toll-like receptor 7 and 8. Science **303:**1526-1529.
25. **Simmons RP, Scully EP, Groden EE, Arnold KB, Chang JJ, Lane K, Lifson J, Rosenberg E, Lauffenburger DA, Altfeld M.** 2013. HIV-1 infection induces strong production of IP-10 through TLR7/9-dependent pathways. AIDS **27:**2505-2517.
26. **Sauter D, Kirchhoff F.** 2016. HIV replication: a game of hide and sense. Curr Opin HIV AIDS **11:**173-181.
27. **Jakobsen MR, Bak RO, Andersen A, Berg RK, Jensen SB, Tengchuan J, Laustsen A, Hansen K, Ostergaard L, Fitzgerald KA, Xiao TS, Mikkelsen JG, Mogensen TH, Paludan SR.** 2013. IFI16 senses DNA forms of the lentiviral replication cycle and controls HIV-1 replication. Proc Natl Acad Sci U S A **110:**E4571-4580.
28. **Solis M, Nakhaei P, Jalalirad M, Lacoste J, Douville R, Arguello M, Zhao T, Laughrea M, Wainberg MA, Hiscott J.** 2011. RIG-I-mediated antiviral signaling is inhibited in HIV-1 infection by a protease-mediated sequestration of RIG-I. J Virol **85:**1224-1236.
29. **Pertel T, Hausmann S, Morger D, Zuger S, Guerra J, Lascano J, Reinhard C, Santoni FA, Uchil PD, Chatel L, Bisiaux A, Albert ML, Strambio-De-Castillia C, Mothes W, Pizzato M, Grutter MG, Luban J.** 2011. TRIM5 is an innate immune sensor for the retrovirus capsid lattice. Nature **472:**361-365.
30. **Galao RP, Le Tortorec A, Pickering S, Kueck T, Neil SJ.** 2012. Innate sensing of HIV-1 assembly by Tetherin induces NFkappaB-dependent proinflammatory responses. Cell Host Microbe **12:**633-644.
31. **Arhel NJ, Souquere-Besse S, Munier S, Souque P, Guadagnini S, Rutherford S, Prevost MC, Allen TD, Charneau P.** 2007. HIV-1 DNA Flap formation promotes uncoating of the pre-integration complex at the nuclear pore. EMBO J **26:**3025-3037.
32. **Lahaye X, Satoh T, Gentili M, Cerboni S, Conrad C, Hurbain I, El Marjou A, Lacabaratz C, Lelievre JD, Manel N.** 2013. The capsids of HIV-1 and HIV-2

determine immune detection of the viral cDNA by the innate sensor cGAS in dendritic cells. Immunity **39:**1132-1142.

33. **Stetson DB, Ko JS, Heidmann T, Medzhitov R.** 2008. Trex1 prevents cell-intrinsic initiation of autoimmunity. Cell **134:**587-598.
34. **Zhao K, Du J, Han X, Goodier JL, Li P, Zhou X, Wei W, Evans SL, Li L, Zhang W, Cheung LE, Wang G, Kazazian HH, Jr., Yu XF.** 2013. Modulation of LINE-1 and Alu/SVA retrotransposition by Aicardi-Goutieres syndrome-related SAMHD1. Cell Rep **4:**1108-1115.
35. **El Hage A, Webb S, Kerr A, Tollervey D.** 2014. Genome-wide distribution of RNA-DNA hybrids identifies RNase H targets in tRNA genes, retrotransposons and mitochondria. PLoS Genet **10:**e1004716.
36. **Chan JK, Greene WC.** 2012. Dynamic roles for NF-kappaB in HTLV-I and HIV-1 retroviral pathogenesis. Immunol Rev **246:**286-310.
37. **Neil SJ, Zang T, Bieniasz PD.** 2008. Tetherin inhibits retrovirus release and is antagonized by HIV-1 Vpu. Nature **451:**425-430.
38. **Laguette N, Bregnard C, Hue P, Basbous J, Yatim A, Larroque M, Kirchhoff F, Constantinou A, Sobhian B, Benkirane M.** 2014. Premature activation of the SLX4 complex by Vpr promotes G2/M arrest and escape from innate immune sensing. Cell **156:**134-145.
39. **Akira S, Uematsu S, Takeuchi O.** 2006. Pathogen recognition and innate immunity. Cell **124:**783-801.
40. **Doyle T, Goujon C, Malim MH.** 2015. HIV-1 and interferons: who's interfering with whom? Nat Rev Microbiol **13:**403-413.
41. **De Andrea M, Ravera R, Gioia D, Gariglio M, Landolfo S.** 2002. The interferon system: an overview. Eur J Paediatr Neurol **6 Suppl A:**A41-46; discussion A55-48.
42. **Liu YJ.** 2005. IPC: professional type 1 interferon-producing cells and plasmacytoid dendritic cell precursors. Annu Rev Immunol **23:**275-306.
43. **Utay NS, Douek DC.** 2016. Interferons and HIV Infection: The Good, the Bad, and the Ugly. Pathog Immun **1:**107-116.
44. **Bosinger SE, Utay NS.** 2015. Type I interferon: understanding its role in HIV pathogenesis and therapy. Curr HIV/AIDS Rep **12:**41-53.
45. **Schoggins JW, Wilson SJ, Panis M, Murphy MY, Jones CT, Bieniasz P, Rice CM.** 2011. A diverse range of gene products are effectors of the type I interferon antiviral response. Nature **472:**481-485.
46. **Pillai SK, Abdel-Mohsen M, Guatelli J, Skasko M, Monto A, Fujimoto K, Yukl S, Greene WC, Kovari H, Rauch A, Fellay J, Battegay M, Hirschel B, Witteck A, Bernasconi E, Ledergerber B, Gunthard HF, Wong JK, Swiss HIVCS.** 2012. Role of retroviral restriction factors in the interferon-alpha-mediated suppression of HIV-1 in vivo. Proc Natl Acad Sci U S A **109:**3035-3040.
47. **Goujon C, Moncorge O, Bauby H, Doyle T, Ward CC, Schaller T, Hue S, Barclay WS, Schulz R, Malim MH.** 2013. Human MX2 is an interferon-induced post-entry inhibitor of HIV-1 infection. Nature **502:**559-562.
48. **Kane M, Yadav SS, Bitzegeio J, Kutluay SB, Zang T, Wilson SJ, Schoggins JW, Rice CM, Yamashita M, Hatziioannou T, Bieniasz PD.** 2013. MX2 is an interferon-induced inhibitor of HIV-1 infection. Nature **502:**563-566.

49. **Schoggins JW, MacDuff DA, Imanaka N, Gainey MD, Shrestha B, Eitson JL, Mar KB, Richardson RB, Ratushny AV, Litvak V, Dabelic R, Manicassamy B, Aitchison JD, Aderem A, Elliott RM, Garcia-Sastre A, Racaniello V, Snijder EJ, Yokoyama WM, Diamond MS, Virgin HW, Rice CM.** 2014. Pan-viral specificity of IFN-induced genes reveals new roles for cGAS in innate immunity. Nature **505:**691-695.
50. **Sandler NG, Bosinger SE, Estes JD, Zhu RT, Tharp GK, Boritz E, Levin D, Wijeyesinghe S, Makamdop KN, del Prete GQ, Hill BJ, Timmer JK, Reiss E, Yarden G, Darko S, Contijoch E, Todd JP, Silvestri G, Nason M, Norgren RB, Jr., Keele BF, Rao S, Langer JA, Lifson JD, Schreiber G, Douek DC.** 2014. Type I interferon responses in rhesus macaques prevent SIV infection and slow disease progression. Nature **511:**601-605.
51. **Lavender KJ, Gibbert K, Peterson KE, Van Dis E, Francois S, Woods T, Messer RJ, Gawanbacht A, Muller JA, Munch J, Phillips K, Race B, Harper MS, Guo K, Lee EJ, Trilling M, Hengel H, Piehler J, Verheyen J, Wilson CC, Santiago ML, Hasenkrug KJ, Dittmer U.** 2016. Interferon Alpha Subtype-Specific Suppression of HIV-1 Infection In Vivo. J Virol **90:**6001-6013.
52. **Harper MS, Guo K, Gibbert K, Lee EJ, Dillon SM, Barrett BS, McCarter MD, Hasenkrug KJ, Dittmer U, Wilson CC, Santiago ML.** 2015. Interferon-alpha Subtypes in an Ex Vivo Model of Acute HIV-1 Infection: Expression, Potency and Effector Mechanisms. PLoS Pathog **11:**e1005254.
53. **Hunt PW, Martin JN, Sinclair E, Bredt B, Hagos E, Lampiris H, Deeks SG.** 2003. T cell activation is associated with lower CD4+ T cell gains in human immunodeficiency virus-infected patients with sustained viral suppression during antiretroviral therapy. J Infect Dis **187:**1534-1543.
54. **Utay NS, Hunt PW.** 2016. Role of immune activation in progression to AIDS. Curr Opin HIV AIDS **11:**131-137.
55. **Stoddart CA, Keir ME, McCune JM.** 2010. IFN-alpha-induced upregulation of CCR5 leads to expanded HIV tropism in vivo. PLoS Pathog **6:**e1000766.
56. **Li Q, Estes JD, Schlievert PM, Duan L, Brosnahan AJ, Southern PJ, Reilly CS, Peterson ML, Schultz-Darken N, Brunner KG, Nephew KR, Pambuccian S, Lifson JD, Carlis JV, Haase AT.** 2009. Glycerol monolaurate prevents mucosal SIV transmission. Nature **458:**1034-1038.
57. **Manion M, Rodriguez B, Medvik K, Hardy G, Harding CV, Schooley RT, Pollard R, Asmuth D, Murphy R, Barker E, Brady KE, Landay A, Funderburg N, Sieg SF, Lederman MM.** 2012. Interferon-alpha administration enhances CD8+ T cell activation in HIV infection. PLoS One **7:**e30306.
58. **Curtsinger JM, Valenzuela JO, Agarwal P, Lins D, Mescher MF.** 2005. Type I IFNs provide a third signal to CD8 T cells to stimulate clonal expansion and differentiation. J Immunol **174:**4465-4469.
59. **Gerlach N, Schimmer S, Weiss S, Kalinke U, Dittmer U.** 2006. Effects of type I interferons on Friend retrovirus infection. J Virol **80:**3438-3444.
60. **Qin X, Gao B.** 2006. The complement system in liver diseases. Cell Mol Immunol **3:**333-340.
61. **Zhou X, Hu W, Qin X.** 2008. The role of complement in the mechanism of action of rituximab for B-cell lymphoma: implications for therapy. Oncologist **13:**954-966.

62. **Morgan BP, Berg CW, Harris CL.** 2005. "Homologous restriction" in complement lysis: roles of membrane complement regulators. Xenotransplantation **12:**258-265.
63. **Mayer MM.** 1984. Complement. Historical perspectives and some current issues. Complement **1:**2-26.
64. **Littwitz-Salomon E, Dittmer U, Sutter K.** 2016. Insufficient natural killer cell responses against retroviruses: how to improve NK cell killing of retrovirus-infected cells. Retrovirology **13:**77.
65. **Hoyler T, Klose CS, Souabni A, Turqueti-Neves A, Pfeifer D, Rawlins EL, Voehringer D, Busslinger M, Diefenbach A.** 2012. The transcription factor GATA-3 controls cell fate and maintenance of type 2 innate lymphoid cells. Immunity **37:**634-648.
66. **Zhou L.** 2012. Striking similarity: GATA-3 regulates ILC2 and Th2 cells. Immunity **37:**589-591.
67. **Eberl G, Colonna M, Di Santo JP, McKenzie AN.** 2015. Innate lymphoid cells. Innate lymphoid cells: a new paradigm in immunology. Science **348:**aaa6566.
68. **Kawamoto H, Minato N.** 2004. Myeloid cells. Int J Biochem Cell Biol **36:**1374-1379.
69. **Wacleche VS, Tremblay CL, Routy JP, Ancuta P.** 2018. The Biology of Monocytes and Dendritic Cells: Contribution to HIV Pathogenesis. Viruses **10**.
70. **Qu C, Brinck-Jensen NS, Zang M, Chen K.** 2014. Monocyte-derived dendritic cells: targets as potent antigen-presenting cells for the design of vaccines against infectious diseases. Int J Infect Dis **19:**1-5.
71. **Ziegler-Heitbrock L, Ancuta P, Crowe S, Dalod M, Grau V, Hart DN, Leenen PJ, Liu YJ, MacPherson G, Randolph GJ, Scherberich J, Schmitz J, Shortman K, Sozzani S, Strobl H, Zembala M, Austyn JM, Lutz MB.** 2010. Nomenclature of monocytes and dendritic cells in blood. Blood **116:**e74-80.
72. **Alexaki A, Liu Y, Wigdahl B.** 2008. Cellular reservoirs of HIV-1 and their role in viral persistence. Curr HIV Res **6:**388-400.
73. **Mege JL, Mehraj V, Capo C.** 2011. Macrophage polarization and bacterial infections. Curr Opin Infect Dis **24:**230-234.
74. **Iannello A, Boulassel MR, Samarani S, Tremblay C, Toma E, Routy JP, Ahmad A.** 2010. HIV-1 causes an imbalance in the production of interleukin-18 and its natural antagonist in HIV-infected individuals: implications for enhanced viral replication. J Infect Dis **201:**608-617.
75. **Cassol E, Cassetta L, Rizzi C, Alfano M, Poli G.** 2009. M1 and M2a polarization of human monocyte-derived macrophages inhibits HIV-1 replication by distinct mechanisms. J Immunol **182:**6237-6246.
76. **Cassol E, Cassetta L, Alfano M, Poli G.** 2010. Macrophage polarization and HIV-1 infection. J Leukoc Biol **87:**599-608.
77. **Honeycutt JB, Thayer WO, Baker CE, Ribeiro RM, Lada SM, Cao Y, Cleary RA, Hudgens MG, Richman DD, Garcia JV.** 2017. HIV persistence in tissue macrophages of humanized myeloid-only mice during antiretroviral therapy. Nat Med **23:**638-643.
78. **Summers C, Rankin SM, Condliffe AM, Singh N, Peters AM, Chilvers ER.** 2010. Neutrophil kinetics in health and disease. Trends Immunol **31:**318-324.
79. **Levine AM, Karim R, Mack W, Gravink DJ, Anastos K, Young M, Cohen M, Newman M, Augenbraun M, Gange S, Watts DH.** 2006. Neutropenia in human immunodeficiency virus infection: data from the women's interagency HIV study. Arch Intern Med **166:**405-410.

80. **Saitoh T, Komano J, Saitoh Y, Misawa T, Takahama M, Kozaki T, Uehata T, Iwasaki H, Omori H, Yamaoka S, Yamamoto N, Akira S.** 2012. Neutrophil extracellular traps mediate a host defense response to human immunodeficiency virus-1. Cell Host Microbe **12:**109-116.
81. **Brinkmann V, Reichard U, Goosmann C, Fauler B, Uhlemann Y, Weiss DS, Weinrauch Y, Zychlinsky A.** 2004. Neutrophil extracellular traps kill bacteria. Science **303:**1532-1535.
82. **Roche PA, Cresswell P.** 1990. Invariant chain association with HLA-DR molecules inhibits immunogenic peptide binding. Nature **345:**615-618.
83. **Bakke O, Dobberstein B.** 1990. MHC class II-associated invariant chain contains a sorting signal for endosomal compartments. Cell **63:**707-716.
84. **Lotteau V, Teyton L, Peleraux A, Nilsson T, Karlsson L, Schmid SL, Quaranta V, Peterson PA.** 1990. Intracellular transport of class II MHC molecules directed by invariant chain. Nature **348:**600-605.
85. **Roche PA, Cresswell P.** 2016. Antigen Processing and Presentation Mechanisms in Myeloid Cells. Microbiol Spectr **4**.
86. **Ke N, Su A, Huang W, Szatmary P, Zhang Z.** 2016. Regulating the expression of CD80/CD86 on dendritic cells to induce immune tolerance after xeno-islet transplantation. Immunobiology **221:**803-812.
87. **Stevenson M.** 2015. Role of myeloid cells in HIV-1-host interplay. J Neurovirol **21:**242-248.
88. **Epelman S, Lavine KJ, Randolph GJ.** 2014. Origin and functions of tissue macrophages. Immunity **41:**21-35.
89. **McElrath MJ, Steinman RM, Cohn ZA.** 1991. Latent HIV-1 infection in enriched populations of blood monocytes and T cells from seropositive patients. J Clin Invest **87:**27-30.
90. **Veenstra M, Leon-Rivera R, Li M, Gama L, Clements JE, Berman JW.** 2017. Mechanisms of CNS Viral Seeding by HIV(+) CD14(+) CD16(+) Monocytes: Establishment and Reseeding of Viral Reservoirs Contributing to HIV-Associated Neurocognitive Disorders. MBio **8**.
91. **Ellery PJ, Tippett E, Chiu YL, Paukovics G, Cameron PU, Solomon A, Lewin SR, Gorry PR, Jaworowski A, Greene WC, Sonza S, Crowe SM.** 2007. The CD16+ monocyte subset is more permissive to infection and preferentially harbors HIV-1 in vivo. J Immunol **178:**6581-6589.
92. **Josefsson L, King MS, Makitalo B, Brannstrom J, Shao W, Maldarelli F, Kearney MF, Hu WS, Chen J, Gaines H, Mellors JW, Albert J, Coffin JM, Palmer SE.** 2011. Majority of CD4+ T cells from peripheral blood of HIV-1-infected individuals contain only one HIV DNA molecule. Proc Natl Acad Sci U S A **108:**11199-11204.
93. **Honeycutt JB, Wahl A, Baker C, Spagnuolo RA, Foster J, Zakharova O, Wietgrefe S, Caro-Vegas C, Madden V, Sharpe G, Haase AT, Eron JJ, Garcia JV.** 2016. Macrophages sustain HIV replication in vivo independently of T cells. J Clin Invest **126:**1353-1366.
94. **Trillo-Pazos G, Diamanturos A, Rislove L, Menza T, Chao W, Belem P, Sadiq S, Morgello S, Sharer L, Volsky DJ.** 2003. Detection of HIV-1 DNA in microglia/macrophages, astrocytes and neurons isolated from brain tissue with HIV-1 encephalitis by laser capture microdissection. Brain Pathol **13:**144-154.

95. **Lebargy F, Branellec A, Deforges L, Bignon J, Bernaudin JF.** 1994. HIV-1 in human alveolar macrophages from infected patients is latent in vivo but replicates after in vitro stimulation. Am J Respir Cell Mol Biol **10:**72-78.
96. **Hufert FT, Schmitz J, Schreiber M, Schmitz H, Racz P, von Laer DD.** 1993. Human Kupffer cells infected with HIV-1 in vivo. J Acquir Immune Defic Syndr **6:**772-777.
97. **Zalar A, Figueroa MI, Ruibal-Ares B, Bare P, Cahn P, de Bracco MM, Belmonte L.** 2010. Macrophage HIV-1 infection in duodenal tissue of patients on long term HAART. Antiviral Res **87:**269-271.
98. **Burleigh L, Lozach PY, Schiffer C, Staropoli I, Pezo V, Porrot F, Canque B, Virelizier JL, Arenzana-Seisdedos F, Amara A.** 2006. Infection of dendritic cells (DCs), not DC-SIGN-mediated internalization of human immunodeficiency virus, is required for long-term transfer of virus to T cells. J Virol **80:**2949-2957.
99. **Gabrilovich DI, Nagaraj S.** 2009. Myeloid-derived suppressor cells as regulators of the immune system. Nat Rev Immunol **9:**162-174.
100. **Medina E, Hartl D.** 2018. Myeloid-Derived Suppressor Cells in Infection: A General Overview. J Innate Immun **10:**407-413.
101. **Vollbrecht T, Stirner R, Tufman A, Roider J, Huber RM, Bogner JR, Lechner A, Bourquin C, Draenert R.** 2012. Chronic progressive HIV-1 infection is associated with elevated levels of myeloid-derived suppressor cells. AIDS **26:**F31-37.
102. **Qin A, Cai W, Pan T, Wu K, Yang Q, Wang N, Liu Y, Yan D, Hu F, Guo P, Chen X, Chen L, Zhang H, Tang X, Zhou J.** 2013. Expansion of monocytic myeloid-derived suppressor cells dampens T cell function in HIV-1-seropositive individuals. J Virol **87:**1477-1490.
103. **Fridlender ZG.** 2018. Myeloid Regulatory Cells - New and Exciting Players in the Immunology of Lung Cancer. Am J Respir Crit Care Med doi:10.1164/rccm.201804-0742ED.
104. **Gabrilovich DI.** 2017. Myeloid-Derived Suppressor Cells. Cancer Immunol Res **5:**3-8.
105. **Gabrilovich DI, Velders MP, Sotomayor EM, Kast WM.** 2001. Mechanism of immune dysfunction in cancer mediated by immature Gr-1+ myeloid cells. J Immunol **166:**5398-5406.
106. **Ostrand-Rosenberg S.** 2010. Myeloid-derived suppressor cells: more mechanisms for inhibiting antitumor immunity. Cancer Immunol Immunother **59:**1593-1600.
107. **Hanson EM, Clements VK, Sinha P, Ilkovitch D, Ostrand-Rosenberg S.** 2009. Myeloid-derived suppressor cells down-regulate L-selectin expression on CD4+ and CD8+ T cells. J Immunol **183:**937-944.
108. **Serafini P, Mgebroff S, Noonan K, Borrello I.** 2008. Myeloid-derived suppressor cells promote cross-tolerance in B-cell lymphoma by expanding regulatory T cells. Cancer Res **68:**5439-5449.
109. **Drabczyk-Pluta M, Werner T, Hoffmann D, Leng Q, Chen L, Dittmer U, Zelinskyy G.** 2017. Granulocytic myeloid-derived suppressor cells suppress virus-specific CD8(+) T cell responses during acute Friend retrovirus infection. Retrovirology **14:**42.
110. **Greaves MF, Brown G.** 1973. A human B lymphocyte specific antigen. Nat New Biol **246:**116-119.
111. **Vignali DA, Collison LW, Workman CJ.** 2008. How regulatory T cells work. Nat Rev Immunol **8:**523-532.

112. **Mills KH.** 2004. Regulatory T cells: friend or foe in immunity to infection? Nat Rev Immunol **4:**841-855.
113. **Veiga-Parga T, Sehrawat S, Rouse BT.** 2013. Role of regulatory T cells during virus infection. Immunol Rev **255:**182-196.
114. **Steinman RM.** 1991. The dendritic cell system and its role in immunogenicity. Annu Rev Immunol **9:**271-296.
115. **Lanzavecchia A, Sallusto F.** 2001. Regulation of T cell immunity by dendritic cells. Cell **106:**263-266.
116. **Hervas-Stubbs S, Riezu-Boj JI, Gonzalez I, Mancheno U, Dubrot J, Azpilicueta A, Gabari I, Palazon A, Aranguren A, Ruiz J, Prieto J, Larrea E, Melero I.** 2010. Effects of IFN-alpha as a signal-3 cytokine on human naive and antigen-experienced CD8(+) T cells. Eur J Immunol **40:**3389-3402.
117. **Curtsinger JM, Mescher MF.** 2010. Inflammatory cytokines as a third signal for T cell activation. Curr Opin Immunol **22:**333-340.
118. **Bachmann MF, Barner M, Viola A, Kopf M.** 1999. Distinct kinetics of cytokine production and cytolysis in effector and memory T cells after viral infection. Eur J Immunol **29:**291-299.
119. **Paliard X, de Waal Malefijt R, Yssel H, Blanchard D, Chretien I, Abrams J, de Vries J, Spits H.** 1988. Simultaneous production of IL-2, IL-4, and IFN-gamma by activated human CD4+ and CD8+ T cell clones. J Immunol **141:**849-855.
120. **Wherry EJ, Ahmed R.** 2004. Memory CD8 T-cell differentiation during viral infection. J Virol **78:**5535-5545.
121. **Schroder K, Hertzog PJ, Ravasi T, Hume DA.** 2004. Interferon-gamma: an overview of signals, mechanisms and functions. J Leukoc Biol **75:**163-189.
122. **Sedger LM, McDermott MF.** 2014. TNF and TNF-receptors: From mediators of cell death and inflammation to therapeutic giants - past, present and future. Cytokine Growth Factor Rev **25:**453-472.
123. **D'Souza WN, Lefrancois L.** 2004. Frontline: An in-depth evaluation of the production of IL-2 by antigen-specific CD8 T cells in vivo. Eur J Immunol **34:**2977-2985.
124. **Pipkin ME, Sacks JA, Cruz-Guilloty F, Lichtenheld MG, Bevan MJ, Rao A.** 2010. Interleukin-2 and inflammation induce distinct transcriptional programs that promote the differentiation of effector cytolytic T cells. Immunity **32:**79-90.
125. **Kamimura D, Bevan MJ.** 2007. Naive CD8+ T cells differentiate into protective memory-like cells after IL-2 anti IL-2 complex treatment in vivo. J Exp Med **204:**1803-1812.
126. **Veugelers K, Motyka B, Goping IS, Shostak I, Sawchuk T, Bleackley RC.** 2006. Granule-mediated killing by granzyme B and perforin requires a mannose 6-phosphate receptor and is augmented by cell surface heparan sulfate. Mol Biol Cell **17:**623-633.
127. **Kagi D, Ledermann B, Burki K, Seiler P, Odermatt B, Olsen KJ, Podack ER, Zinkernagel RM, Hengartner H.** 1994. Cytotoxicity mediated by T cells and natural killer cells is greatly impaired in perforin-deficient mice. Nature **369:**31-37.
128. **Pham CT, Ley TJ.** 1997. The role of granzyme B cluster proteases in cell-mediated cytotoxicity. Semin Immunol **9:**127-133.
129. **Barry M, Bleackley RC.** 2002. Cytotoxic T lymphocytes: all roads lead to death. Nat Rev Immunol **2:**401-409.

130. **Sun J, Bird CH, Sutton V, McDonald L, Coughlin PB, De Jong TA, Trapani JA, Bird PI.** 1996. A cytosolic granzyme B inhibitor related to the viral apoptotic regulator cytokine response modifier A is present in cytotoxic lymphocytes. J Biol Chem **271:**27802-27809.
131. **Van Parijs L, Abbas AK.** 1996. Role of Fas-mediated cell death in the regulation of immune responses. Curr Opin Immunol **8:**355-361.
132. **Wiley SR, Schooley K, Smolak PJ, Din WS, Huang CP, Nicholl JK, Sutherland GR, Smith TD, Rauch C, Smith CA, et al.** 1995. Identification and characterization of a new member of the TNF family that induces apoptosis. Immunity **3:**673-682.
133. **Badovinac VP, Porter BB, Harty JT.** 2002. Programmed contraction of CD8(+) T cells after infection. Nat Immunol **3:**619-626.
134. **Kaech SM, Tan JT, Wherry EJ, Konieczny BT, Surh CD, Ahmed R.** 2003. Selective expression of the interleukin 7 receptor identifies effector CD8 T cells that give rise to long-lived memory cells. Nat Immunol **4:**1191-1198.
135. **Fuller MJ, Zajac AJ.** 2003. Ablation of CD8 and CD4 T cell responses by high viral loads. J Immunol **170:**477-486.
136. **Zelinskyy G, Myers L, Dietze KK, Gibbert K, Roggendorf M, Liu J, Lu M, Kraft AR, Teichgraber V, Hasenkrug KJ, Dittmer U.** 2011. Virus-specific CD8+ T cells upregulate programmed death-1 expression during acute friend retrovirus infection but are highly cytotoxic and control virus replication. J Immunol **187:**3730-3737.
137. **Odorizzi PM, Wherry EJ.** 2012. Inhibitory receptors on lymphocytes: insights from infections. J Immunol **188:**2957-2965.
138. **Buchbinder EI, Desai A.** 2016. CTLA-4 and PD-1 Pathways: Similarities, Differences, and Implications of Their Inhibition. Am J Clin Oncol **39:**98-106.
139. **Jin HT, Anderson AC, Tan WG, West EE, Ha SJ, Araki K, Freeman GJ, Kuchroo VK, Ahmed R.** 2010. Cooperation of Tim-3 and PD-1 in CD8 T-cell exhaustion during chronic viral infection. Proc Natl Acad Sci U S A **107:**14733-14738.
140. **Rodriguez-Manzanet R, DeKruyff R, Kuchroo VK, Umetsu DT.** 2009. The costimulatory role of TIM molecules. Immunol Rev **229:**259-270.
141. **Barber DL, Wherry EJ, Masopust D, Zhu B, Allison JP, Sharpe AH, Freeman GJ, Ahmed R.** 2006. Restoring function in exhausted CD8 T cells during chronic viral infection. Nature **439:**682-687.
142. **Blackburn SD, Shin H, Haining WN, Zou T, Workman CJ, Polley A, Betts MR, Freeman GJ, Vignali DA, Wherry EJ.** 2009. Coregulation of CD8+ T cell exhaustion by multiple inhibitory receptors during chronic viral infection. Nat Immunol **10:**29-37.
143. **Thaventhiran JE, Hoffmann A, Magiera L, de la Roche M, Lingel H, Brunner-Weinzierl M, Fearon DT.** 2012. Activation of the Hippo pathway by CTLA-4 regulates the expression of Blimp-1 in the CD8+ T cell. Proc Natl Acad Sci U S A **109:**E2223-2229.
144. **Lipson EJ, Drake CG.** 2011. Ipilimumab: an anti-CTLA-4 antibody for metastatic melanoma. Clin Cancer Res **17:**6958-6962.
145. **Workman CJ, Cauley LS, Kim IJ, Blackman MA, Woodland DL, Vignali DA.** 2004. Lymphocyte activation gene-3 (CD223) regulates the size of the expanding T cell population following antigen activation in vivo. J Immunol **172:**5450-5455.

146. **Hannier S, Tournier M, Bismuth G, Triebel F.** 1998. CD3/TCR complex-associated lymphocyte activation gene-3 molecules inhibit CD3/TCR signaling. J Immunol **161:**4058-4065.
147. **Du W, Yang M, Turner A, Xu C, Ferris RL, Huang J, Kane LP, Lu B.** 2017. TIM-3 as a Target for Cancer Immunotherapy and Mechanisms of Action. Int J Mol Sci **18**.
148. **Zhu C, Anderson AC, Kuchroo VK.** 2011. TIM-3 and its regulatory role in immune responses. Curr Top Microbiol Immunol **350:**1-15.
149. **Boles KS, Stepp SE, Bennett M, Kumar V, Mathew PA.** 2001. 2B4 (CD244) and CS1: novel members of the CD2 subset of the immunoglobulin superfamily molecules expressed on natural killer cells and other leukocytes. Immunol Rev **181:**234-249.
150. **Mathew PA, Garni-Wagner BA, Land K, Takashima A, Stoneman E, Bennett M, Kumar V.** 1993. Cloning and characterization of the 2B4 gene encoding a molecule associated with non-MHC-restricted killing mediated by activated natural killer cells and T cells. J Immunol **151:**5328-5337.
151. **Garni-Wagner BA, Purohit A, Mathew PA, Bennett M, Kumar V.** 1993. A novel function-associated molecule related to non-MHC-restricted cytotoxicity mediated by activated natural killer cells and T cells. J Immunol **151:**60-70.
152. **Latchman Y, Reiser H.** 1998. Enhanced murine CD4+ T cell responses induced by the CD2 ligand CD48. Eur J Immunol **28:**4325-4331.
153. **Brown MH, Boles K, van der Merwe PA, Kumar V, Mathew PA, Barclay AN.** 1998. 2B4, the natural killer and T cell immunoglobulin superfamily surface protein, is a ligand for CD48. J Exp Med **188:**2083-2090.
154. **Assarsson E, Kambayashi T, Persson CM, Chambers BJ, Ljunggren HG.** 2005. 2B4/CD48-mediated regulation of lymphocyte activation and function. J Immunol **175:**2045-2049.
155. **Cai G, Freeman GJ.** 2009. The CD160, BTLA, LIGHT/HVEM pathway: a bidirectional switch regulating T-cell activation. Immunol Rev **229:**244-258.
156. **Imaizumi T, Kumagai M, Sasaki N, Kurotaki H, Mori F, Seki M, Nishi N, Fujimoto K, Tanji K, Shibata T, Tamo W, Matsumiya T, Yoshida H, Cui XF, Takanashi S, Hanada K, Okumura K, Yagihashi S, Wakabayashi K, Nakamura T, Hirashima M, Satoh K.** 2002. Interferon-gamma stimulates the expression of galectin-9 in cultured human endothelial cells. J Leukoc Biol **72:**486-491.
157. **Keir ME, Butte MJ, Freeman GJ, Sharpe AH.** 2008. PD-1 and its ligands in tolerance and immunity. Annu Rev Immunol **26:**677-704.
158. **Wherry EJ, Kurachi M.** 2015. Molecular and cellular insights into T cell exhaustion. Nat Rev Immunol **15:**486-499.
159. **Sakaguchi S, Yamaguchi T, Nomura T, Ono M.** 2008. Regulatory T cells and immune tolerance. Cell **133:**775-787.
160. **Malek TR.** 2003. The main function of IL-2 is to promote the development of T regulatory cells. J Leukoc Biol **74:**961-965.
161. **Malek TR, Castro I.** 2010. Interleukin-2 receptor signaling: at the interface between tolerance and immunity. Immunity **33:**153-165.
162. **Weiss JM, Bilate AM, Gobert M, Ding Y, Curotto de Lafaille MA, Parkhurst CN, Xiong H, Dolpady J, Frey AB, Ruocco MG, Yang Y, Floess S, Huehn J, Oh S, Li MO, Niec RE, Rudensky AY, Dustin ML, Littman DR, Lafaille JJ.** 2012. Neuropilin

1 is expressed on thymus-derived natural regulatory T cells, but not mucosa-generated induced Foxp3+ T reg cells. J Exp Med **209:**1723-1742, S1721.

163. **Yadav M, Louvet C, Davini D, Gardner JM, Martinez-Llordella M, Bailey-Bucktrout S, Anthony BA, Sverdrup FM, Head R, Kuster DJ, Ruminski P, Weiss D, Von Schack D, Bluestone JA.** 2012. Neuropilin-1 distinguishes natural and inducible regulatory T cells among regulatory T cell subsets in vivo. J Exp Med **209:**1713-1722, S1711-1719.
164. **Nakamura K, Kitani A, Strober W.** 2001. Cell contact-dependent immunosuppression by CD4(+)CD25(+) regulatory T cells is mediated by cell surface-bound transforming growth factor beta. J Exp Med **194:**629-644.
165. **Kingsley CI, Karim M, Bushell AR, Wood KJ.** 2002. CD25+CD4+ regulatory T cells prevent graft rejection: CTLA-4- and IL-10-dependent immunoregulation of alloresponses. J Immunol **168:**1080-1086.
166. **Ebinuma H, Nakamoto N, Li Y, Price DA, Gostick E, Levine BL, Tobias J, Kwok WW, Chang KM.** 2008. Identification and in vitro expansion of functional antigen-specific CD25+ FoxP3+ regulatory T cells in hepatitis C virus infection. J Virol **82:**5043-5053.
167. **Antonioli L, Pacher P, Vizi ES, Hasko G.** 2013. CD39 and CD73 in immunity and inflammation. Trends Mol Med **19:**355-367.
168. **Borsellino G, Kleinewietfeld M, Di Mitri D, Sternjak A, Diamantini A, Giometto R, Hopner S, Centonze D, Bernardi G, Dell'Acqua ML, Rossini PM, Battistini L, Rotzschke O, Falk K.** 2007. Expression of ectonucleotidase CD39 by Foxp3+ Treg cells: hydrolysis of extracellular ATP and immune suppression. Blood **110:**1225-1232.
169. **Onishi Y, Fehervari Z, Yamaguchi T, Sakaguchi S.** 2008. Foxp3+ natural regulatory T cells preferentially form aggregates on dendritic cells in vitro and actively inhibit their maturation. Proc Natl Acad Sci U S A **105:**10113-10118.
170. **Huang CT, Workman CJ, Flies D, Pan X, Marson AL, Zhou G, Hipkiss EL, Ravi S, Kowalski J, Levitsky HI, Powell JD, Pardoll DM, Drake CG, Vignali DA.** 2004. Role of LAG-3 in regulatory T cells. Immunity **21:**503-513.
171. **Serra P, Amrani A, Yamanouchi J, Han B, Thiessen S, Utsugi T, Verdaguer J, Santamaria P.** 2003. CD40 ligation releases immature dendritic cells from the control of regulatory CD4+CD25+ T cells. Immunity **19:**877-889.
172. **Fallarino F, Grohmann U, Hwang KW, Orabona C, Vacca C, Bianchi R, Belladonna ML, Fioretti MC, Alegre ML, Puccetti P.** 2003. Modulation of tryptophan catabolism by regulatory T cells. Nat Immunol **4:**1206-1212.
173. **Oderup C, Cederbom L, Makowska A, Cilio CM, Ivars F.** 2006. Cytotoxic T lymphocyte antigen-4-dependent down-modulation of costimulatory molecules on dendritic cells in CD4+ CD25+ regulatory T-cell-mediated suppression. Immunology **118:**240-249.
174. **Windmann S, Otto L, Hrycak CP, Malyshkina A, Bongard N, David P, Gunzer M, Dittmer U, Bayer W.** 2019. Infection of B Cell Follicle-Resident Cells by Friend Retrovirus Occurs during Acute Infection and Is Maintained during Viral Persistence. MBio **10**.
175. **Akhmetzyanova I, Drabczyk M, Neff CP, Gibbert K, Dietze KK, Werner T, Liu J, Chen L, Lang KS, Palmer BE, Dittmer U, Zelinskyy G.** 2015. PD-L1 Expression on

Retrovirus-Infected Cells Mediates Immune Escape from CD8+ T Cell Killing. PLoS Pathog **11:**e1005224.

176. **Zaynagetdinov R, Sherrill TP, Kendall PL, Segal BH, Weller KP, Tighe RM, Blackwell TS.** 2013. Identification of myeloid cell subsets in murine lungs using flow cytometry. Am J Respir Cell Mol Biol **49:**180-189.
177. **Rose S, Misharin A, Perlman H.** 2012. A novel Ly6C/Ly6G-based strategy to analyze the mouse splenic myeloid compartment. Cytometry A **81:**343-350.
178. **Rozali EN, Hato SV, Robinson BW, Lake RA, Lesterhuis WJ.** 2012. Programmed death ligand 2 in cancer-induced immune suppression. Clin Dev Immunol **2012:**656340.
179. **del Rio ML, Lucas CL, Buhler L, Rayat G, Rodriguez-Barbosa JI.** 2010. HVEM/LIGHT/BTLA/CD160 cosignaling pathways as targets for immune regulation. J Leukoc Biol **87:**223-235.
180. **Vasu C, Wang A, Gorla SR, Kaithamana S, Prabhakar BS, Holterman MJ.** 2003. CD80 and CD86 C domains play an important role in receptor binding and co-stimulatory properties. Int Immunol **15:**167-175.
181. **Carreno BM, Collins M.** 2002. The B7 family of ligands and its receptors: new pathways for costimulation and inhibition of immune responses. Annu Rev Immunol **20:**29-53.
182. **Gorczynski R, Chen Z, Kai Y, Lee L, Wong S, Marsden PA.** 2004. CD200 is a ligand for all members of the CD200R family of immunoregulatory molecules. J Immunol **172:**7744-7749.
183. **McArdel SL, Terhorst C, Sharpe AH.** 2016. Roles of CD48 in regulating immunity and tolerance. Clin Immunol **164:**10-20.
184. **Chen W, Qin H, Chesebro B, Cheever MA.** 1996. Identification of a gag-encoded cytotoxic T-lymphocyte epitope from FBL-3 leukemia shared by Friend, Moloney, and Rauscher murine leukemia virus-induced tumors. J Virol **70:**7773-7782.
185. **Shui JW, Kronenberg M.** 2013. HVEM: An unusual TNF receptor family member important for mucosal innate immune responses to microbes. Gut Microbes **4:**146-151.
186. **Elliott LA, Doherty GA, Sheahan K, Ryan EJ.** 2017. Human Tumor-Infiltrating Myeloid Cells: Phenotypic and Functional Diversity. Front Immunol **8:**86.
187. **Yu YR, Hotten DF, Malakhau Y, Volker E, Ghio AJ, Noble PW, Kraft M, Hollingsworth JW, Gunn MD, Tighe RM.** 2016. Flow Cytometric Analysis of Myeloid Cells in Human Blood, Bronchoalveolar Lavage, and Lung Tissues. Am J Respir Cell Mol Biol **54:**13-24.
188. **Hassan J, Browne K, De Gascun C.** 2016. HIV-1 in Monocytes and Macrophages: An Overlooked Reservoir? Viral Immunol **29:**532-533.
189. **Rodrigues V, Ruffin N, San-Roman M, Benaroch P.** 2017. Myeloid Cell Interaction with HIV: A Complex Relationship. Front Immunol **8:**1698.
190. **Bayat Mokhtari R, Homayouni TS, Baluch N, Morgatskaya E, Kumar S, Das B, Yeger H.** 2017. Combination therapy in combating cancer. Oncotarget **8:**38022-38043.
191. **Paul N, Han SH.** 2011. Combination Therapy for Chronic Hepatitis B: Current Indications. Curr Hepat Rep **10:**98-105.
192. **Rasi G, Pierimarchi P, Sinibaldi Vallebona P, Colella F, Garaci E.** 2003. Combination therapy in the treatment of chronic viral hepatitis and prevention of hepatocellular carcinoma. Int Immunopharmacol **3:**1169-1176.

193. **Dietze KK, Zelinskyy G, Liu J, Kretzmer F, Schimmer S, Dittmer U.** 2013. Combining regulatory T cell depletion and inhibitory receptor blockade improves reactivation of exhausted virus-specific CD8+ T cells and efficiently reduces chronic retroviral loads. PLoS Pathog **9:**e1003798.
194. **Lahl K, Loddenkemper C, Drouin C, Freyer J, Arnason J, Eberl G, Hamann A, Wagner H, Huehn J, Sparwasser T.** 2007. Selective depletion of Foxp3+ regulatory T cells induces a scurfy-like disease. J Exp Med **204:**57-63.
195. **Nair SR, Zelinskyy G, Schimmer S, Gerlach N, Kassiotis G, Dittmer U.** 2010. Mechanisms of control of acute Friend virus infection by CD4+ T helper cells and their functional impairment by regulatory T cells. J Gen Virol **91:**440-451.
196. **Manzke N, Akhmetzyanova I, Hasenkrug KJ, Trilling M, Zelinskyy G, Dittmer U.** 2013. CD4+ T cells develop antiretroviral cytotoxic activity in the absence of regulatory T cells and CD8+ T cells. J Virol **87:**6306-6313.
197. **Zelinskyy G, Dietze K, Sparwasser T, Dittmer U.** 2009. Regulatory T cells suppress antiviral immune responses and increase viral loads during acute infection with a lymphotropic retrovirus. PLoS Pathog **5:**e1000406.
198. **Durrant LG, Ballantyne KC, Armitage NC, Robins RA, Marksman R, Hardcastle JD, Baldwin RW.** 1987. Quantitation of MHC antigen expression on colorectal tumours and its association with tumour progression. Br J Cancer **56:**425-432.
199. **Thibodeau J, Bourgeois-Daigneault MC, Lapointe R.** 2012. Targeting the MHC Class II antigen presentation pathway in cancer immunotherapy. Oncoimmunology **1:**908-916.
200. **Hemon P, Jean-Louis F, Ramgolam K, Brignone C, Viguier M, Bachelez H, Triebel F, Charron D, Aoudjit F, Al-Daccak R, Michel L.** 2011. MHC class II engagement by its ligand LAG-3 (CD223) contributes to melanoma resistance to apoptosis. J Immunol **186:**5173-5183.
201. **Maruhashi T, Okazaki IM, Sugiura D, Takahashi S, Maeda TK, Shimizu K, Okazaki T.** 2018. LAG-3 inhibits the activation of CD4(+) T cells that recognize stable pMHCII through its conformation-dependent recognition of pMHCII. Nat Immunol **19:**1415-1426.
202. **Vandenborre K, Van Gool SW, Kasran A, Ceuppens JL, Boogaerts MA, Vandenberghe P.** 1999. Interaction of CTLA-4 (CD152) with CD80 or CD86 inhibits human T-cell activation. Immunology **98:**413-421.
203. **Scholzen T, Gerdes J.** 2000. The Ki-67 protein: from the known and the unknown. J Cell Physiol **182:**311-322.
204. **Allard B, Longhi MS, Robson SC, Stagg J.** 2017. The ectonucleotidases CD39 and CD73: Novel checkpoint inhibitor targets. Immunol Rev **276:**121-144.
205. **Yang S, Wang J, Brand DD, Zheng SG.** 2018. Role of TNF-TNF Receptor 2 Signal in Regulatory T Cells and Its Therapeutic Implications. Front Immunol **9:**784.
206. **Vanamee ES, Faustman DL.** 2017. TNFR2: A Novel Target for Cancer Immunotherapy. Trends Mol Med **23:**1037-1046.
207. **Joedicke JJ, Myers L, Carmody AB, Messer RJ, Wajant H, Lang KS, Lang PA, Mak TW, Hasenkrug KJ, Dittmer U.** 2014. Activated CD8+ T cells induce expansion of Vbeta5+ regulatory T cells via TNFR2 signaling. J Immunol **193:**2952-2960.
208. **Honke N, Shaabani N, Cadeddu G, Sorg UR, Zhang DE, Trilling M, Klingel K, Sauter M, Kandolf R, Gailus N, van Rooijen N, Burkart C, Baldus SE, Grusdat M, Lohning M, Hengel H, Pfeffer K, Tanaka M, Haussinger D, Recher M, Lang PA,**

Lang KS. 2011. Enforced viral replication activates adaptive immunity and is essential for the control of a cytopathic virus. Nat Immunol **13:**51-57.

209. **Shaabani N, Duhan V, Khairnar V, Gassa A, Ferrer-Tur R, Haussinger D, Recher M, Zelinskyy G, Liu J, Dittmer U, Trilling M, Scheu S, Hardt C, Lang PA, Honke N, Lang KS.** 2016. CD169(+) macrophages regulate PD-L1 expression via type I interferon and thereby prevent severe immunopathology after LCMV infection. Cell Death Dis **7:**e2446.
210. **Martinez-Picado J, McLaren PJ, Telenti A, Izquierdo-Useros N.** 2017. Retroviruses As Myeloid Cell Riders: What Natural Human Siglec-1 "Knockouts" Tell Us About Pathogenesis. Front Immunol **8:**1593.
211. **Hladik F, Sakchalathorn P, Ballweber L, Lentz G, Fialkow M, Eschenbach D, McElrath MJ.** 2007. Initial events in establishing vaginal entry and infection by human immunodeficiency virus type-1. Immunity **26:**257-270.
212. **Zhang Z, Schuler T, Zupancic M, Wietgrefe S, Staskus KA, Reimann KA, Reinhart TA, Rogan M, Cavert W, Miller CJ, Veazey RS, Notermans D, Little S, Danner SA, Richman DD, Havlir D, Wong J, Jordan HL, Schacker TW, Racz P, Tenner-Racz K, Letvin NL, Wolinsky S, Haase AT.** 1999. Sexual transmission and propagation of SIV and HIV in resting and activated CD4+ T cells. Science **286:**1353-1357.
213. **Zhou Z, Barry de Longchamps N, Schmitt A, Zerbib M, Vacher-Lavenu MC, Bomsel M, Ganor Y.** 2011. HIV-1 efficient entry in inner foreskin is mediated by elevated CCL5/RANTES that recruits T cells and fuels conjugate formation with Langerhans cells. PLoS Pathog **7:**e1002100.
214. **Cameron PU, Freudenthal PS, Barker JM, Gezelter S, Inaba K, Steinman RM.** 1992. Dendritic cells exposed to human immunodeficiency virus type-1 transmit a vigorous cytopathic infection to CD4+ T cells. Science **257:**383-387.
215. **Lore K, Smed-Sorensen A, Vasudevan J, Mascola JR, Koup RA.** 2005. Myeloid and plasmacytoid dendritic cells transfer HIV-1 preferentially to antigen-specific CD4+ T cells. J Exp Med **201:**2023-2033.
216. **Spiegel H, Herbst H, Niedobitek G, Foss HD, Stein H.** 1992. Follicular dendritic cells are a major reservoir for human immunodeficiency virus type 1 in lymphoid tissues facilitating infection of CD4+ T-helper cells. Am J Pathol **140:**15-22.
217. **Heesters BA, Lindqvist M, Vagefi PA, Scully EP, Schildberg FA, Altfeld M, Walker BD, Kaufmann DE, Carroll MC.** 2015. Follicular Dendritic Cells Retain Infectious HIV in Cycling Endosomes. PLoS Pathog **11:**e1005285.
218. **Heath SL, Tew JG, Tew JG, Szakal AK, Burton GF.** 1995. Follicular dendritic cells and human immunodeficiency virus infectivity. Nature **377:**740-744.
219. **Honeycutt JB, Thayer WO, Baker CE, Ribeiro RM, Lada SM, Cao Y, Cleary RA, Hudgens MG, Richman DD, Garcia JV.** 2017. HIV persistence in tissue macrophages of humanized myeloid-only mice during antiretroviral therapy. Nature Medicine **23:**638.
220. **Klepper A, Branch AD.** 2015. Macrophages and the Viral Dissemination Super Highway. EC Microbiol **2:**328-336.
221. **Gendelman HE, Narayan O, Molineaux S, Clements JE, Ghotbi Z.** 1985. Slow, persistent replication of lentiviruses: role of tissue macrophages and macrophage precursors in bone marrow. Proc Natl Acad Sci U S A **82:**7086-7090.
222. **Zon LI, Arkin C, Groopman JE.** 1987. Haematologic manifestations of the human immune deficiency virus (HIV). Br J Haematol **66:**251-256.

223. **Kuritzkes DR.** 2000. Neutropenia, neutrophil dysfunction, and bacterial infection in patients with human immunodeficiency virus disease: the role of granulocyte colony-stimulating factor. Clin Infect Dis **30:**256-260.
224. **Shi X, Sims MD, Hanna MM, Xie M, Gulick PG, Zheng YH, Basson MD, Zhang P.** 2014. Neutropenia during HIV infection: adverse consequences and remedies. Int Rev Immunol **33:**511-536.
225. **Zelinskyy G, Dietze KK, Husecken YP, Schimmer S, Nair S, Werner T, Gibbert K, Kershaw O, Gruber AD, Sparwasser T, Dittmer U.** 2009. The regulatory T-cell response during acute retroviral infection is locally defined and controls the magnitude and duration of the virus-specific cytotoxic T-cell response. Blood **114:**3199-3207.
226. **Teigler JE, Zelinskyy G, Eller MA, Bolton DL, Marovich M, Gordon AD, Alrubayyi A, Alter G, Robb ML, Martin JN, Deeks SG, Michael NL, Dittmer U, Streeck H.** 2017. Differential Inhibitory Receptor Expression on T Cells Delineates Functional Capacities in Chronic Viral Infection. J Virol **91**.
227. **Attanasio J, Wherry EJ.** 2016. Costimulatory and Coinhibitory Receptor Pathways in Infectious Disease. Immunity **44:**1052-1068.
228. **Bardhan K, Anagnostou T, Boussiotis VA.** 2016. The PD1:PD-L1/2 Pathway from Discovery to Clinical Implementation. Front Immunol **7:**550.
229. **Ghiotto M, Gauthier L, Serriari N, Pastor S, Truneh A, Nunes JA, Olive D.** 2010. PD-L1 and PD-L2 differ in their molecular mechanisms of interaction with PD-1. Int Immunol **22:**651-660.
230. **Ishida M, Iwai Y, Tanaka Y, Okazaki T, Freeman GJ, Minato N, Honjo T.** 2002. Differential expression of PD-L1 and PD-L2, ligands for an inhibitory receptor PD-1, in the cells of lymphohematopoietic tissues. Immunol Lett **84:**57-62.
231. **David P, Megger DA, Kaiser T, Werner T, Liu J, Chen L, Sitek B, Dittmer U, Zelinskyy G.** 2019. The PD-1/PD-L1 Pathway Affects the Expansion and Function of Cytotoxic CD8(+) T Cells During an Acute Retroviral Infection. Front Immunol **10:**54.
232. **Meier A, Bagchi A, Sidhu HK, Alter G, Suscovich TJ, Kavanagh DG, Streeck H, Brockman MA, LeGall S, Hellman J, Altfeld M.** 2008. Upregulation of PD-L1 on monocytes and dendritic cells by HIV-1 derived TLR ligands. AIDS **22:**655-658.
233. **Sachdeva M, Fischl MA, Pahwa R, Sachdeva N, Pahwa S.** 2010. Immune exhaustion occurs concomitantly with immune activation and decrease in regulatory T cells in viremic chronically HIV-1-infected patients. J Acquir Immune Defic Syndr **54:**447-454.
234. **Wang X, Zhang Z, Zhang S, Fu J, Yao J, Jiao Y, Wu H, Wang FS.** 2008. B7-H1 up-regulation impairs myeloid DC and correlates with disease progression in chronic HIV-1 infection. Eur J Immunol **38:**3226-3236.
235. **Boasso A, Hardy AW, Landay AL, Martinson JL, Anderson SA, Dolan MJ, Clerici M, Shearer GM.** 2008. PDL-1 upregulation on monocytes and T cells by HIV via type I interferon: restricted expression of type I interferon receptor by CCR5-expressing leukocytes. Clin Immunol **129:**132-144.
236. **Rodriguez-Garcia M, Porichis F, de Jong OG, Levi K, Diefenbach TJ, Lifson JD, Freeman GJ, Walker BD, Kaufmann DE, Kavanagh DG.** 2011. Expression of PD-L1 and PD-L2 on human macrophages is up-regulated by HIV-1 and differentially modulated by IL-10. J Leukoc Biol **89:**507-515.
237. **Muthumani K, Shedlock DJ, Choo DK, Fagone P, Kawalekar OU, Goodman J, Bian CB, Ramanathan AA, Atman P, Tebas P, Chattergoon MA, Choo AY, Weiner DB.**

2011. HIV-mediated phosphatidylinositol 3-kinase/serine-threonine kinase activation in APCs leads to programmed death-1 ligand upregulation and suppression of HIV-specific CD8 T cells. J Immunol **187:**2932-2943.

238. **Dickens AM, Yoo SW, Chin AC, Xu J, Johnson TP, Trout AL, Hauser KF, Haughey NJ.** 2017. Chronic low-level expression of HIV-1 Tat promotes a neurodegenerative phenotype with aging. Sci Rep **7:**7748.
239. **Planes R, BenMohamed L, Leghmari K, Delobel P, Izopet J, Bahraoui E.** 2014. HIV-1 Tat protein induces PD-L1 (B7-H1) expression on dendritic cells through tumor necrosis factor alpha- and toll-like receptor 4-mediated mechanisms. J Virol **88:**6672-6689.
240. **Lesterhuis WJ, Punt CJ, Hato SV, Eleveld-Trancikova D, Jansen BJ, Nierkens S, Schreibelt G, de Boer A, Van Herpen CM, Kaanders JH, van Krieken JH, Adema GJ, Figdor CG, de Vries IJ.** 2011. Platinum-based drugs disrupt STAT6-mediated suppression of immune responses against cancer in humans and mice. J Clin Invest **121:**3100-3108.
241. **Yamazaki T, Akiba H, Iwai H, Matsuda H, Aoki M, Tanno Y, Shin T, Tsuchiya H, Pardoll DM, Okumura K, Azuma M, Yagita H.** 2002. Expression of programmed death 1 ligands by murine T cells and APC. J Immunol **169:**5538-5545.
242. **Stanciu LA, Bellettato CM, Laza-Stanca V, Coyle AJ, Papi A, Johnston SL.** 2006. Expression of programmed death-1 ligand (PD-L) 1, PD-L2, B7-H3, and inducible costimulator ligand on human respiratory tract epithelial cells and regulation by respiratory syncytial virus and type 1 and 2 cytokines. J Infect Dis **193:**404-412.
243. **Hatam LJ, Devoti JA, Rosenthal DW, Lam F, Abramson AL, Steinberg BM, Bonagura VR.** 2012. Immune suppression in premalignant respiratory papillomas: enriched functional CD4+Foxp3+ regulatory T cells and PD-1/PD-L1/L2 expression. Clin Cancer Res **18:**1925-1935.
244. **Matsuyama-Kato A, Murata S, Isezaki M, Takasaki S, Kano R, Konnai S, Ohashi K.** 2014. Expression analysis of programmed death ligand 2 in tumors caused by the avian oncovirus Marek's disease virus. Arch Virol **159:**2123-2126.
245. **Raftery MJ, Abdelaziz MO, Hofmann J, Schonrich G.** 2018. Hantavirus-Driven PD-L1/PD-L2 Upregulation: An Imperfect Viral Immune Evasion Mechanism. Front Immunol **9:**2560.
246. **Messal N, Serriari NE, Pastor S, Nunes JA, Olive D.** 2011. PD-L2 is expressed on activated human T cells and regulates their function. Mol Immunol **48:**2214-2219.
247. **Iwamura K, Kato T, Miyahara Y, Naota H, Mineno J, Ikeda H, Shiku H.** 2012. siRNA-mediated silencing of PD-1 ligands enhances tumor-specific human T-cell effector functions. Gene Ther **19:**959-966.
248. **Chen F, Liu Z, Wu W, Rozo C, Bowdridge S, Millman A, Van Rooijen N, Urban JF, Jr., Wynn TA, Gause WC.** 2012. An essential role for TH2-type responses in limiting acute tissue damage during experimental helminth infection. Nat Med **18:**260-266.
249. **Nazareth MR, Broderick L, Simpson-Abelson MR, Kelleher RJ, Jr., Yokota SJ, Bankert RB.** 2007. Characterization of human lung tumor-associated fibroblasts and their ability to modulate the activation of tumor-associated T cells. J Immunol **178:**5552-5562.
250. **Ohigashi Y, Sho M, Yamada Y, Tsurui Y, Hamada K, Ikeda N, Mizuno T, Yoriki R, Kashizuka H, Yane K, Tsushima F, Otsuki N, Yagita H, Azuma M, Nakajima Y.**

2005. Clinical significance of programmed death-1 ligand-1 and programmed death-1 ligand-2 expression in human esophageal cancer. Clin Cancer Res **11:**2947-2953.

251. **Gao Q, Wang XY, Qiu SJ, Yamato I, Sho M, Nakajima Y, Zhou J, Li BZ, Shi YH, Xiao YS, Xu Y, Fan J.** 2009. Overexpression of PD-L1 significantly associates with tumor aggressiveness and postoperative recurrence in human hepatocellular carcinoma. Clin Cancer Res **15:**971-979.
252. **del Rio ML, Fernandez-Renedo C, Chaloin O, Scheu S, Pfeffer K, Shintani Y, Perez-Simon JA, Schneider P, Rodriguez-Barbosa JI.** 2016. Immunotherapeutic targeting of LIGHT/LTbetaR/HVEM pathway fully recapitulates the reduced cytotoxic phenotype of LIGHT-deficient T cells. MAbs **8:**478-490.
253. **Inoue T, Sho M, Yasuda S, Nishiwada S, Nakamura S, Ueda T, Nishigori N, Kawasaki K, Obara S, Nakamoto T, Koyama F, Fujii H, Nakajima Y.** 2015. HVEM expression contributes to tumor progression and prognosis in human colorectal cancer. Anticancer Res **35:**1361-1367.
254. **Derre L, Rivals JP, Jandus C, Pastor S, Rimoldi D, Romero P, Michielin O, Olive D, Speiser DE.** 2010. BTLA mediates inhibition of human tumor-specific CD8+ T cells that can be partially reversed by vaccination. J Clin Invest **120:**157-167.
255. **Murphy KM, Nelson CA, Sedy JR.** 2006. Balancing co-stimulation and inhibition with BTLA and HVEM. Nat Rev Immunol **6:**671-681.
256. **Ramsay AG, Clear AJ, Fatah R, Gribben JG.** 2012. Multiple inhibitory ligands induce impaired T-cell immunologic synapse function in chronic lymphocytic leukemia that can be blocked with lenalidomide: establishing a reversible immune evasion mechanism in human cancer. Blood **120:**1412-1421.
257. **Vigano S, Banga R, Bellanger F, Pellaton C, Farina A, Comte D, Harari A, Perreau M.** 2014. CD160-associated CD8 T-cell functional impairment is independent of PD-1 expression. PLoS Pathog **10:**e1004380.
258. **Wherry EJ, Ha SJ, Kaech SM, Haining WN, Sarkar S, Kalia V, Subramaniam S, Blattman JN, Barber DL, Ahmed R.** 2007. Molecular signature of CD8+ T cell exhaustion during chronic viral infection. Immunity **27:**670-684.
259. **Bensussan A, Rabian C, Schiavon V, Bengoufa D, Leca G, Boumsell L.** 1993. Significant enlargement of a specific subset of CD3+CD8+ peripheral blood leukocytes mediating cytotoxic T-lymphocyte activity during human immunodeficiency virus infection. Proc Natl Acad Sci U S A **90:**9427-9430.
260. **Peretz Y, He Z, Shi Y, Yassine-Diab B, Goulet JP, Bordi R, Filali-Mouhim A, Loubert JB, El-Far M, Dupuy FP, Boulassel MR, Tremblay C, Routy JP, Bernard N, Balderas R, Haddad EK, Sekaly RP.** 2012. CD160 and PD-1 co-expression on HIV-specific CD8 T cells defines a subset with advanced dysfunction. PLoS Pathog **8:**e1002840.
261. **Muscate F, Stetter N, Schramm C, Schulze Zur Wiesch J, Bosurgi L, Jacobs T.** 2018. HVEM and CD160: Regulators of Immunopathology During Malaria Blood-Stage. Front Immunol **9:**2611.
262. **Flynn R, Hutchinson T, Murphy KM, Ware CF, Croft M, Salek-Ardakani S.** 2013. CD8 T cell memory to a viral pathogen requires trans cosignaling between HVEM and BTLA. PLoS One **8:**e77991.

263. **Steinberg MW, Huang Y, Wang-Zhu Y, Ware CF, Cheroutre H, Kronenberg M.** 2013. BTLA interaction with HVEM expressed on CD8(+) T cells promotes survival and memory generation in response to a bacterial infection. PLoS One **8:**e77992.
264. **Rosenblum MD, Olasz EB, Yancey KB, Woodliff JE, Lazarova Z, Gerber KA, Truitt RL.** 2004. Expression of CD200 on epithelial cells of the murine hair follicle: a role in tissue-specific immune tolerance? J Invest Dermatol **123:**880-887.
265. **Wright GJ, Jones M, Puklavec MJ, Brown MH, Barclay AN.** 2001. The unusual distribution of the neuronal/lymphoid cell surface CD200 (OX2) glycoprotein is conserved in humans. Immunology **102:**173-179.
266. **Koning N, Swaab DF, Hoek RM, Huitinga I.** 2009. Distribution of the immune inhibitory molecules CD200 and CD200R in the normal central nervous system and multiple sclerosis lesions suggests neuron-glia and glia-glia interactions. J Neuropathol Exp Neurol **68:**159-167.
267. **Snelgrove RJ, Goulding J, Didierlaurent AM, Lyonga D, Vekaria S, Edwards L, Gwyer E, Sedgwick JD, Barclay AN, Hussell T.** 2008. A critical function for CD200 in lung immune homeostasis and the severity of influenza infection. Nat Immunol **9:**1074-1083.
268. **Curry A, Khatri I, Kos O, Zhu F, Gorczynski R.** 2017. Importance of CD200 expression by tumor or host cells to regulation of immunotherapy in a mouse breast cancer model. PLoS One **12:**e0171586.
269. **Cook KD, Whitmire JK.** 2016. LAG-3 Confers a Competitive Disadvantage upon Antiviral CD8+ T Cell Responses. J Immunol **197:**119-127.
270. **Richter K, Agnellini P, Oxenius A.** 2010. On the role of the inhibitory receptor LAG-3 in acute and chronic LCMV infection. Int Immunol **22:**13-23.
271. **Lichtenegger FS, Rothe M, Schnorfeil FM, Deiser K, Krupka C, Augsberger C, Schluter M, Neitz J, Subklewe M.** 2018. Targeting LAG-3 and PD-1 to Enhance T Cell Activation by Antigen-Presenting Cells. Front Immunol **9:**385.
272. **Moretta A, Bottino C, Vitale M, Pende D, Cantoni C, Mingari MC, Biassoni R, Moretta L.** 2001. Activating receptors and coreceptors involved in human natural killer cell-mediated cytolysis. Annu Rev Immunol **19:**197-223.
273. **Peritt D, Sesok-Pizzini DA, Schretzenmair R, Macgregor RR, Valiante NM, Tu X, Trinchieri G, Kamoun M.** 1999. C1.7 antigen expression on CD8+ T cells is activation dependent: increased proportion of C1.7+CD8+ T cells in HIV-1-infected patients with progressing disease. J Immunol **162:**7563-7568.
274. **Bengsch B, Seigel B, Ruhl M, Timm J, Kuntz M, Blum HE, Pircher H, Thimme R.** 2010. Coexpression of PD-1, 2B4, CD160 and KLRG1 on exhausted HCV-specific CD8+ T cells is linked to antigen recognition and T cell differentiation. PLoS Pathog **6:**e1000947.
275. **Aldy KN, Horton NC, Mathew PA, Mathew SO.** 2011. 2B4+ CD8+ T cells play an inhibitory role against constrained HIV epitopes. Biochem Biophys Res Commun **405:**503-507.
276. **Sakuishi K, Apetoh L, Sullivan JM, Blazar BR, Kuchroo VK, Anderson AC.** 2010. Targeting Tim-3 and PD-1 pathways to reverse T cell exhaustion and restore anti-tumor immunity. J Exp Med **207:**2187-2194.

277. **Ngiow SF, von Scheidt B, Akiba H, Yagita H, Teng MW, Smyth MJ.** 2011. Anti-TIM3 antibody promotes T cell IFN-gamma-mediated antitumor immunity and suppresses established tumors. Cancer Res **71:**3540-3551.
278. **Fourcade J, Sun Z, Benallaoua M, Guillaume P, Luescher IF, Sander C, Kirkwood JM, Kuchroo V, Zarour HM.** 2010. Upregulation of Tim-3 and PD-1 expression is associated with tumor antigen-specific CD8+ T cell dysfunction in melanoma patients. J Exp Med **207:**2175-2186.
279. **Gao X, Zhu Y, Li G, Huang H, Zhang G, Wang F, Sun J, Yang Q, Zhang X, Lu B.** 2012. TIM-3 expression characterizes regulatory T cells in tumor tissues and is associated with lung cancer progression. PLoS One **7:**e30676.
280. **Greenwald RJ, Freeman GJ, Sharpe AH.** 2005. The B7 family revisited. Annu Rev Immunol **23:**515-548.
281. **Lespagnard L, Mettens P, Urbain J, Moser M.** 1997. Role of B7 costimulation in the induction of T and B cell responses by dendritic cells in vivo. Adv Exp Med Biol **417:**529-533.
282. **Chang CS, Chang JH, Hsu NC, Lin HY, Chung CY.** 2007. Expression of CD80 and CD86 costimulatory molecules are potential markers for better survival in nasopharyngeal carcinoma. BMC Cancer **7:**88.
283. **Belkaid Y, Tarbell K.** 2009. Regulatory T cells in the control of host-microorganism interactions (*). Annu Rev Immunol **27:**551-589.
284. **Melero I, Berman DM, Aznar MA, Korman AJ, Perez Gracia JL, Haanen J.** 2015. Evolving synergistic combinations of targeted immunotherapies to combat cancer. Nat Rev Cancer **15:**457-472.
285. **Gide TN, Quek C, Menzies AM, Tasker AT, Shang P, Holst J, Madore J, Lim SY, Velickovic R, Wongchenko M, Yan Y, Lo S, Carlino MS, Guminski A, Saw RPM, Pang A, McGuire HM, Palendira U, Thompson JF, Rizos H, Silva IPD, Batten M, Scolyer RA, Long GV, Wilmott JS.** 2019. Distinct Immune Cell Populations Define Response to Anti-PD-1 Monotherapy and Anti-PD-1/Anti-CTLA-4 Combined Therapy. Cancer Cell **35:**238-255 e236.
286. **Champiat S, Lambotte O, Barreau E, Belkhir R, Berdelou A, Carbonnel F, Cauquil C, Chanson P, Collins M, Durrbach A, Ederhy S, Feuillet S, Francois H, Lazarovici J, Le Pavec J, De Martin E, Mateus C, Michot JM, Samuel D, Soria JC, Robert C, Eggermont A, Marabelle A.** 2016. Management of immune checkpoint blockade dysimmune toxicities: a collaborative position paper. Ann Oncol **27:**559-574.
287. **Hodi FS, Butler M, Oble DA, Seiden MV, Haluska FG, Kruse A, Macrae S, Nelson M, Canning C, Lowy I, Korman A, Lautz D, Russell S, Jaklitsch MT, Ramaiya N, Chen TC, Neuberg D, Allison JP, Mihm MC, Dranoff G.** 2008. Immunologic and clinical effects of antibody blockade of cytotoxic T lymphocyte-associated antigen 4 in previously vaccinated cancer patients. Proc Natl Acad Sci U S A **105:**3005-3010.
288. **Liakou CI, Kamat A, Tang DN, Chen H, Sun J, Troncoso P, Logothetis C, Sharma P.** 2008. CTLA-4 blockade increases IFNgamma-producing CD4+ICOShi cells to shift the ratio of effector to regulatory T cells in cancer patients. Proc Natl Acad Sci U S A **105:**14987-14992.
289. **Romano E, Kusio-Kobialka M, Foukas PG, Baumgaertner P, Meyer C, Ballabeni P, Michielin O, Weide B, Romero P, Speiser DE.** 2015. Ipilimumab-dependent cell-

mediated cytotoxicity of regulatory T cells ex vivo by nonclassical monocytes in melanoma patients. Proc Natl Acad Sci U S A **112:**6140-6145.

290. **Wang DY, Salem JE, Cohen JV, Chandra S, Menzer C, Ye F, Zhao S, Das S, Beckermann KE, Ha L, Rathmell WK, Ancell KK, Balko JM, Bowman C, Davis EJ, Chism DD, Horn L, Long GV, Carlino MS, Lebrun-Vignes B, Eroglu Z, Hassel JC, Menzies AM, Sosman JA, Sullivan RJ, Moslehi JJ, Johnson DB.** 2018. Fatal Toxic Effects Associated With Immune Checkpoint Inhibitors: A Systematic Review and Meta-analysis. JAMA Oncol **4:**1721-1728.

291. **Fleming V, Hu X, Weber R, Nagibin V, Groth C, Altevogt P, Utikal J, Umansky V.** 2018. Targeting Myeloid-Derived Suppressor Cells to Bypass Tumor-Induced Immunosuppression. Front Immunol **9:**398.

9. Appendix

9.1 List of Abbreviations

Abbreviations	Full form
5FU	5- Fluorouracil
°C	Degree Celsius
γδ T cells	Gamma delta T cells
µl	Microlitre
ADCC	Antibody dependent cell mediated cytotoxicity
AF 488	Alexa Fluor 488
AF 647	Alexa Fluor 647
AF 700	Alexa Fluor 700
AIDS	Acquired immunodeficiency syndrome
APC	Antigen presenting cells
APC	Allophycocyanin
APC-Cy7	Allophycocyanin – cyanine 7
Arg	Arginase
ART	Antiretroviral therapy
ATRA	All – trans retinoic acid
BM	Bone marrow
BSA	Bovine serum albumin
BTLA	B and T lymphocyte attenuator
BV	Brilliant violet 421
Caecam	Carcinoembryonic antigen related cell adhesion molecule 1
cAMP	Cyclic adenosine monophosphate
CD	Cluster of differentiation
CFSE	Carboxyfluoresceinsuccinimidyl ester
CLL	Chronic lymphocytic leukemia
CNS	Central nervous system
CRC	Colorectal cancer
CTL	Cytotoxic T lymphocytes
CTLA-4	Cytotoxic T lymphocyte Antigen 4
DC	Dendritic cells
DEREG	Depletion of regulatory T cells
DMSO	Dimethyl sulfoxide
DNA	Deoxyribonucleic acid
dpi	Days post infection
DT	Diphtheria toxin
DTR	Diphtheria toxin receptor
EDTA	Ethylene diamine tetra acetic acid
ER	Endoplasmic reticulum
ERManI	Endoplasmic reticulum a1,2-mannisidase I
Env	envelope

Eomes	Eomesdermin
FACS	Fluorescence activated cell sorting
FCS	Fetal calf serum
FELASA	Federation of European Laboratory Animal Science Association
FIV	Feline immunodeficiency virus
FITC	Fluorescein isothiocyanate
FL	Follicular B cell non-Hodgkin lymphoma
F-MuLV	Friend murine leukemia virus
FoxP3	Forkhead box P3
FSC	Forward scatter channel
FV	Friend Virus
FVD	Fixable viable dye
G	Gram
Gag	Group specific antigen
Gal-9	Galectin - 9
Gata-3	Gata binding protein 3
GBP	Guanylate binding protein
GFP	Green fluorescent protein
gMDSC	Granulocytic myeloid derived suppressor cell
GIST	Gastrointestinal stromal tumors
Gzm	Granzyme
HAART	High active antiretroviral therapy
HBV	Hepatitis B virus
HCC	Hepatocellular carcinoma
HCV	Hepatitis C virus
HIV	Human immunodeficiency virus
HNSCC	Head and neck squamous cell carcinoma
HLA	Human leukocytes antigen
HSV	Herpes simplex virus
HVEM	Herpes virus entry mediator
HTLV-1	Human T cell leukemia virus-1
IBD	Inflammatory bowel disease
IDO	indoleamine 2,3- dioxygenase
Ii	Invariant chain
i.p	intraperitoneal
iNOS	Induced nitric oxide synthetase
i.v	Intravenous
IFN-g	Interferon gamma
Ig	Immunoglobulin
IL	Interleukin
IgSF	Immunoglobulin superfamily
iTregs	Induced regulatory T cells
KLRG-1	Killer cell lectin like receptor subfamily G member 1

L	liter
LAG-3	Lymphocyte activation gene 3
LCMV	Lymphocytic choriomeningitis virus
Lin-	Lineage neagtive
LTa	Lymphotoxin alpha
LTR	Long terminal repeat
Mab	Monoclonal antibody
MAB	Membrane attack complex
MBL	Mannose binding lectin
MCMV	Murine cytomegalovirus
mDC	Myeloid dendritic cell
MDSC	Myeloid derived suppressor cell
MFI	Mean fluorescent intensity
mg	Milligram
MHC	Major histocompatibility complex
ml	Milliliter
mm	Melanoma
mMDSC	Monocytic myeloid derived suppressor cell
mRNA	Messenger ribonucleic acid
mTOR	Mammalian target of rapamycin
NK	Natural killer cells
NLR	Nod like receptors
NOS	Nitric oxide synthase
NSCLC	Non-small cell lung cancer
nTregs	Natural regulatory T cells
PAMPs	Pathogen associated molecular pattern
PBBS	Phosphate buffer saline containing glucose
PBS	Phosphate buffer saline
PBMC	Peripheral blood mononuclear cells
PD-1	Programmed cell death
PD-L1	Programmed cell death ligand 1
PE	Phycoerythrin
PE Cy5	Phycoerythrin – Cyanine 5
PE Cy7	Phycoerythrin – Cyanine 7
PerCP	Peridinin chlorophyll protein complex
PHA	Phytohaemagglutin
PI	Propidium iodide
PI3K	Phosphoinisitide 3-kinase
PMNs	Polymorphonuclear
Pol	Polymerase
PRR	Pathogen recognition receptors
PtdSer	Phosphatidyl serine
RLR	Retinoic acid inducible gene I like receptors
RNA	Ribonucleic acid
ROS	Reactive oxygen species

RPMI-1640	Rosewell park memorial institute medium 1640
RSV	Rous sarcoma virus
RT	Reverse transcriptase
SAMHD 1	Sterile alpha motif and histidine-aspartate domain 1
SERINC3/5	Serine incorporator
SFFV	Spleen focus forming virus
SIV	Simian immunodeficiency virus
SLAM	Signaling lymphocytic activation molecule
SSC	Side scatter channel
ssRNA	Single stranded ribonucleic acid
STAT	Signal transducer and activator of transcription
TCR	T cell recptor
Tetr	Tetramer
TGF-b	Transforming growth factor beta
Th	T helper
Tim-3	T cell immunoglobulin domain and mucin domain-3
TLR	Toll like recptor
TNFR	Tumor necrosis factor recptor
TNF-a	Tumor necrosis factor alpha
TNFRSF14	Tumor necrosis factor receptor super family
TRAIL	Tumor necrosis factor related apoptosis inducing ligand
tRNA	Transfer ribonucleic acid
Tregs	Regulatory T cells
TSPO	Translocator protein
ZAP	Zinc finger antiviral protein

9.2 Figure list

9.3 Table list

9.4 List of publication

- **Paul David**, Dominik Megger, Tamara Kaiser, Tanja Werner, Jia Liu, Lieping Chen , Barbara Sitek, Ulf Dittmer & Gennadiy Zelinskyy. ‘’The PD-1/PD-L1 pathway effects the expansion and function of cytotoxic CD8+ T cells during an acute retroviral infection’’, Frontiers in immunology. 2019Jan
- Sonja Windmann, Lucas Otto, Camilla Hrycak, Anna Malyshkina, Nadine Bongard, **PaulDavid**, Matthias Gunzer, Ulf Dittmer, and Wibke Bayer. "Infection of B cell follicle-resident cells by Friend retrovirus occurs during acute infection and is maintained during viral persistence", mBio. 2019 Jan

9.5 Acknowledgement

Firstly I would like to thank God almighty for bringing me to Germany, giving me good health and helping me find favor in the eyes of my supervisors.

I would like to express my sincere gratitude to both my supervisors Dr Gennadiy Zelinskyy and Prof. Ulf Dittmer for their continuous support of my PhD study and related research for their patience, motivation and immense knowledge. Their guidance helped me in all the time of research and writing of this thesis. I could not have imagined having a better advisor and mentor for my Ph.D study.

Beside my advisors, I would like to thank everyone from Institute of Virology starting from Prof Dittmer's group, present and past (Wibke, Kathrin, Kirsten, Elisabeth, Gosia, Nadine, Camilla, Lucas, Aleks, Anja, Sonja, Julia I, Julia D, Rouven, Sandra, Jaana and Philip) for their constant encouragement and help.

I would also like to extend my thanks to Tanja Werner and Simone Schimmer for their useful technical advice and also to Ursula, Katrin and Delia for helping me with all the official work.

I would specially like to thank DFG and the funding sources that supported (TRR60) me during my Ph.D. My sincere appreciation and thanks to Asmae Gassa for forwarding me the PhD application.

I also want to thank Tanja Becker, Benny, Mira, Silke, Chris for their time and timely help. I would like to thank Mirko, Daniel, Sandra and Ruth for the healthy discussions during Biome student lectures.

A special thanks to my family. Words cannot express how grateful I am to my mother, my mother-in law, father-in-law, and other very dear members of my family for all of the sacrifices that you've made on my behalf. Your prayer for me was what sustained me thus far. I would also like to thank all of my friends, members from Christ Church who supported me in writing, and incented me to strive towards my goal. At the end, I would like express appreciation to my beloved wife Kanika who was always my support in the moments when there was no one to answer my queries.

9.6 Curriculum vitae

‘’The curriculum vitae is not included in the online version for reasons of data protection’’.

9.7 Erklärung:

Hiermit erkläre ich, gem. § 6 Abs. (2) e) der Promotionsordnung der Fakultät für Biologie zur Erlangung des Dr. rer. nat., dass ich keine anderen Promotionen bzw. Promotionsversuche in der Vergangenheit durchgeführt habe.

Essen, den _____ _____

Unterschrift des Doktoranden

Erklärung:

Hiermit erkläre ich, gemäß § 6 Abs. (2) f) der Promotionsordnung der Fakultät für Biologie, dass mir die Gelegenheit zum vorliegenden Promotionsverfahren nicht kommerziell vermittelt worden ist. Insbesondere habe ich keine Organisation eingeschaltet, die gegen Entgelt Betreuerinnen und Betreuer für die Anfertigung von Dissertationen sucht oder die mir obliegenden Pflichten hinsichtlich der Prüfungsleistungen für mich ganz oder teilweise erledigt. Hilfe Dritter wurde bis jetzt und wird auch künftig nur in wissenschaftlich vertretbarem und prüfungsrechtlich zulässigem Ausmaß in Anspruch genommen.
Mir ist bekannt, dass Unwahrheiten hinsichtlich der vorstehenden Erklärung die Zulassung zur Promotion ausschließen bzw. später zum Verfahrensabbruch oder zur Rücknahme des Titels führen können.

Essen, den _____ _____

Unterschrift des Doktoranden

Erklärung:

Hiermit erkläre ich, gem. § 6 Abs. (2) g) der Promotionsordnung der Fakultät für Biologie zur Erlangung der Dr. rer. nat., dass ich das Arbeitsgebiet, dem das Thema *"**Retrovirus induced expression of inhibitory ligands on myeloid cells and the regulation of cytotoxic CD8+ T cells**"* zuzuordnen ist, in Forschung und Lehre vertrete und den Antrag von ***(Paul David)*** befürworte und die Betreuung auch im Falle eines Weggangs, wenn nicht wichtige Gründe dem entgegenstehen, weiterführen werde.

Essen, den _____ _____

Unterschrift eines Mitglieds der Universität Duisburg-Essen

DOI: 10.17185/duepublico/70226
URN: urn:nbn:de:hbz:464-20190627-104210-0